

10
I 29 A

CIVIL ENGINEERING STUDIES

no. 156
cop. 2

STRUCTURAL RESEARCH SERIES NO. 156

Metz Reference Room
Civil Engineering Department
Rm 606 C. E. Building
University of Illinois
Urbana, Illinois 61801



**AN INVESTIGATION OF RIVETED AND BOLTED
COLUMN-BASE AND BEAM-TO-COLUMN CONNECTIONS
UNDER SLOW AND RAPID LOADING**

By
D. McDonald
A. Ang
and
J. M. Massard

Final Report to
RESEARCH DIRECTORATE
AIR FORCE SPECIAL WEAPONS CENTER
Air Research and Development Command
Contract AF 33(616)-3780
Project 1080
Task 10803

UNIVERSITY OF ILLINOIS
URBANA, ILLINOIS
FEBRUARY 1958

AN INVESTIGATION OF RIVETED AND BOLTED COLUMN-BASE
AND BEAM-TO-COLUMN CONNECTIONS UNDER
SLOW AND RAPID LOADING

by

D. McDonald

A. Ang

and

J. M. Massard

University of Illinois

Department of Civil Engineering

February 1958

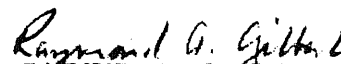
RESEARCH DIRECTORATE
AIR FORCE SPECIAL WEAPONS CENTER
Air Research and Development Command
Kirtland Air Force Base, New Mexico

Project : 1080
Task : 10803
Contract : AF 33(616)-3780

Approved:



ERIC H. WANG
Chief
Structures Division


RAYMOND A. GILBERT
Colonel, USAF
Director

ABSTRACT

This report contains a description of slow and rapid load tests of riveted and bolted column-base and beam-to-column connections, and the results which were obtained. Measurements of load, deflection, strain, and acceleration were taken in order to evaluate the resistance characteristics of the connections.

The small number of specimens and variety of connection types limited the scope of the investigation. The tests clearly indicated that the rate of deformation had an effect on the resistance of the connection; rapidly deformed specimens had a greater resistance at a given deflection than those tested slowly. In these tests, the type of fastener, rivet or high strength bolt, had little effect on the moment-rotation characteristics of the connections studied. With respect to the evaluation of specific moment resistance characteristics of connections subjected to rapid loading, this limited pilot study served only to indicate the nature of the resistance function which could be expected for connections of the type tested.

Also presented in this report is a procedure for evaluating the resistance of a frame with semi-rigid connections as it is loaded into the inelastic range. The method of analysis is such that the resistance characteristics of the connection, as well as that of the members, are taken into consideration. The method is of particular interest from the research standpoint since strain hardening is included.

PUBLICATION REVIEW

This report has been reviewed and is approved.

FOR THE COMMANDER:



IRVING L. BRANCH
Colonel, USAF
Deputy Commander

AN INVESTIGATION OF RIVETED AND BOLTED COLUMN-BASE
AND BEAM-TO-COLUMN CONNECTIONS UNDER
SLOW AND RAPID LOADING

CONTENTS

	<u>Page</u>
1. INTRODUCTION	
1.1 Object and Scope	1
1.2 Results and Conclusions.	4
1.3 Background	6
1.4 Acknowledgment	7
2. PRELIMINARY INVESTIGATION	
2.1 Comments	9
2.2 Conclusions.	9
3. A METHOD FOR DETERMINING THE RESISTANCE OF FRAMES WITH SEMI-RIGID CONNECTIONS WHEN SUBJECTED TO INELASTIC DEFORMATION	
3.1 Introductory Remarks	11
3.2 Notation	12
3.3 The Analytical Method.	13
3.4 Example: Multi-Story, Multi-Bay Frame With Semi-Rigid Connections.	16
4. SLOW AND RAPID TESTS OF RIVETED AND BOLTED COLUMN-BASE AND BEAM-TO-COLUMN CONNECTIONS	
4.1 Testing Apparatus.	23
4.1.1 Loading and Straining Apparatus	23
4.1.2 Instrumentation and Calibration	24
4.2 Column-Base Connection Tests	27
4.2.1 Testing Program	27
4.2.2 The Results of Column-Base Tests.	28

CONTENTS (Continued)

	<u>Page</u>
4.3 Beam-To-Column Connection Tests.	29
4.3.1 Testing Program	29
4.3.2 Results of Tests.	30
4.4 Comparison of Resistance-Deformation Characteristics	30
4.4.1 Determination of Resistances.	30
4.4.2 Comparison of Resistance-Deformation Characteristics. .	32
4.4.3 Empirical Relationships for Slow Deformation Tests. . .	33
4.5 Comments on Connection Behavior and Material Properties. . . .	35
BIBLIOGRAPHY.	37
APPENDIX A: Recorded Data From Connection Tests.	76
APPENDIX B: Photographs of Specimens After Testing	127

LIST OF TABLES

	<u>Page</u>
1. Computation of Resisting Moments for Example Problem	44
2. Summary of Column-Base Connection Tests.	59
3a. Summary of Beam-To-Column Connection Tests	60
3b. Summary of Beam-To-Column Connection Tests	61

LIST OF FIGURES

	<u>Page</u>
1a. Moment-End Slope Relationships for WF Sections of ASTM A-7 Steel (for Member with Contraflexure)	39
1b. Moment-End Slope Relationships for WF Sections of ASTM A-7 Steel (for Member with Contraflexure)	40
2. Moment-End Slope Relationships for WF Sections of ASTM A-7 Steel (for Member without Contraflexure).	41
3. Assumed Moment-Rotation Relationship for Beam-to-Column Connections	42
4. Assumed Moment-Rotation Relationship for Column-Base Connections.	43
5. General View of Testing Apparatus.	48
6. View of Instruments and Pressure Panel	49
7. View of Axial Loading and End Reaction System.	50
8. Schematic Drawing of Testing Arrangement for Column-Base Connections.	51
8a. Details of Column-Base Connections	52
9. Schematic Drawing of Testing Arrangement for Beam-to-Column Connections	53
9a. Details of Beam-to-Column Connections.	54
10a. Wiring Diagram for SR-4 Strain Bridges--Column-Base Connections.	55
10b. Wiring Diagram for SR-4 Strain Bridges--Beam-to-Column Connections.	56
11. Wiring Diagram for Deflection Gages.	57
12. Schematic Drawing of Axial Load Tie Rod System	58
13. Measured Lateral Resistance Versus Midspan Deflection of Column-Base Connections CB1 and CB2	62
14. Measured Lateral Resistance Versus Midspan Deflection of Column-Base Connections CB3 and CB4	63
15. Measured Lateral Resistance Versus Midspan Deflection of Column-Base Connection CB6.	64

LIST OF FIGURES (Continued)

	<u>Page</u>
16. Measured Lateral Resistance Versus Midspan Deflection of Column-Base Connections CB7 and CB8.	65
17. Measured Lateral Resisting Moment Versus Rotation of Column-Base Connections CB1 and CB2.	66
18. Measured Lateral Resisting Moment Versus Rotation of Column-Base Connections CB3 and CB4.	67
19. Measured Lateral Resisting Moment Versus Rotation of Column-Base Connection CB6	68
20. Measured Lateral Resisting Moment Versus Rotation of Column-Base Connections CB7 and CB8.	69
21. Measured Resisting Moment Versus Beam Rotation of Beam-to-Column Connections CTBS and CTBR	70
22. Measured Resisting Moment Versus Beam Rotation of Beam-to-Column Connections CTBS and CTBR	71
23. Measured Resisting Moment Versus Beam Rotation of Beam-to-Column Connections CWBS and CWBR	72
24. Measured Resisting Moment Versus Beam Rotation of Beam-to-Column Connections CWBS and CWBR	73
25. Measured Resisting Moment Versus Beam Rotation of Beam-to-Column Connections CFBS and CFBR	74
26. Measured Resisting Moment Versus Beam Rotation of Beam-to-Column Connections CFRS and CFRR	75

AN INVESTIGATION OF RIVETED AND BOLTED COLUMN-BASE
AND BEAM-TO-COLUMN CONNECTIONS UNDER
SLOW AND RAPID LOADING

1. INTRODUCTION

1.1 Object and Scope

The investigation performed at the University of Illinois under Contract AF 33(616)-3780 was concerned with the performance of tests and analyses to obtain information pertaining to the behavior of riveted and bolted column-base and beam-to-column connections when subjected to known static and transient dynamic loadings that produced extensive inelastic deformations.

Little work has been done in this field; a brief review of the literature on frame type connections revealed very little in the way of test data or methods of analysis by means of which the moment-deformation characteristics of riveted or bolted connections could be estimated with fair accuracy. Essentially nothing was known concerning the resistance of connections under rapid loading conditions.

The moment resistance of connections is of great importance in studies of building response in which inelastic behavior is considered. Commonly, in limit analyses, the connections are considered to be rigid, i.e., capable of transmitting the resisting moment of the attached frame member. Under such conditions the "plastic hinges" are assumed to form in the members at critical sections, i.e., at points of maximum moment; these occur at load points or points of structural discontinuity. The order of formation of hinges is dependent on the magnitude of the moment and the moment resistant capacity of the member at the critical section; moreover,

as the applied load and thereby the moment at a connection increases, the hinge will form in the weaker of the two components, either the connection or the beam. Thus, it should be clear that connections are critical items in inelastic analysis and design, since they often occur at points of maximum moment, and in general always represent a point of structural discontinuity. In steel frame structures, connections are of two general types, namely welded and riveted or bolted. Properly designed welded connections may realistically be assumed as rigid. Riveted or bolted connections may be of various designs, of which the types studied in this investigation are typical. In general, such connections may be classed as rigid, semi-rigid, or flexible. Actually, the so-called rigid type of riveted or bolted connection may not be extremely rigid; this of course depends on the particular design. In studying the response of structures with riveted or bolted connections, it is necessary to know the resistance characteristics of the connection as well as those of the connected members. At a point of junction, the plastic hinge will form in (a) the member or (b) the connection, whichever has the lesser resistance. Normally the connection would have the lesser resistance and this is the item under study in this program.

A brief study was made of the accuracy with which the maximum resistance and deformation of such connections could be determined using extreme simplification. This is discussed in Section 2 of this report.

In studying the response of steel structures, it is common to neglect the strain hardening effect which occurs following yielding; the effect of strain hardening is to increase the resistance. Such an assumption simplifies the analysis in that it permits one to assume a constant

level of moment resistance in the inelastic range. In most applications, approximations of this nature are justified and lead to engineering results of the desired accuracy. However, in research studies it is often desirable to consider the effect of strain hardening (or alternately, the effect of a decreasing resisting function following the peak resistance). As another phase of the present investigation the method presented under Contract AF 33(616)-170 for determining the resistance of steel frame structures to inelastic deformation^{17*} was extended to include the effect of inelastic deformation of the connections (as might be typical of semi-rigid connections). This work is presented in Section 3. It should be emphasized that this particular portion of the study should be considered primarily as a research tool, and is not well adapted for general structural analysis purposes.

Since the analytical determination of the resistance-deformation characteristics of riveted or bolted column-base and beam-to-column connections of the usual complex form seemed a hopeless task, the major objective of the investigation conducted at the University of Illinois under Contract AF 33(616)-3780 was to obtain experimental information pertaining to the behavior of such connections as they respond to slow and rapid loadings. To provide this information, ten sets of connection specimens were tested; four sets were of the column-base type and six sets were of the beam-to-column type. Each set contained two matching specimens, one of which was tested with a slowly applied lateral load, and the other with a rapidly applied lateral load. In addition to the lateral load, the column-base connections were subjected to a relatively constant thrust applied

* Numbers refer to entries in Bibliography

initially along the axis of the "columns". In these tests a double cantilever arrangement was used in which two beams were framed into a center loading stub by means of the connections to be tested.

1.2 Results and Conclusions

1. In order to more realistically study the response of structures in the inelastic range, it is necessary to know the resistance characteristics of riveted and bolted connections under both statically and rapidly applied loads. Specifically, a knowledge of the moment resistance characteristics of the connections as well as those of the attached members is required in order to realistically evaluate the hinge formation in inelastic analysis or design studies. The small number of specimens and variety of connection types limited the scope of the present investigation. As a result, rather than indicating general relationships which could be used for estimating the resistance of various types and sizes of connections subjected to rapid loading, this pilot study served to indicate the nature of the resistance function which could be expected for connections of the type tested. This in itself is of considerable value since no results were previously available; moreover, such information will prove extremely useful in future investigations. The more definite conclusions resulting from the study are listed below.

2. The rate of deformation had a definite effect on the resistance of the connections tested in that those specimens deformed rapidly had a greater resistance at a given deflection than those tested slowly.

3. The relative dynamic increase of the moment resistance is greater in the beam-to-column connections than in the column-base connections.

4. The dynamic increase in resistance was greater in the more flexible connections.

5. The type of fastener, rivet or high strength bolt, had little effect on the moment-rotation characteristics of a connection. The maximum resistance of the connection was affected slightly, and the mode of failure was affected to the extent that several rivets failed but no failures occurred in high strength bolts.

6. In the column-base connections tested, the behavior was governed by the anchor bolts and deformation of the angles used as the column connection. The type of fastener between the angle and column was of little importance.

7. The failure process of connections in which the angles were the weakest components was terminated in several cases by brittle fracture of the angle under either slow or rapid loading. However, these failures were obtained only after much inelastic deformation with consequent "exhaustion" of ductility in the critical angle itself, so that the energy absorbed by the connection was reduced little if any over that absorbed by similar specimens in which no terminal brittle fracture occurred. The "shear lip" associated with the brittle fracture was large, usually covering about ten percent of the cross section.

8. A method of analysis is presented by means of which the resistance of frames having non-rigid connections can be determined for all deformations including the range of strain hardening. Although the method is completely general in nature, it is believed its primary usefulness is limited to research applications.

1.3 Background

A search of the literature reveals field tests of riveted beam connections as far back as 1908¹. Also some analytical work has been done in the prediction of the moment-rotation characteristics of connections^{7,8} and methods of estimating the ultimate moment resistance.⁶ An excellent bibliography is given in reference (9) for those interested in pursuing this study further.

As regards studies pertaining to column-base connections, direct pull-out tests of anchor bolts set in concrete^{5,16}, as well as compression tests of column bases have been reported^{2,3}. However, very little experimental work has been reported on the behavior of column-base anchorages subjected to moment as well as direct force. The available analytical information seems to be limited to equations derived for one general type of column anchorage¹². These can be used to determine the maximum value of the resisting moment and the minimum rotation at that moment. Also, a procedure is outlined by means of which a few points on the moment-rotation curve can be obtained.

Some analytical work concerned with the behavior of structures under transient loading has been done using practicable assumptions concerning the resistance of the structures or structural elements considered^{10,13,14}. Also, some experimental investigations of the behavior of structures and their components have been accomplished^{15,19,20}, although the major portion of such work has been laboratory studies of small-scale specimens or field tests of full-scale structures¹¹, most of the results of which are classified under U. S. Government Security regulations. It is believed that the tests described in this report are the first transient loading tests of structural connections.

1.4 Acknowledgment

The work described in this report was performed by staff members of the University of Illinois in cooperation with the Blast Effects Group, Wright Air Development Center, now the Structures Division, Research Directorate, Air Force Special Weapons Center, Department of the Air Force, under Contract AF 33(616)-3780. The project was conducted in the Structural Research Laboratory of the Department of Civil Engineering under the general direction of N. M. Newmark, Professor of Civil Engineering and Head of the Department. The Project was under the direct supervision of J. M. Massard, Research Assistant Professor of Civil Engineering.

The preliminary studies were made by W. Egger, Research Associate in Civil Engineering. A. Ang, Research Assistant in Civil Engineering, was responsible for the analytical procedure for determining the inelastic resistance of frames having semi-rigid connections. This formed a part of his M. S. dissertation¹⁸. D. McDonald, Research Assistant in Civil Engineering, had the direct responsibility for the experimental work on the column-base and beam-to-column connections. The column-base tests were used by Mr. McDonald as the basis of his M. S. dissertation¹⁹. R. F. Wojcieszak, Research Associate in Civil Engineering, aided the performance of the project generally. His assistance was especially valuable in the performance of tests and interpretation of test data. The instrumentation used was the responsibility of V. J. McDonald, Associate Professor of Civil Engineering, and his assistants O. H. Ray, Instrument Maker, and H. H. Dalrymple, Laboratory Technician.

In addition to the persons named above, the assistance of the personnel of the Civil Engineering Shop, and student assistants, particularly H. A. Mitchell, is gratefully acknowledged.

Certain portions of the final report were revised and edited by W. J. Hall, Associate Professor of Civil Engineering.

2. PRELIMINARY INVESTIGATION

2.1 Comments

The complexity of a typical riveted or bolted connection in both construction and function precludes the possibility of accurate analysis. In the so-called elastic range the performance of the connection is governed by, and, in fact, depends upon residual stresses which are largely indeterminate. In the range of inelastic deformation residual stresses may no longer be important but complex forces associated with the large deformations act upon the components of the connection. Attempts have been made by many investigators including the project staff at the University of Illinois to compute maximum resistance and deformation of such connections assuming extreme simplification of the manner in which the connections resist deformation. The accuracy obtainable by such procedures is mainly dependent upon the experience and judgment of the "analyst", but in most cases is no more than sufficient to indicate limiting values useful in designing specimens and the associated testing apparatus. Since the studies made at the University of Illinois were based upon arbitrary approximations which could not be reduced easily to generally applicable form, the procedures used and the results obtained are not presented. It is sufficient to say that the usefulness of such computations in determining structural behavior is very limited since complete resistance-deformation characteristics are not obtained.

2.2 Conclusions

It was evident from the preliminary study that information concerning the resistance-deformation characteristics of riveted or bolted

column-base and beam-to-column connections can best be determined from empirical relationships based upon reliable test data. Therefore, it was decided that "analysis" associated with connections tested under Contract AF 33(616)-3780 would be limited to determination of empirical relationships of the form proposed by Professor Johnston and his associates¹², and that, for conditions of rapid loading and deformation, an attempt would be made to obtain modifications of these relationships necessary to take into account the increased rate of deformation.

3. A METHOD FOR DETERMINING THE RESISTANCE OF FRAMES WITH SEMI-RIGID CONNECTIONS WHEN SUBJECTED TO INELASTIC DEFORMATION

3.1 Introductory Remarks

A method for the analysis of frames with rigid connections subjected to inelastic deformation into the range of strain hardening was presented in a Technical Report prepared under Contract AF 33(616)-170¹⁷. In this section, an extension of the method to include the effect of non-rigid inelastic connections will be described. Only the essentials of the basic method are described here; for a discussion of the assumption and limitations associated with the procedure, the reader is referred to the original report mentioned above.

The procedure can be used for determining the resistance of frame structures composed of elements having individual resistance-deformation characteristics of any monotonically increasing form that can be described graphically. The resisting moments which correspond to a given set of displacements of the "loaded" joints in a structure are found by means of a modified "moment distribution" procedure made convenient by use of moment-end slope curves for the individual members and moment-rotation curves for the semi-rigid connections. After the compatible set of resisting moments have been obtained, the corresponding set of loads required to produce the particular joint displacements are computed. By solving a set of such problems, load-joint displacement relationships can be obtained for a range of loads, or conversely, for a range of displacements.

For use with the procedure, resistance-deformation relationships are required for each of the structural elements of the frame under consideration. In Figs. 1 and 2, which are reproduced from Reference (17),

are presented dimensionless moment-end slope curves representing with an error of less than ± 3 percent these characteristics for all wide flange beams and columns made of a "typical" ASTM A7 steel. The derivation of these moment-end slope curves was based upon the following assumptions:

1. The members are prismatic, and there is no change in shear along the length of any member.
2. Only flexural stresses are considered in the computation of the moment-curvature relationships.
3. Clockwise end moments are positive.
4. An end slope is positive if the rotation is in the same direction as the moment.
5. Relative lateral displacements of entire members can be described in terms of an angle change times the original length of a member.

In Figs. 3 and 4, reproduced from Reference (18), are given, respectively, the moment-rotation relationships for the beam-to-column and column-base connections which will be used in the example problem used in this text.

3.2 Notation

The following notation has been used in this section:

Superscripts: ij designates the member considered
 c designates connection considered
 o designates a quantity used as the
reference value in a problem

Subscripts: e designates elastic limit condition
 fp designates fully plastic condition
 ij designates end i of member ij

Sectional Properties

I = moment of inertia about the centroidal axis of the cross section - in.⁴

d = overall depth of structural section - in.

S = section modulus ($I/d/2$) - in.³

Loads

P = applied lateral load - kips

M = total moment at a section - kip ft

M_e^{ij} = elastic limit resisting moment of member ij

M_{fp}^{ij} = fully plastic resisting moment of member ij

M_{ji} = total moment at end j of member ji

M_{ji}^C = moment of the connection at j of member ji

Stress

σ_e = static yield stress of the material - ksi

Deformation

θ^{ij} = total angle change along the full length of member ij - rad.

θ_e^{ij} = elastic limit angle change of member ij

θ_e^O = elastic limit angle change of a particular member used as a standard unit of rotation in a problem

ϕ_{ji} = end slope at end j of member ji - rad.

ϕ_{ji}^C = rotation of the connection at j of member ji

3.3 The Analytical Method

The assumptions underlying the method of analysis are as follows:

1. The relationships between the external forces acting upon a structural element and its pertinent deformation can be presented in a form similar to Figs. 1, 2, 3 and 4.

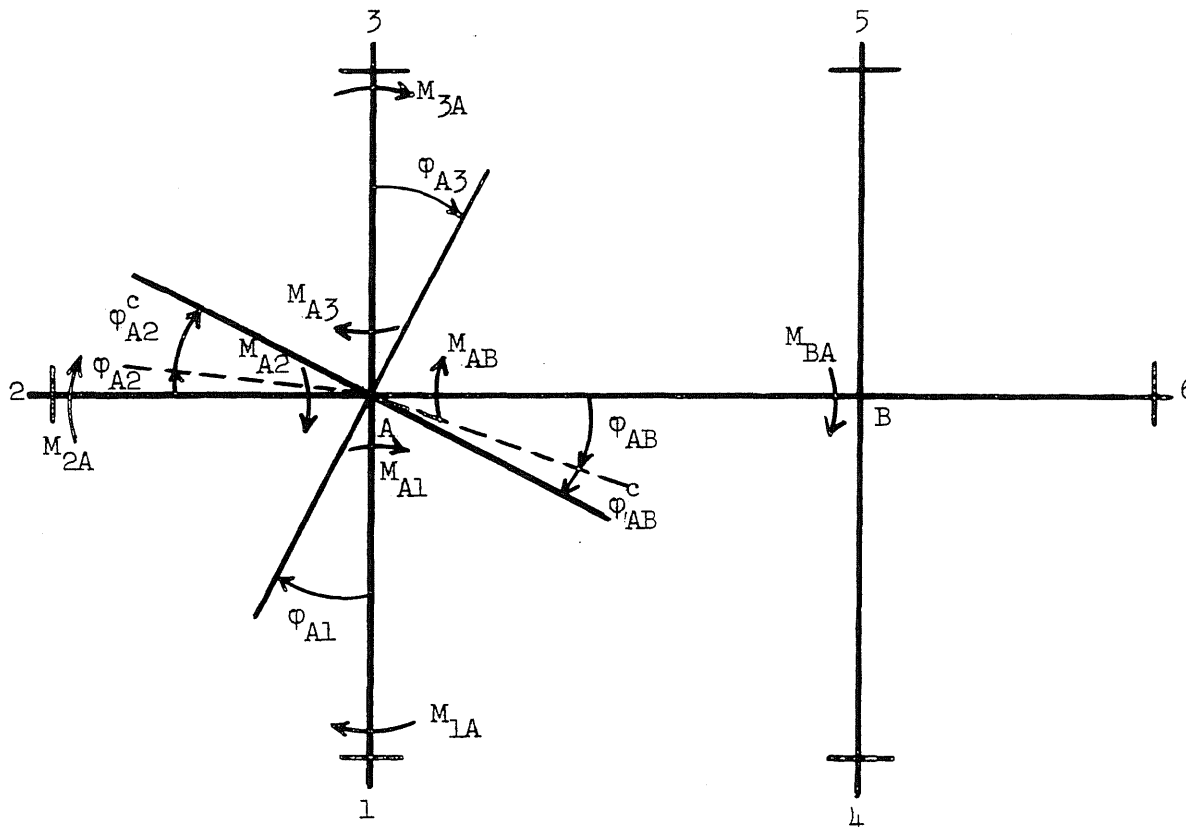
2. External loads are assumed to be concentrated at the joints and are always increasing. There are no loads at intermediate points of any member. (A load could be applied at an intermediate point on a member by considering that point as a joint.)

3. For a rigid joint, full continuity at the joint is maintained; thus the moment up to and including the ultimate moment can be transmitted. For a semi-rigid joint, the moment-rotation characteristic of the connection must be defined up to and including the ultimate moment; the rotation of both the connection and the member must be considered at a joint.

Moment distribution as used in the analysis of linearly elastic structures is based upon the principle of superposition, and the stiffnesses and carry-over factors used in the distribution process are constant for each member. In inelastic structures, however, the application of superposition is restricted. Moments can no longer be added or subtracted indiscriminately; a correct direction of moment must be known; and the stiffnesses and carry-over factors must be those corresponding to the final end moments.

As an alternative procedure the moment, M_{ji} , at the near end of a flexural member, can be found that will produce the required rotation, ϕ_{ji} , at the near end, with a given or assumed far end moment. In addition to this, compatible resisting moments and deformations of the connections must be determined so that in the final solution, equilibrium of forces and moments, and physical continuity have been obtained. In order to use the procedure outlined here, the direction of the end moments must be known; the direction of the end moments acting on a member determines whether Fig. 1 or Fig. 2 is to be used for obtaining the end slope.

There are perhaps many possible ways to proceed in the solution of a problem of this type. One of these will be described with reference to the following sketch.



In this illustration (as in the example problem to follow) the columns are assumed to be continuous, so that no concentrated rotations occur in the columns themselves at the intermediate floor connections.

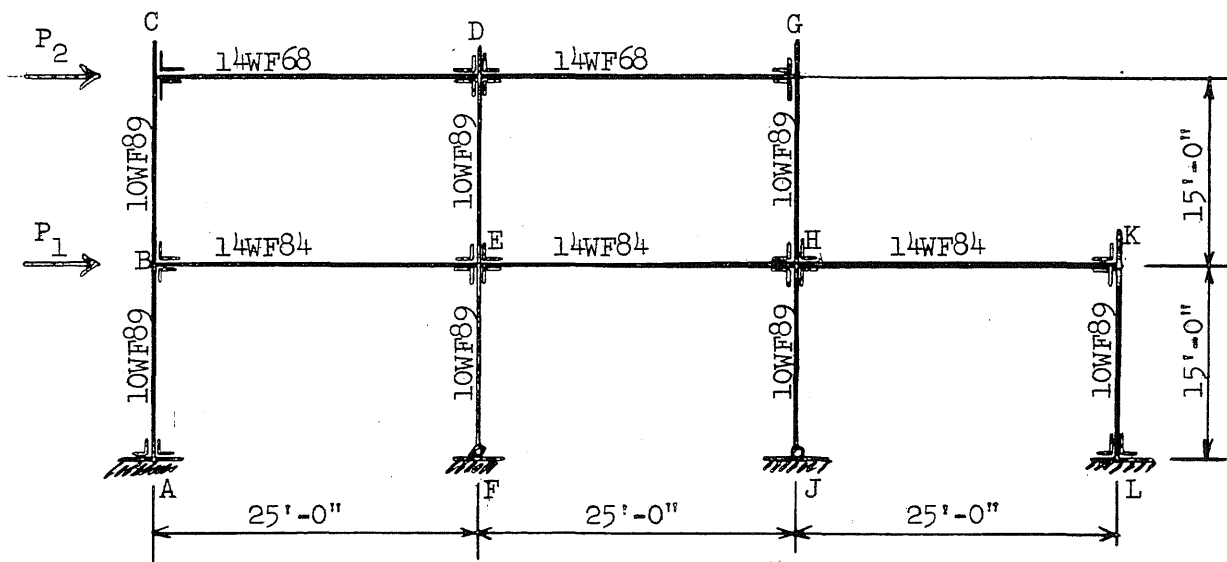
At the start of the procedure, magnitudes of the far end moments, M_{BA} , M_{1A} , M_{2A} , and M_{3A} are assumed or known. The moments M_{AB} , M_{A1} , M_{A2} , and M_{A3} are determined by trial and error from the moment-end slope relationships of the members and the moment-rotation relationships of the connections, so that at A the end rotations are equal; that is, $\phi_{A3} = \phi_{A1} = \phi_{A2} + \phi_{A2}^c = \phi_{AB} + \phi_{AB}^c$ and in addition the moments must be in equilibrium. The procedure

is carried out to every joint until moment convergence to within the desired accuracy has been achieved.

An example of the method applied to frames with inelastic connections follows.

3.4 Example: Multi-Story, Multi-Bay Frame with Semi-Rigid Connections

The same problem used in Example B of Reference (18) will be solved considering that the joints are semi-rigid and have the moment-rotation relationships for beam-to-column and column-base connections given in Figs. 3 and 4 respectively. These moment-rotation relationships are assumed for purposes of illustration only. For convenience, the moments and rotations are expressed, respectively, in terms of M_{fp} and θ_e of the connected members.



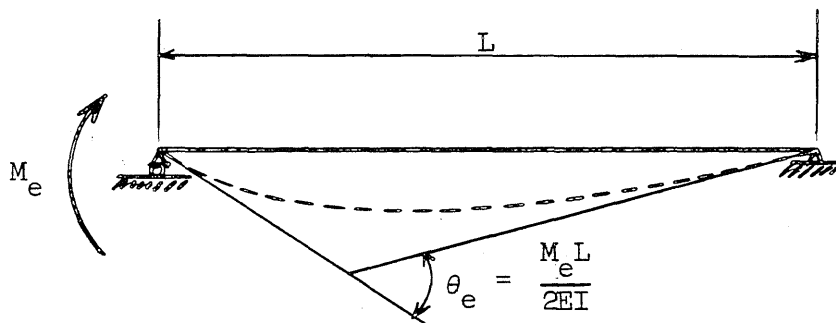
Properties of Members:

	I	S	Shape Factors
14WF84:	928.4 in. ⁴	130.9 in. ³	1.107
14WF68:	724.1 in. ⁴	103.0 in. ³	1.113
10WF89:	542.4 in. ⁴	99.7 in. ³	1.146

Using $\sigma_e = 32$ ksi, the M_e and M_{fp} are:

	M_e (kip-in.)	M_{fp} (kip-in.)	M_{fp}/M_{fp}^o
14WF84:	4,188.8	4,640	<u>1.268</u>
14WF68:	3,296.0	3,670	<u>1.003</u>
10WF89:	3,190.4	3,660(reference)	<u>1.000</u>

the elastic limit angle changes, θ_e , as used in Figs. 1 through 4 are illustrated below.



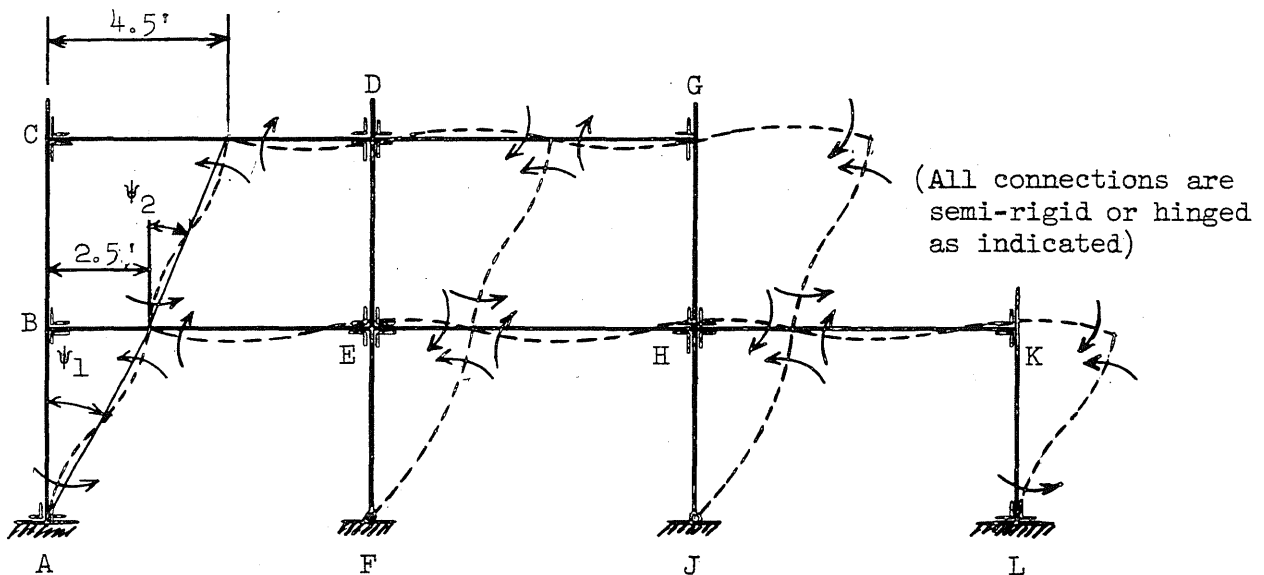
The elastic limit angle changes (θ_e) for the members used in this illustration are computed below.

$$\theta_e^{14WF84 (25')} = \frac{4,188.8 \times 25 \times 12}{2 \times 30,000 \times 928.4} = 0.023 \text{ rad.}$$

$$\theta_e^{14WF68 (25')} = \frac{3,296.0 \times 25 \times 12}{2 \times 30,000 \times 724.1} = 0.023 \text{ rad.}$$

$$\theta_e^{10WF89 (15')} = \theta_e^o = \frac{3,190.4 \times 15 \times 12}{2 \times 30,000 \times 542.4} = 0.018 \text{ rad. (reference)}$$

Given: $\Delta_{AB} = 2.5 \text{ ft}$; $\Delta_{AC} = 4.5 \text{ ft}$; Find P_1 and P_2 .



Deflected Structure and Direction of Moments

The displacement angles ψ_1 and ψ_2 corresponding to the given displacements may be expressed in terms of θ_e^0 as follows:

$$\psi_1 = \frac{2.5}{15} = 9.26 \theta_e^0$$

$$\psi_2 = \frac{2}{15} = 7.41 \theta_e^0$$

where,

$$\theta_e^0 = \theta_e^{\text{LOWF89 (15')}} = 0.018 \text{ rad.}$$

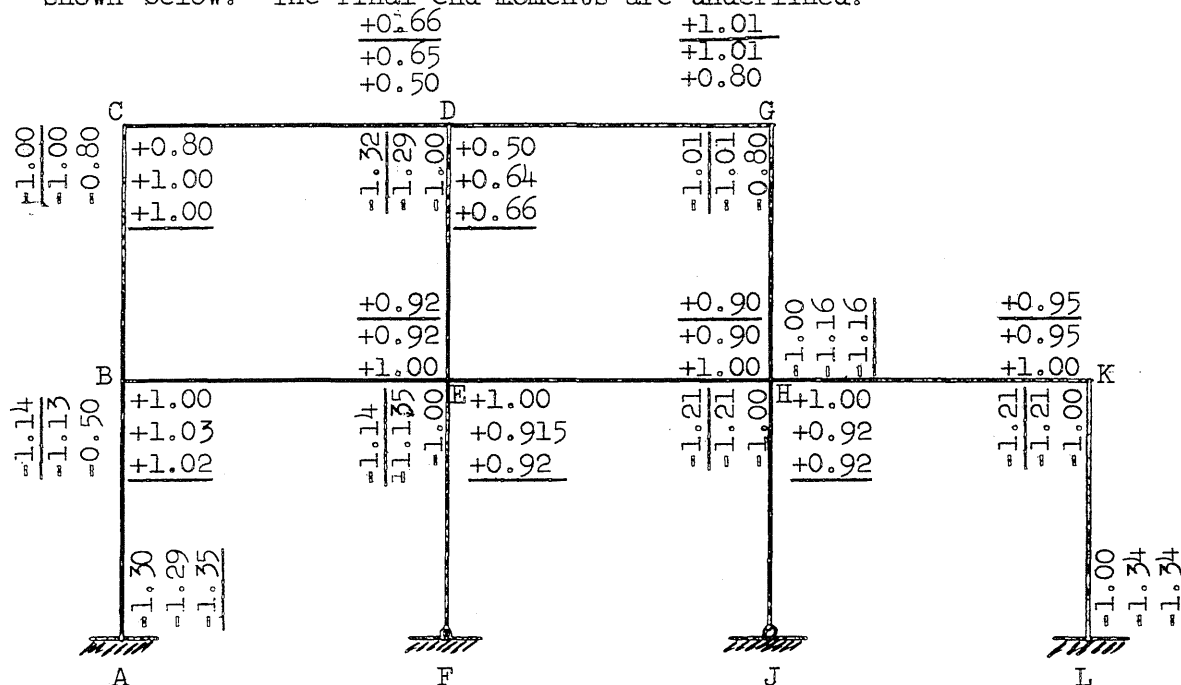
The assumed end moments (in terms of M_{fp}^{ji}) are given in the first line of moments (nearest the member) in the figure on page 21. From these the "correct" moments are determined by trial and error iteration with the use of Figs. 1a or 1b and Figs. 3 and 4; the iteration procedure is illustrated in Table 1.

Joint A is arbitrarily chosen as the starting point. The end moment, M_{AB} , as shown, is assumed to be $1.30 M_{fp}^0 = 1.30 M_{fp}^{AB}$. From Fig. 1a or 1b, the end-slope $\phi_{ji} = \phi_{AB}$ corresponding to $M_{ji} = M_{AB} = 1.30 M_{fp}^{AB}$ and $M_{ij} = M_{BA} = 0.50 M_{fp}^{AB}$ is found to be $6.70 \theta_e^{AB}$, and $\phi_{ji} = \phi_{AB}^c$ corresponding to $M_{ji}^c = M_{AB}^c = 1.30 M_{fp}^{AB}$ is found from Fig. 4 to be $2.80 \theta_e^{AB}$. By definition, $\phi_{AB} + \phi_{AB}^c$ must be equal to ψ_1 . Since $\phi_{AB} + \phi_{AB}^c = 6.70 \theta_e^{AB} + 2.80 \theta_e^{AB} = 9.50 \theta_e^{AB} \neq \psi_1$, (ψ_1 was originally calculated to be equal to $9.26 \theta_e^0 = 9.26 \theta_e^{AB}$) the assumed moment, $M_{AB} = 1.30 M_{fp}$, is incorrect. The correct

moment is found to be $1.29 M_{fp}$. The trial iteration may be observed in Cycle 1, Joint A, Table 1. In Table 1, the column M_{ji}/M_{fp}^O allows one to sum moments quickly about a joint. The column M_{ji}/M_{fp}^{ij} is used in conjunction with Figs. 1 through 4.

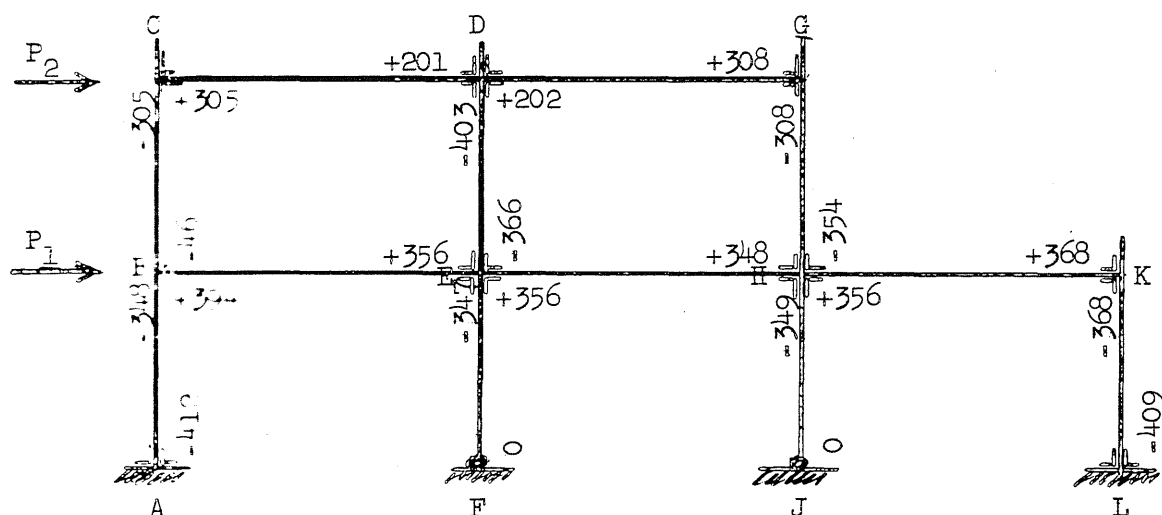
Going to Joint B, the end moment, M_{BA} , (in the final iteration) is assumed to be $1.13 M_{fp}^O = 1.13 M_{fp}$. From Fig. 1a or 1b, the end-slope $\phi_{ji} = \phi_{BA}$ corresponding to $M_{ji} = M_{BA} = 1.13 M_{fp}$ and $M_{ij} = M_{AB} = 1.29 M_{fp}$ is found to be $1.70 \theta_e^{BA}$. The rotation of BA at B is therefore $9.26 \theta_e^{BA} - 1.70 \theta_e^{BA} = 7.56 \theta_e^{BA} = 7.56 \theta_e^O$. (θ_e^{BA} is considered as θ_e^O in this problem.) Since the columns are assumed continuous, the rotation of BC at B also must be equal to $7.56 \theta_e^O = 7.56 \theta_e^{BC}$, so that the end-slope $\phi_{BC} = \psi_2 - 7.56 \theta_e^{BC} = 7.41 \theta_e^{BC} - 7.56 \theta_e^{BC} = -0.15 \theta_e^{BC}$. The moment, M_{BC} , corresponding to this end-slope and a far-end moment of $0.80 M_{fp}$ is $0.18 M_{fp} = 0.18 M_{fp}^O$ (from Fig. 1a or 1b). From the chosen deflection configuration, $M_{BE} = M_{BA} + M_{BC} = 1.13 M_{fp}^O + 0.18 M_{fp}^O = 1.31 M_{fp}^O = 1.03 M_{fp}^{BE}$. The end-slope ϕ_{BE} , (from Fig. 1a or 1b) corresponding to $M_{ji} = M_{BE} = 1.03 M_{fp}$ and $M_{ij} = M_{EB} = 1.00 M_{fp}$ is $0.85 \theta_e^{BE}$, and the connection rotation, $\phi_{ji}^c = \phi_{BE}^c$, (from Fig. 3) corresponding to $M_{ji}^c = M_{BE}^c = 1.03 M_{fp}$ is $5.20 \theta_e^{BE}$. ($\phi_{BE} + \phi_{BE}^c = 0.85 \theta_e^{BE} + 5.20 \theta_e^{BE} = 6.05 \theta_e^{BE} = 7.73 \theta_e^O$.) Since this total rotation is approximately equal to the rotation of the column at B, the assumed moments are correct. The complete

solution for moments is given in Table 1, and the convergence of moments is shown below. The final end moments are underlined.



Moments Given in Terms of Fully Plastic Moment, M_p

The structure with the final moments in ft-kips is shown below:



The loads P_1 and P_2 may be computed as indicated below.

$$P_2 = \frac{305 + 46}{15} + \frac{403 + 366}{15} + \frac{308 + 354}{15}$$

$$= 118.8 \text{ kips.}$$

$$P_1 = \frac{348 + 412}{15} + \frac{347}{15} + \frac{349}{15} + \frac{368 + 409}{15} - 118.8$$

$$= 148.87 - 118.8$$

$$= 30.07 \text{ kips.}$$

4. SLOW AND RAPID TESTS OF RIVETED AND BOLTED COLUMN-BASE AND BEAM-TO-COLUMN CONNECTIONS

4.1 Testing Apparatus

4.1.1 Loading and Straining Apparatus. A general view of the testing apparatus used in the column-base and beam-to-column connection investigation is shown in Fig. 5. In the rapid tests the lateral load was applied by a 60-kip loading unit, similar to that shown in Fig. 5. A complete description of the rapid loading units is presented in another report²¹. In the slow tests a hydraulic jack, driven by an electric pump, was used so that the deflection of the specimen was increased continuously throughout the duration of the test. In both slow and rapid tests a transverse pin allowed relative rotation between the piston rod and the stub in the plane of the specimen.

The axial thrust in the column-base connection tests was supplied by two pneumatic loading units which were capable of sustaining loads up to 55 kips. These units, one at each end of the specimen, were connected with tie rods so that the axial loading assembly was self contained. Each unit was equipped with mechanisms to limit movement if specimen collapse occurred.

Schematic drawings of the testing apparatus and end loading arrangement are given in Figs. 8, 9 and 12. A view of the end reaction system is shown in Fig. 7.

To conserve specimen material the steel beam extensions shown in Figs. 8 and 9 were incorporated into the testing arrangement and used throughout the test series.

The end reaction system allows rotation and translation in the plane of the specimen and provides partial restraint against motion in the

four other possible degrees of freedom. The distance between end reaction systems was selected for a favorable relation between moment and applied load.

4.1.2 Instrumentation and Calibration. In all tests, applied loads, strains in the connections, and deflections occurring along the length of the beams were recorded oscillographically as functions of time. In addition, acceleration of the loading point was recorded during rapid tests. A photograph of the recording instruments is shown in Fig. 6.

The lateral load was measured by means of a dynamometer attached to the end of the piston of the lateral loading unit. Strain gages mounted on the end reaction units were used to measure axial thrust. Five slide wire deflection gages were located symmetrically on the specimen, with one at the loading point, one 16 inches, and one 36 inches away from the center-line of the specimen. The locations of the post yield SR-4 strain gages are shown in Figs. 10a and 10b. An accelerometer was mounted on the loading stub in the rapid tests.

Measurements in these tests may be divided into three groups: (1) the measurements of various strains (in this group are included all load measurements since the load data were obtained through the use of standard SR-4 strain gages attached to dynamometers and calibrated in terms of pounds of load); (2) the measurement of specimen deflection; and finally, (3) the general problems of sequence and timing.

Strain measurements were taken with standard SR-4 gages connected as conventional Wheatstone bridges which were excited with a 3,000 cps carrier wave produced by an oscillator having added regulation so that the output voltage remained constant within one percent even under open circuit

conditions. A diagram of one such bridge is shown in Fig. 10. The output of five strain bridges were "fed" into slightly modified Hathaway Company MRC 18 carrier system amplifiers, whose output in turn fed Hathaway OC 2 group 23 galvanometers in a pair of S14C magnetic oscillographs. This combination had a frequency response that is flat within 10 percent to about 450 cycles per second. One channel of this carrier system was used to record the output of an AMS20A accelerometer and was in all respects identical to the other channels except that the accelerometer exciting voltage was limited to one volt instead of the four volts used in the strain channels.

Deflections of the specimen were measured using slide wire gages which were constructed in the laboratory and whose maximum range was about 18 inches. These gages formed two legs of a DC excited Wheatstone bridge circuit. The other two legs of the Wheatstone bridges were formed by calibrating devices. All gages were connected in series and excited with the same regulated DC current. The outputs of these bridges were fed into Hathaway magnetic oscillograph channels in which were used Hathaway OC2 group 23 recording galvanometers. These deflection measuring channels were flat in response within 10 percent from 0 to 450 cps. The deflection circuits are shown schematically in Fig. 11.

Because of limitations in the amount of equipment available it was necessary to record the information discussed above on two six-channel magnetic oscillographs. Therefore, in addition to the standard timing signals, it was necessary to add synchronizing signals so that the two records could be measured with respect to the same time reference. To provide this synchronization, an electrical signal of known frequency was obtained from a common source and applied to one galvanometer in each of the two oscillographs.

The timing signal was modulated in amplitude by means of a mechanically driven switch to insure that a given cycle of a timing wave could be identified on each of the two records.

Strain channels were calibrated by the conventional method of shunting one arm of the measuring bridge with resistances whose equivalencies in terms of strain had been measured previously. The dynamometers used to measure loads and reactions were calibrated under static loading. During these calibrations, shunting resistances were placed in the circuit so that the equivalent values in terms of load could be determined.

Prior to use, the slide wire deflection gages were calibrated by recording the gage output for various measured amounts of mechanical displacement. During the calibration period, the gage was returned to its zero position and the switches on the calibration arms of the bridge were closed in sequence. By this procedure, the value of the calibration switch positions were obtained in terms of mechanical movement of the gage. These values were then used for calibration in the actual test. That is, prior to a test, the calibration switches were closed in sequence with the result that a series of steps was produced on the oscillograph record whose equivalencies in terms of mechanical deflection were known.

The AMS20A accelerometer which was used to record movement of the center of the specimen was calibrated by driving it mechanically with a series of sinusoidal movements of measured amplitude and period. During the calibrations, equivalent electrical output was obtained through the use of calibrating inductors. Thus, as in the case of the deflections in strains, calibration marks were determined. These were then used prior to an actual test to show the sensitivity of the recording system.

The basic timing signal used was checked by use of a Potter Instrument Company Model 830 frequency meter, which in turn was checked periodically by comparing its timing intervals with a standard timing signal.

4.2 Column-Base Connection Tests

4.2.1 Testing Program. The specimens tested in this portion of the investigation simulated typical column anchorages as found in small steel frame buildings. Two basic types of connections were used: (1) angles connected to the flanges of the columns, referred to as flange-angle connections; (2) angles connected to the web of the column, referred to as web-angle connections. Rivets were used as angle-to-beam fasteners on half of the specimens of each basic type and high tensile strength bolts on the remaining specimens. Anchor bolts, threaded at both ends and continuous through the loading stub, were used to connect the angles to the stub. A resumé of the types of connections, types of stub, and manner of failure for each specimen is given in Table 2. Details of the connections may be obtained from a study of Figs. 8 and 8a and the photographs in Appendix B. As noted in the table two types of stubs were used, a reinforced concrete block, and a welded assemblage of steel plates. The columns in all specimens were 8WF35 sections; the anchor bolts through the stub were one inch diameter mild steel; the fasteners were either 3/4 inch diameter rivets or bolts.

Two specimens of each type were fabricated, one of which was tested with a slowly applied loading and the other with a load applied rapidly. At the beginning of a test, the column-base connection specimens were subjected to a 40-kip axial force which was maintained at a relatively constant value throughout the duration of the test.

4.2.2 The Results of Column-Base Tests. The phenomena measured versus time during each of the column-base connection tests were the lateral load, the deflections at various points along the lengths of the specimen, the axial load, and strains in the connection angles. In addition, the acceleration of the loading point was measured in the rapid tests. These quantities, plotted as functions of time, are presented in Appendix A, along with the measured resistance determined as described in Section 4.4.

Photographs of the specimens after testing are given in Appendix B. It should be noted that in the process of being removed from the testing frame, the specimens were straightened to some extent.

Two types of failures were encountered in the column-base connection tests, excluding failure by excessive deformation of those specimens which struck the bottom of the loading frame prior to actual fracture of any component. One type of failure was a fracture of the bottom anchor bolt, which failed in ductile tension in two cases and by shearing of the threads in another. Large elongation of the anchor bolts occurred outside of the loading stub and therefore the bolts were subjected to high bending stresses as well as to shearing and tensile stresses. The other type of failure obtained in these tests was brittle fracture of the connection angle, which occurred both in web-angle tests and flange-angle tests, with the fracture located at the toe of the angle fillet on that leg of the angle adjacent to the base plate. Such failures were obtained only after much inelastic deformation of the critical angle had occurred, so that the energies absorbed by the connections in such cases were reduced little if any over those absorbed by similar specimens with completely ductile failure. The brittle fracture surface was in every case accompanied by a "shear lip" covering ten percent or so of the section area, predominately on the side at which the failure was initiated.

4.3 Beam-to-Column Connection Tests

4.3.1 Testing Program. The specimens tested in this portion of the investigation were representative of riveted and bolted beam-to-column connections found in steel frame buildings. The form of the specimens are shown in Figs. 9 and 9a and the testing program and some of the results are outlined in Table 3. Photographs of the specimens, taken after testing, are shown in Appendix B.

The loading stub, or column, in all connections was an 8WF35 section; the beams were 14WF34; and the fasteners were either 3/4 inch rivets or high tensile strength bolts. Three types of connection were used to attach the beams to the column flanges: (1) tees connected to the top and bottom flanges of the beam plus angles attached to the web (designated as T connection), (2) angles connected to the top and bottom flanges of the beam (designated as F connection), (3) angles connected to the web of the beam (designated as W connection). All connections were framed into the flanges of the loading stub. Rivets (R) were used as fasteners on half of the specimens of each type, and high tensile strength bolts (B) on the remainder.

Two identical specimens of each of the three types (1, 2, or 3) were fabricated with bolts as fasteners; one was loaded slowly (S), and the other rapidly (R). A similar set of two specimens of the same three types with rivets as fasteners was fabricated and tested in the same manner. Thus, 12 specimens were tested and the variables in the four tests of any one type of connection were the fasteners and the rate of loading.

As may be deduced from the letters given in parentheses above, the specimen and type of loading are identified by the designation based on the

following code: connection (C), type (T, F, or W), fastener (B or R), and manner of loading (S or R).

4.3.2 Results of Tests. The phenomena measured during each of the tests were lateral load, acceleration of the loading point (in rapid tests only) the deflections at various points along the length of the specimen, and strains in the connection angles, all of which were measured versus time. These quantities plotted as functions of time are presented in Appendix A, along with the measured resistance determined as described in Section 4.4. Photographs of the specimens after testing are shown in Appendix B.

All beam-to-column connections failed either by ductile fracture of the fasteners or by brittle fracture of the connection angles. Fastener failures were obtained only in riveted connections. In no case did a fracture of a high tensile strength bolt occur.

Brittle fracture of the bottom angle was obtained in both the slow and the rapid test in the top and seat angle bolted connections. As was the case in the column-base connection tests, the brittle fractures occurred after considerable inelastic deformation of the critical angles, so that the energy absorbed in these cases was comparable to that absorbed by similar specimens which failed in a completely ductile manner.

4.4 Comparison of Resistance-Deformation Characteristics

4.4.1 Determination of Resistances. The "measured" resistances of the specimens were determined by assuming that the deflection-time relationship obtained during the test considered could be approximated as that resulting from the application of the measured loading function to an equivalent single-degree-of-freedom system, the governing equation of which is

$$M\ddot{x} + Q(x) = F(t),$$

in which

M = the effective mass of the equivalent system

x = the displacement of the loading point

\ddot{x} = the acceleration of the loading point

$Q(x)$ = the "measured" resistance of the specimen, considered to be
a function of displacement only

$F(t)$ = the applied (measured) loading function

t = time

For all rapid tests, both $F(t)$ and \ddot{x} were measured; therefore, it was expected that $Q(x)$ could be obtained by using a reasonable value of M . The effective mass is by definition that mass which causes the equivalent system to have the same kinetic energy as the original system. The kinetic energy of the specimen was computed on the basis of the assumption that the beams underwent a rigid-bar rotation and that all of the angle-change was concentrated at the connections. Thus the acceleration of any point of the specimen was expressed as a function of the acceleration of the loading stub and the total kinetic energy of the system was computed. Equating the kinetic energy of the specimen with that of the equivalent system yields the effective mass. For the slow tests, it was assumed that accelerations were negligible, so that $Q(x) = F(t)$.

In every rapid test, the record produced by the output of the accelerometer was quite erratic and the results seemed unreliable. Therefore, the accelerations were calculated by twice differentiating the center point deflection-time curve measured during the test considered. The differentiation was accomplished by visual estimation of the slope of the

deflection-time curve at a number of points. These values were then plotted versus time as a velocity-time relationship. This curve was integrated by use of a polar planimeter and the results compared with the original deflection-time curve. Necessary adjustments were made in the velocity-time graph so that the curves were compatible. The differentiation process was repeated on the velocity-time curve, thereby obtaining accelerations as a function of time. Using these accelerations and the data obtained from the load time curve, the resistance, $Q(x)$, of the specimen could be computed as previously outlined.

4.4.2 Comparison of Resistance Deformation Characteristics. The results of the column-base connection tests are presented in two ways: (1) curves which express the specimen resistance to lateral deformation versus the corresponding midspan deflection; (2) curves which express the total resisting moment versus the beam rotation. These curves are presented in Figs. 13 through 20, with the corresponding slow and rapid test results shown on the same graph.

In computing the rotations for the moment-rotation curves, it was assumed that the beams underwent rigid bar rotations, i.e., that rotation is the midspan lateral deflection divided by the distance between the reaction and the face of the loading stub. The acceptability of this assumption was verified, within limits of experimental error, by comparing at a gage point away from the center of the specimen the deflection computed from the measured center deflection with the deflection measured at that point during tests. Data concerning the center of rotation were not considered to be worth the difficulties associated with its determination.

The results of the beam-to-column connection tests are presented in Figs. 21 through 26 in the form of curves expressing resisting moment

versus rotation of the beams. The same assumptions used in the column-base connection curves were used in computing the rotations for the beam-to-column connection curves.

Oscillations, in some cases quite violent, were obtained in the applied load versus time records. Therefore, in computing the resistances of the various specimens, a smooth curve was passed through the measured curve and the approximation used in computing the resistances of the connections, as is shown for example in Appendix A, Fig. A 15a.

The first specimen tested rapidly in the column-base connection series, CB2, was subjected to an arbitrary load which did not cause failure. Application of a second and higher load resulted in an anchor bolt fracture.

No deflection records were obtained from tests CB5 due to a malfunction of the oscillographic equipment.

4.4.3 Empirical Relationships for Slow Deformation Tests. As was mentioned earlier in this report, Prof. Johnston and his associates at the University of Michigan have determined empirical relationships which fit well some of the data published on beam-to-column connections¹². For top and seat angle connections, web angle connections, and top and bottom tee connections, they have suggested a relationship of the form:

$$M = X \log_{10} (Y \phi + 1)$$

in which

M = moment

ϕ = rotation.

Using the considerable amount of data available for top and seat angle connections, they have related the parameters X and Y to beam depth and top

angle (the bottom angle in the tests reported herein) thickness, two of the more important factors in the behavior of such connections. A correction factor for the area of top angle rivets is included for use in determining the proper value of the parameter X .

For use with connections having top and bottom tees, they suggest, on the basis of one series of tests, a constant value of Y and an expression for X which includes the area of the tension rivets in the critical tee and the depth of the beam.

They do give values of the parameters X and Y for a typical web angle connection, but indicate that the data available are insufficient to permit distinction between the effects of variables because of the great experimental scatter in test results for this type of connection.

Values of the parameters X and Y in the relationships given above were computed to fit the results obtained from the slow loading tests of the top and seat angle, and top and bottom tee with web angle connections tested as a part of this program. These relationships with the values of the parameters given are presented in Figs. 21, 22, 25 and 26. Because of the shape of the moment-rotation curves obtained in tests of the web angle connections where eventual contact of the beam flanges with the column caused a considerable increase in resistance, no attempt was made to fit the relationship used above to these test results. Also, this relationship was not applicable to the test results for the column-base connections which had constant axial thrust with consequent eventual decay in measured resistance to lateral deformation. Such a relationship could probably be used for the total moment resistance of the column-base connection, including that resulting from the axial force. However, that was not done in this investigation.

4.5 Comments on Connection Behavior and Material Properties

Because of the many materials comprising each connection specimen, it was not possible within the limited time and funds available to determine material properties completely. However, "static" mechanical properties were determined for some of the angles used. The results obtained were typical for ASTM A-7 steel formed into sections of these types, and, therefore, are not included in this report.

A brief investigation of the possibility of estimating the increase in resistance of a connection to be expected under rapid deformation, by using delayed yielding and rate of yielding information²⁰ typical of mild steel, was not successful, mainly because of the difficulty in estimating the rates of straining at critical locations in the connection considered. However, on the basis of the experimental results obtained in the connection tests and the rate of general yielding information mentioned above, it can be said that the governing rates of straining in the rapid tests were on the order of 0.1 to 1.0 in./in./sec. In general, the resistance of the column-base and beam-to-column connections to rapid lateral load was somewhat higher than the resistance corresponding to slow loading. However, the rapid load resistance of the column-base connections was not consistently higher than the slow load resistance, as was the case for the beam-to-column connections. Undoubtedly the presence of the axial load in the case of the column base connection served to alter the resistance pattern. In any case, on the basis of the information presented in this report, it does not seem possible to do more than only roughly estimate the nature of resistance function which could be expected for connections of the type tested. However, this in itself is of considerable value since no

results were previously available. Until such time as additional data become available, the information presented herein should be of value in evaluating the nature of the resistance of connections similar to the type tested.

BIBLIOGRAPHY

1. American Bridge Company, "Beam Connection Tests" American Bridge Company, 1908.
2. Columbia University, "Report of Compression Tests on Riveted and Welded Beam Connections" Report No. 2193, Department of Civil Engineering, Columbia University, March 1920.
3. Edwards, J. H., Whittemore, H. C., and Stang, A. H., "Compressive Tests of Bases for Subway Columns" MBSJ Research, Vol. 5, p. 619, 1930.
4. Johnston, B. G. and Godfrey, H. J., "Analysis of Lehigh University Tests of Beam-Column Connections" Lehigh University Tests for Bethlehem Steel Company, October 1940.
5. Graham, H. E., "Strength of Steel Anchors in Concrete" Engineering News Record, Vol. 130, pp. 560-1, April 1943.
6. Hechtman, R. A., and Johnston, B. G., "Riveted Semi-Rigid Beam-to-Column Building Connections" AISC Publication No. 206, November 1947.
7. Beaufroy, L. A., and Muharram, A., "Derived Moment-Angle Curves for Web-Cleat Connection" Third Congress, International Association of Bridge and Structural Engineering - Preliminary Publication, Vol. III, pp. 105-18, 1948.
8. Lothers, J. E., "Elastic Restraint Equations for Semi-Rigid Connections" Proceedings Amer. Soc. of Civ. Eng., Vol. 76, No. 5, February 1950.
9. Hu, L. S., Byce, R. C., and Johnston, B. G., "Steel Beams, Connections, Columns, and Frames" Engineering Research Institute, University of Michigan, March 1952.
10. Johnston, B. G., "Structural Steel Members and Frames", Proc. on Earthquake and Blast Effects on Structures, Earthquake Engineering Research Institute and Univ. of Calif., Los Angeles, Calif., June 1952, p. 148.
11. Newmark, N. M., and Chan, S. P., "A Comparison of Numerical Methods for Analyzing the Dynamic Response of Structures," Univ. of Ill. Civil Engr. Studies, Struct. Res. Series No. 36, October 1952.
12. Schenker, L., Salmon, C. G., Johnston, B. G., "Structural Steel Connections" University of Michigan Tech. Report No. 352 to AFSWP, June 1954.
13. Thomson, W. T., "Plastic Behavior of Beams Under Long Duration Impulsive Loads," Univ. of Calif., Los Angeles, Dept. of Engr., Rept. 54-92, October 1954, ASTIA AD 52844.

14. Howland, F. L., "Inelastic Behavior of Mild Steel Beams Subjected to Transverse Impact," Univ. of Ill. Civil Engr. Studies, Struct. Res. Series No. 106, Contract AF 33(616)-170, August 1955.
15. Mayerjak, R. J., "A Study of the Resistance of Model Frames to Dynamic Lateral Load," Univ. of Ill. Civil Engr. Studies, Struct. Res. Series No. 108, August 1955.
16. Adams, R. F., "Some Factors Which Influence the Strength of Bolt Anchors in Concrete" Journal Amer. Conc. Inst., Vol. 27, No. 2, October 1955.
17. Ang, A. and Massard, J. M., "A Method for the Analysis of Frames Subjected to Inelastic Deformation into the Range of Strain Hardening", Univ. of Ill. Tech. Report AFSWC-TR-56-47 under Contract AF 33(616)-170, November 1956.
18. Ang, A., "A Method for the Analysis of Frames Subjected to Inelastic Deformation into the Range of Strain Hardening", M. S. Thesis, Univ. of Ill., Feb. 1957.
19. McDonald, D., "Tests of Column-Base Connections Under Slow and Rapid Loading", M. S. Thesis, Univ. of Ill., June 1957.
20. Wojcieszak, R. F., and Massard, J. M., "Slow and Rapid Lateral Loading Tests of Simply Supported Beams and Beam-Columns" Univ. of Ill., Technical Report AFSWC-TR-57-21, Contract AF 33(616)-170, June 1957.
21. Egger, W., "60 Kip Capacity Slow or Rapid Loading Apparatus", Univ. of Ill., Technical Report AFSWC-TR-57-22, Contract AF 33(616)-170, June 1957.

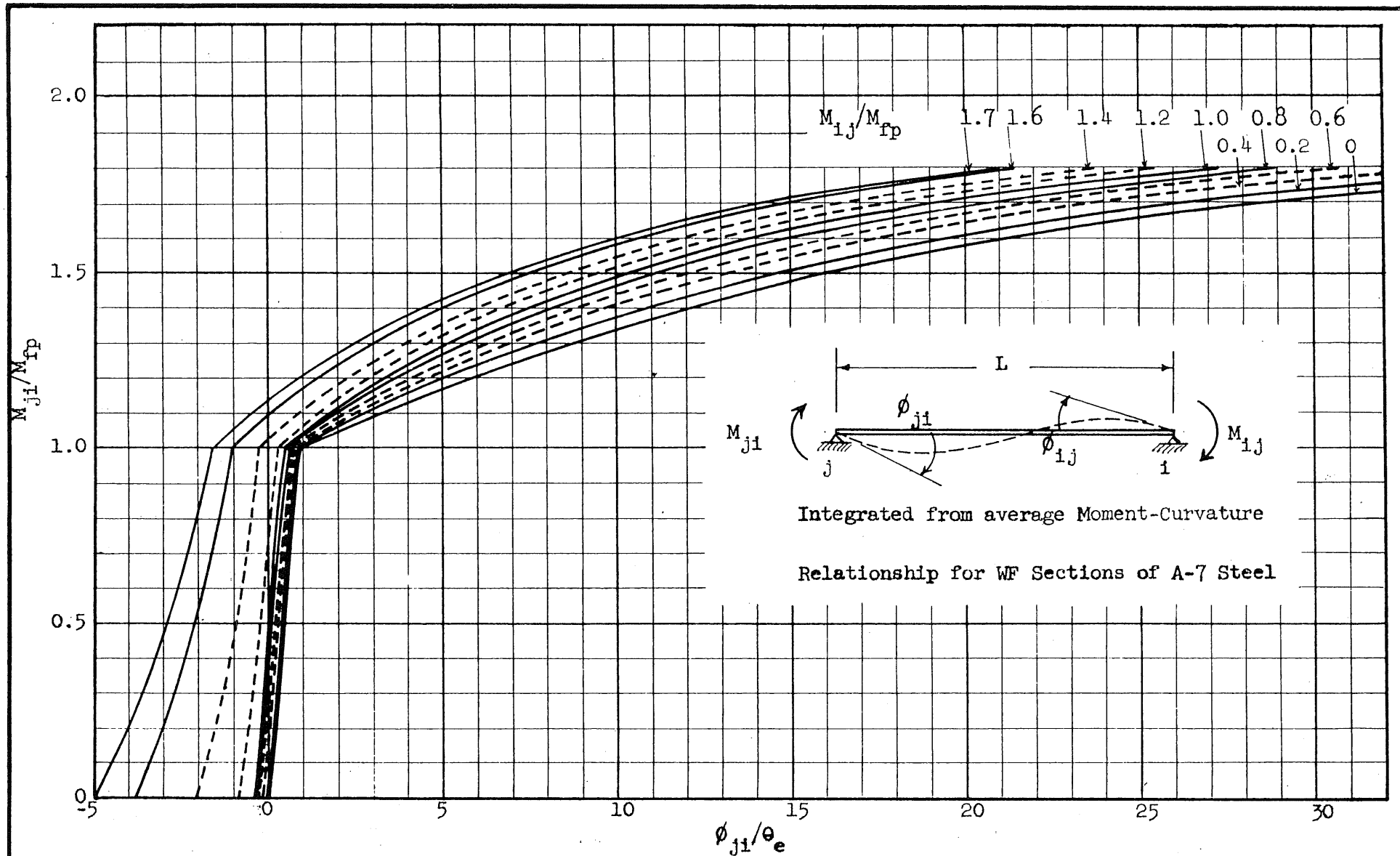


FIG. 1a: MOMENT-END SLOPE RELATIONSHIPS FOR WF SECTIONS OF ASTM A7 STEEL (For member with contraflexure)

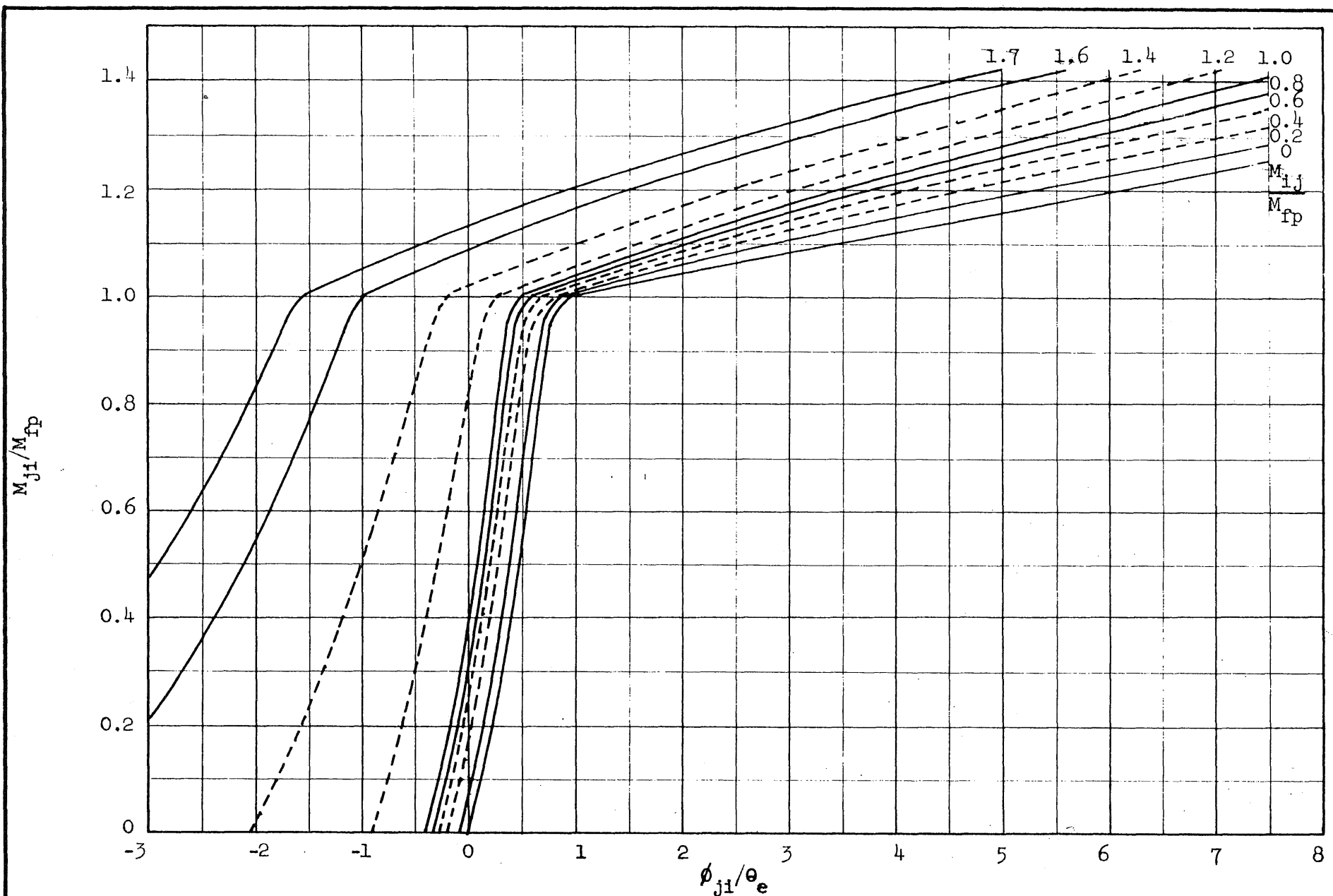


FIG. 1b: MOMENT-END SLOPE RELATIONSHIPS FOR WF SECTIONS OF ASTM A7 STEEL (For member with contraflexure)

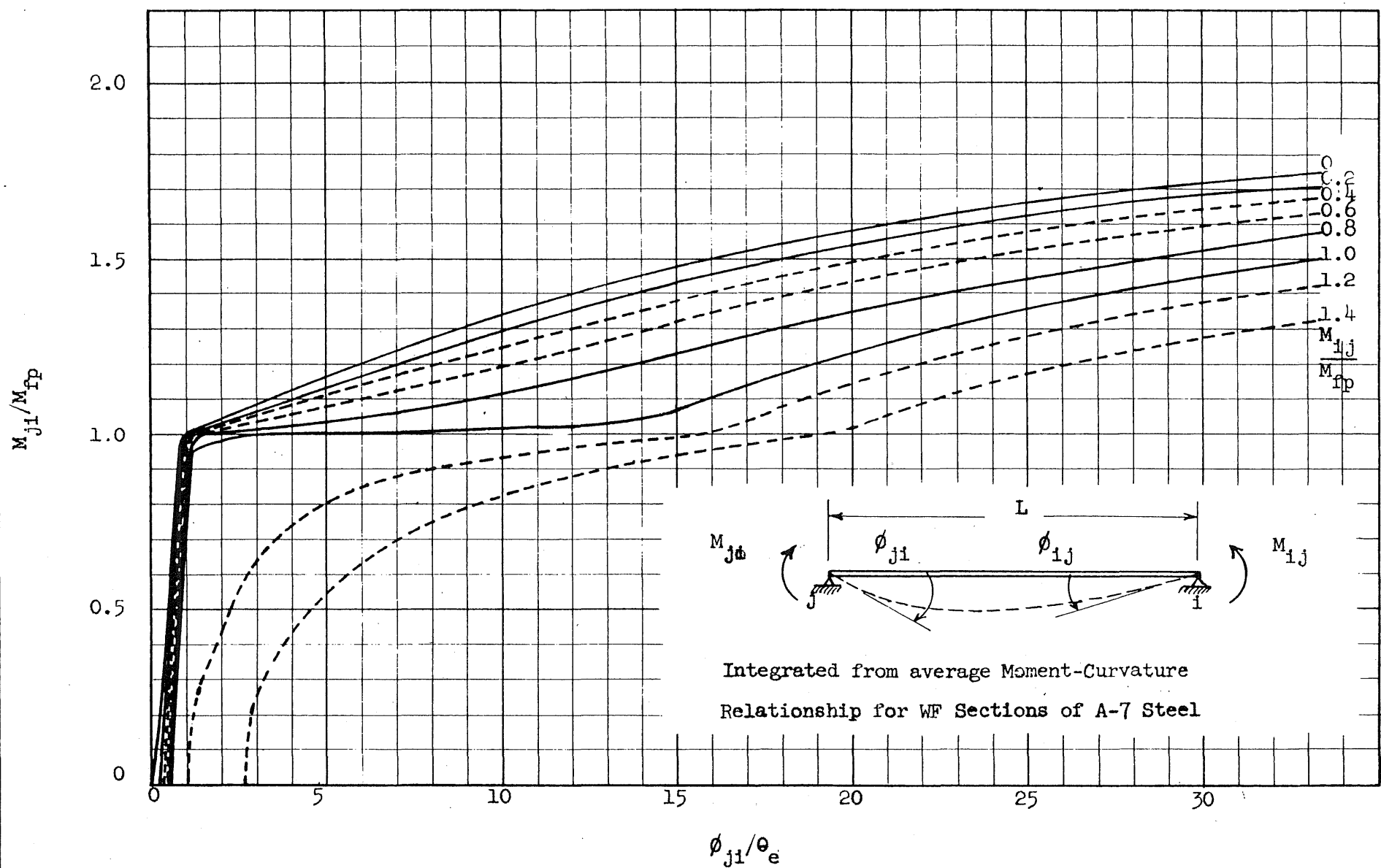


FIG. 2: MOMENT-END SLOPE RELATIONSHIPS FOR WF SECTIONS OF ASTM A7 STEEL (For member without contraflexure)

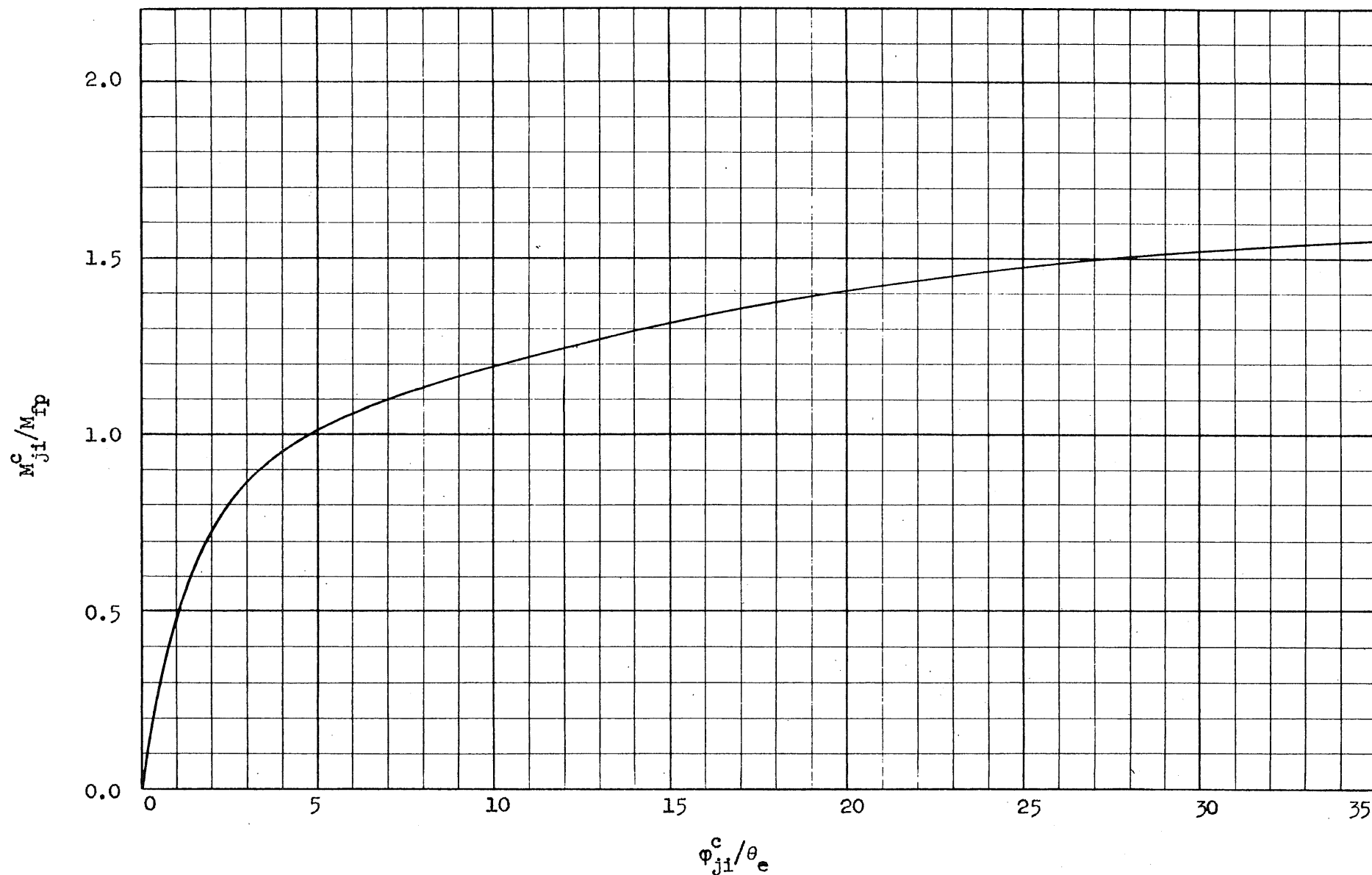


FIG. 3: ASSUMED MOMENT-ROTATION RELATIONSHIP OF BEAM-TO-COLUMN CONNECTIONS

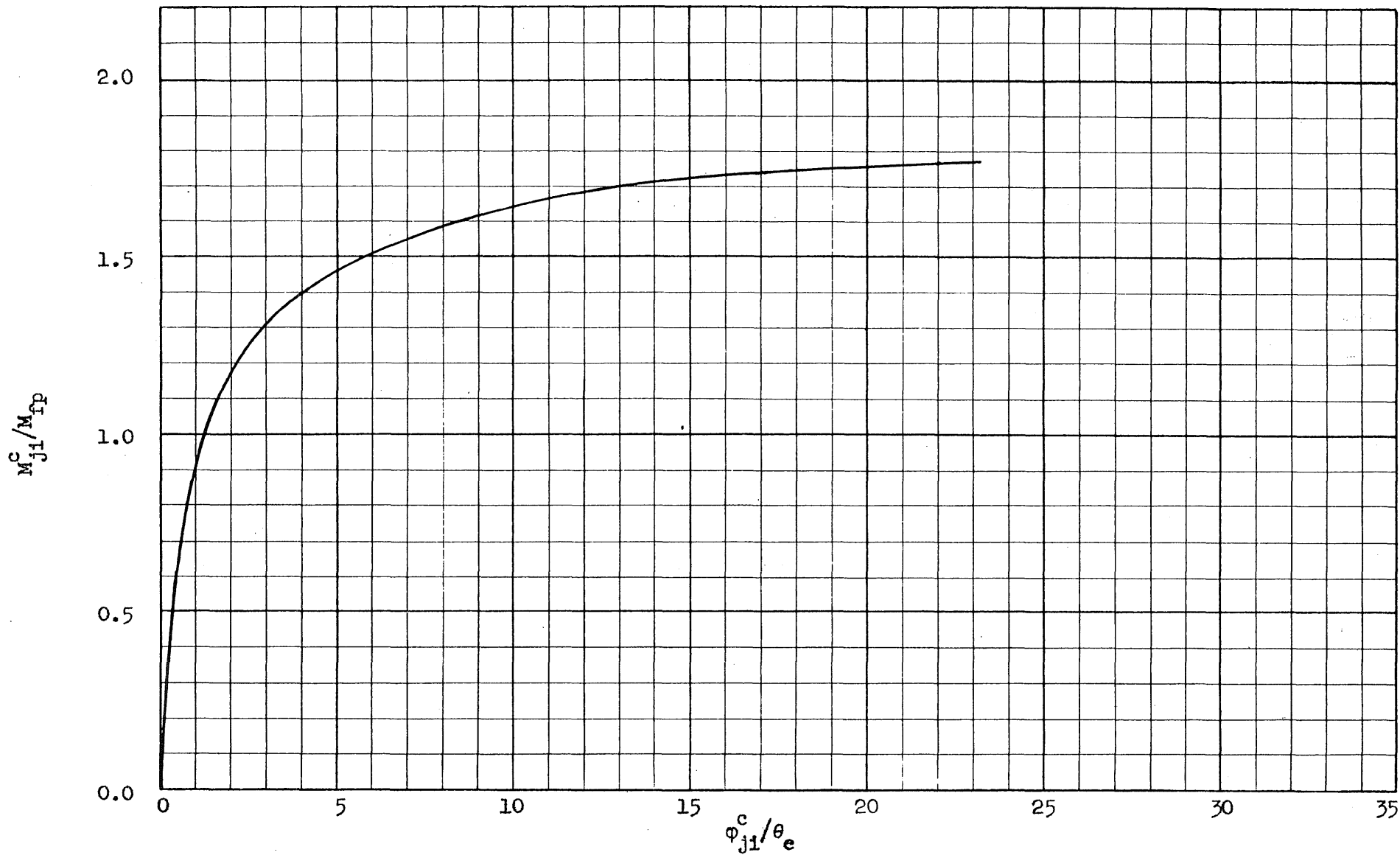


FIG. 4: ASSUMED MOMENT-ROTATION RELATIONSHIP OF COLUMN-BASE CONNECTIONS

TABLE 1

COMPUTATION OF RESISTING MOMENTS FOR EXAMPLE PROBLEM

Cycle No. 1:

Joint	ji	$\frac{M_{ji}}{M_{fp}^o}$		$\frac{\phi_{ji}}{\theta_e^{ji}}$	$\frac{\phi_{ji}^c}{\theta_e^{ji}}$	Rotation at Joint	
						$\div \theta_e^{ji}$	$\div \theta_e^o$
A	AB	Ass. 1.30	1.30	6.70	2.80	-	-
		Ass. 1.28	1.28	6.10	2.70	-	-
		Ass. 1.29	<u>1.29</u>	6.35	2.80	-	-
B	BA	Ass. 0.60	0.60	-0.45	0	9.71	9.71
	BC	Impossible		-2.30	0	9.71	9.71
B	BA	Ass. 1.10	1.10	1.25	0	8.01	8.01
	BC	Impossible		-0.60	0	8.01	8.01
B	BA	Ass. 1.13	<u>1.13</u>	1.70	0	7.56	7.56
	BC	0.18	<u>0.18</u>	-0.15	0	7.56	7.56
	BE	1.31	<u>1.03</u>	0.85	5.20	6.05	7.73
C	CB	Ass. 1.00	<u>1.00</u>	0.90	0	6.57	6.57
	CD	1.00	<u>1.00</u>	0.75	4.60	5.35	6.84
D	DC	Ass. 0.50	0.50	0.05	1.00	1.05	1.05
	DG	0.48	0.48	0.10	0.95	1.05	1.05
	DE	0.98	0.98	0.40	0	7.01	5.48
D	DC	Ass. 0.60	0.60	0.12	1.35	1.47	1.47
	DG	0.59	0.59	0.19	1.30	1.49	1.49
	DE	1.19	1.19	3.20	0	4.21	3.29
D	DC	Ass. 0.65	<u>0.65</u>	0.15	1.60	1.75	1.75
	DG	0.64	<u>0.64</u>	0.23	1.50	1.73	1.73
	DE	1.29	<u>1.29</u>	5.05	0	2.36	1.85
E	ED	Ass. 1.20	1.20	2.65	0	4.76	4.76
	EF	1.14	1.14	4.50	0	4.76	4.76
	EB	1.15	0.91	0.30	3.40	3.70	4.73
	EH	1.19	0.94	0.35	3.80	4.15	5.30
E	ED	Ass. 1.19	<u>1.19</u>	2.50	0	4.91	4.91
	EF	<u>1.135</u>	<u>1.135</u>	4.35	0	4.91	4.91
	EB	1.165	<u>0.92</u>	0.33	3.50	3.83	4.89
	EH	1.16	<u>0.915</u>	0.30	3.50	3.80	4.86

TABLE 1 (Continued)

Joint	ji		$\frac{M_{ji}}{M_{fp}^O}$	$\frac{M_{ji}}{M_{fp}^{ji}}$	$\frac{\phi_{ji}}{\theta_e^{ji}}$	$\frac{\phi_{ji}^c}{\theta_e^{ji}}$	Rotation at Joint	
							$\div \theta_e^{ji}$	$\div \theta_e^O$
G	GH	Ass.	1.00	1.00	0.45	0	6.96	6.96
	GD		1.00	1.00	0.65	4.60	5.25	6.71
G	GH	Ass.	1.01	<u>1.01</u>	0.55	0	6.86	6.86
	GD		1.01	<u>1.01</u>	0.75	4.80	5.55	7.09
H	HG	Ass.	1.10	1.10	1.80	0	5.61	5.61
	HJ		1.11	1.11	3.65	0	5.61	5.61
	HE		1.22	0.96	0.42	4.00	4.42	5.65
	HK		0.99	0.78	0.25	2.20	2.45	3.13
H	HG	Ass.	1.15	1.15	2.55	0	4.86	4.86
	HJ		1.135	1.135	4.40	0	4.86	4.86
	HE		1.16	0.915	0.37	3.50	3.87	4.94
	HK		1.125	0.89	0.30	3.20	3.50	4.47
H	HG	Ass.	1.16	<u>1.16</u>	2.75	0	4.66	4.66
	HJ		1.145	<u>1.145</u>	4.65	0	4.65	4.65
	HE		1.14	<u>0.90</u>	0.35	3.30	3.65	4.66
	HK		1.165	<u>0.92</u>	0.33	3.50	3.83	4.89
K	KL	Ass.	1.10	1.10	1.80	0	7.46	7.46
	KH		1.10	0.87	0.35	3.00	3.35	4.28
K	KL	Ass.	1.15	1.15	2.60	0	6.66	6.66
	KH		1.15	0.91	0.37	3.40	3.77	4.82
K	KL	Ass.	1.20	1.20	3.40	0	5.86	5.86
	KE		1.20	0.95	0.40	3.90	4.30	5.50
K	KL	Ass.	1.21	<u>1.21</u>	3.60	0	5.66	5.66
	KE		1.21	<u>0.95</u>	0.40	3.90	4.30	5.50
L	LK	Ass.	1.30	1.30	4.60	2.80	-	-
	LK	Ass.	1.35	1.35	6.25	3.40	-	-
	LK	Ass.	1.34	<u>1.34</u>	6.10	3.20	-	-

TABLE 1 (Continued)

Cycle No. 2:

Joint	ji	$\frac{M_{ji}}{M_{fp}^O}$		$\frac{\varphi_{ji}}{\theta_e^{ji}}$		Rotation at Joint	
		Ass.				$\div \theta_e^{ji}$	$\div \theta_e^O$
A	AB	Ass.	1.30	1.30	4.90	2.80	-
	AB	Ass.	1.35	<u>1.35</u>	5.90	3.30	-
B	BA	Ass.	1.15	1.15	1.75	0	7.51
	BC		0.31	0.31	-0.10	0	7.51
	BE		1.46	1.15	1.75	8.30	10.05
B	BA	Ass.	1.13	1.13	1.50	0	7.76
	BC		0.06	0.06	-0.35	0	7.76
	BE		1.19	0.94	0.40	3.80	4.20
B	BA	Ass.	1.14	<u>1.14</u>	1.60	0	7.66
	BC		0.15	<u>0.15</u>	-0.25	0	7.66
	BE		1.29	<u>1.02</u>	0.75	5.00	5.75
C	CB	Ass.	1.00	<u>1.00</u>	0.90	0	6.51
	CD		1.00	<u>1.00</u>	0.65	4.60	5.25
D	DC	Ass.	0.65	0.65	0.15	1.60	1.75
	DG		0.65	0.65	0.15	1.60	1.75
	DE		1.30	1.30	4.70	0	2.71
D	DC	Ass.	0.66	<u>0.66</u>	0.16	1.60	1.76
	DG		0.66	<u>0.66</u>	0.16	1.60	1.76
	DE		1.32	<u>1.32</u>	5.10	0	2.31
E	ED	Ass.	1.20	<u>1.20</u>	2.60	0	4.81
	EF		1.14	<u>1.14</u>	4.45	0	4.81
	EB		1.17	<u>0.92</u>	0.30	3.50	3.80
	EH		1.17	<u>0.92</u>	0.37	3.50	3.87
G	GH	Ass.	1.01	<u>1.01</u>	0.40	0	7.01
	GD		1.01	<u>1.01</u>	0.75	4.80	5.55
H	HG	Ass.	1.16	<u>1.16</u>	2.75	0	4.66
	HJ		1.145	<u>1.145</u>	4.65	0	4.65
	HE		1.14	<u>0.90</u>	0.35	3.30	3.65
	HK		1.165	<u>0.92</u>	0.35	3.50	3.85
K	KL	Ass.	1.21	<u>1.21</u>	3.60	0	5.66
	KH		1.21	<u>0.95</u>	0.40	3.90	4.30

TABLE 1 (Continued)

Cycle No. 3:

The far end moments of all joints did not have significant changes from those of Cycle No. 2; therefore, the results of Cycle No. 2 are correct.

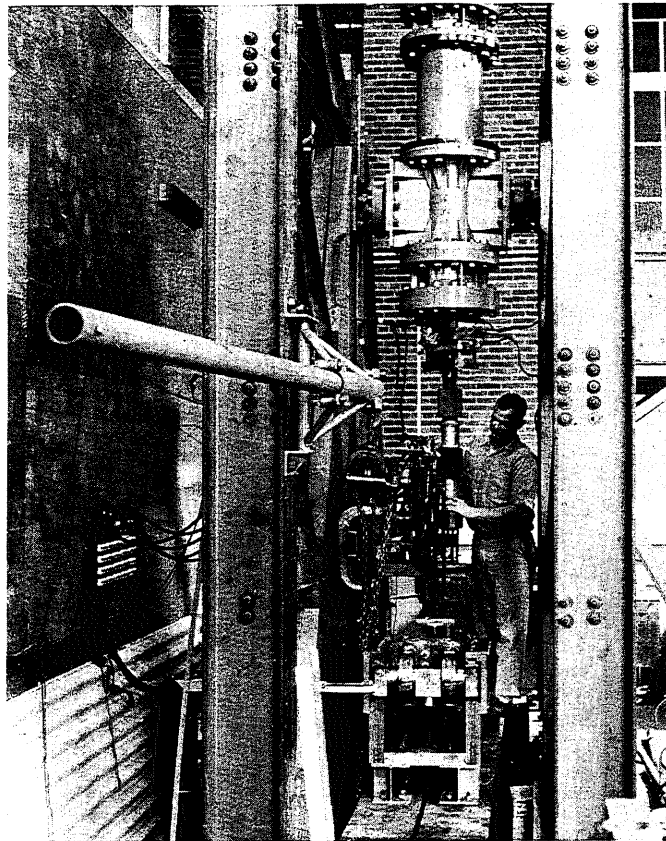


FIG. 5 GENERAL VIEW OF TESTING APPARATUS

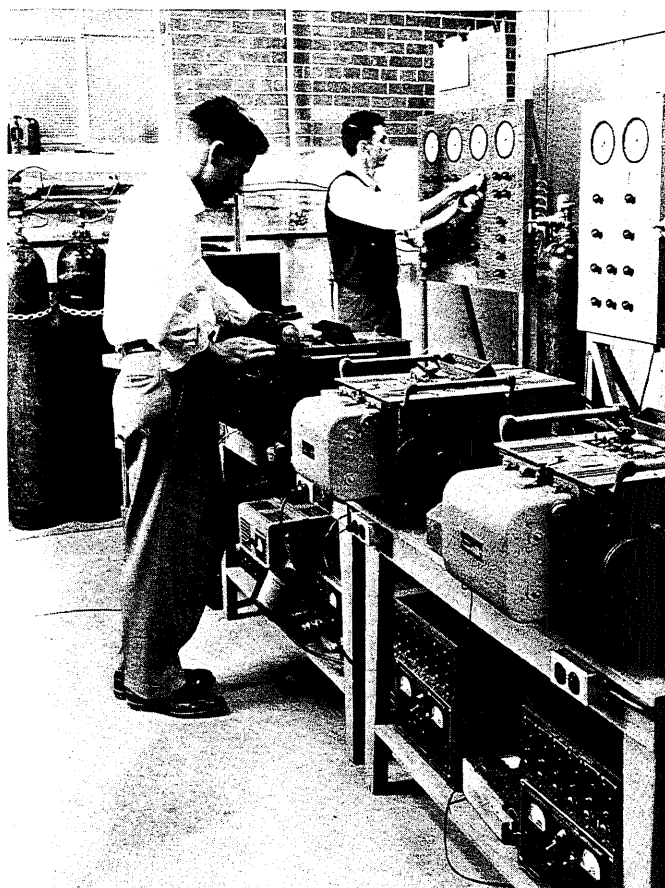


FIG. 6 . VIEW OF INSTRUMENTS AND PRESSURE PANEL

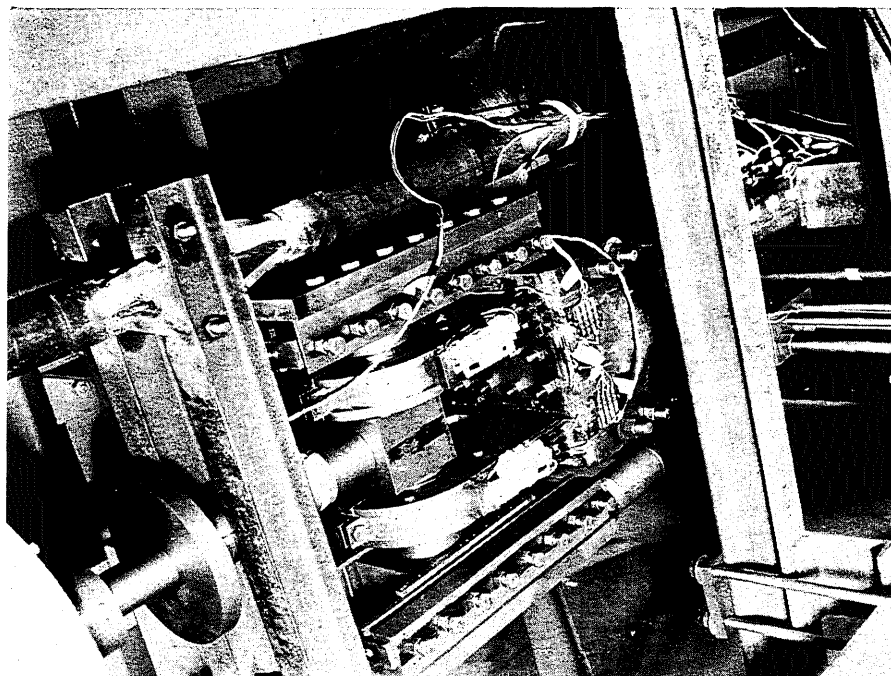


FIG. 7 VIEW OF AXIAL LOADING AND END REACTION SYSTEM

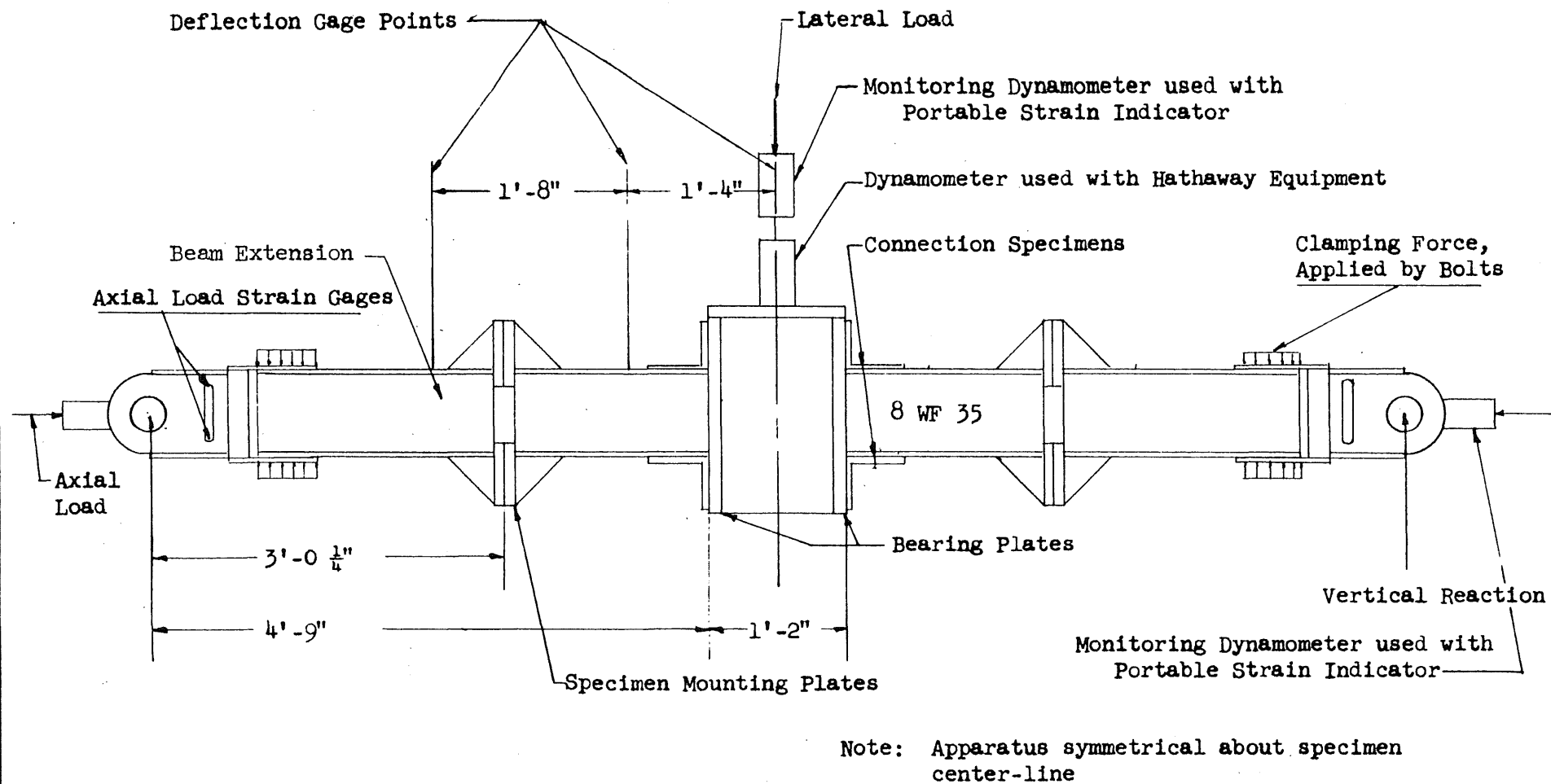
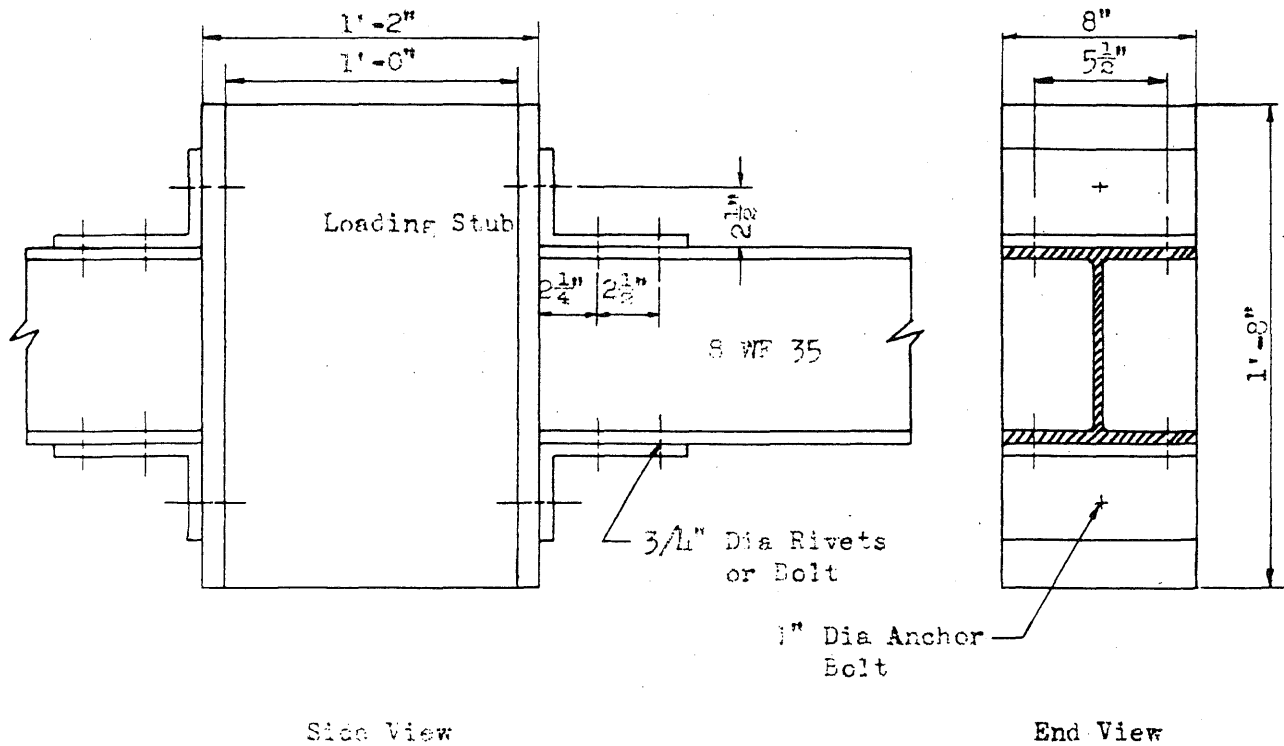
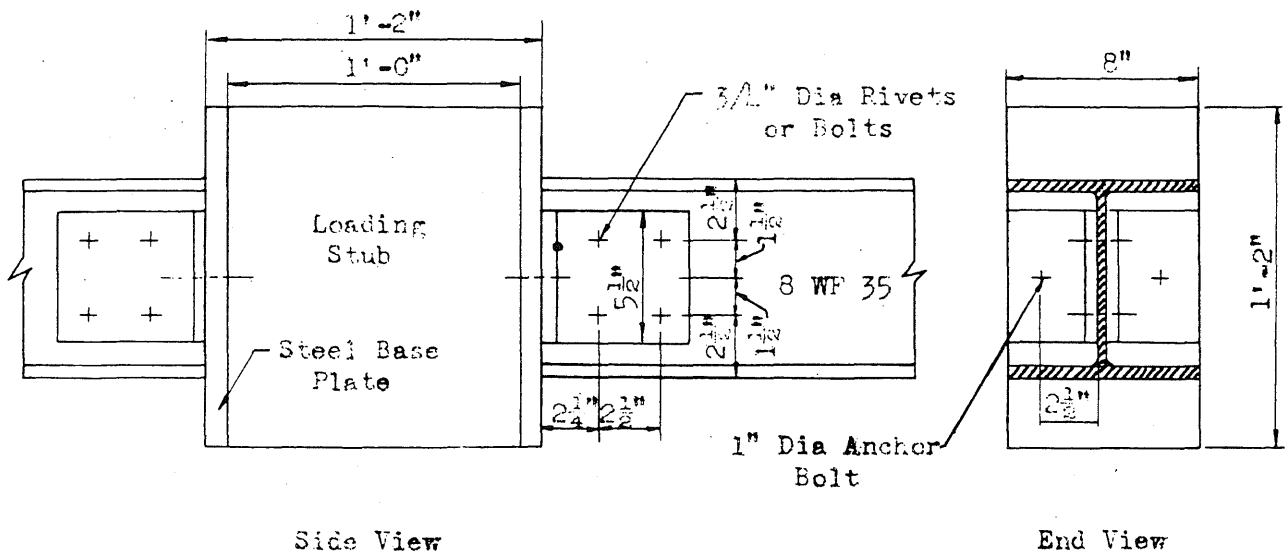


FIG. 8: SCHEMATIC DRAWING OF TESTING ARRANGEMENT FOR COLUMN-BASE CONNECTIONS



Scale $1\frac{1}{2}" = 1'0"$

Fig. 8a. Details of Column Base Connections

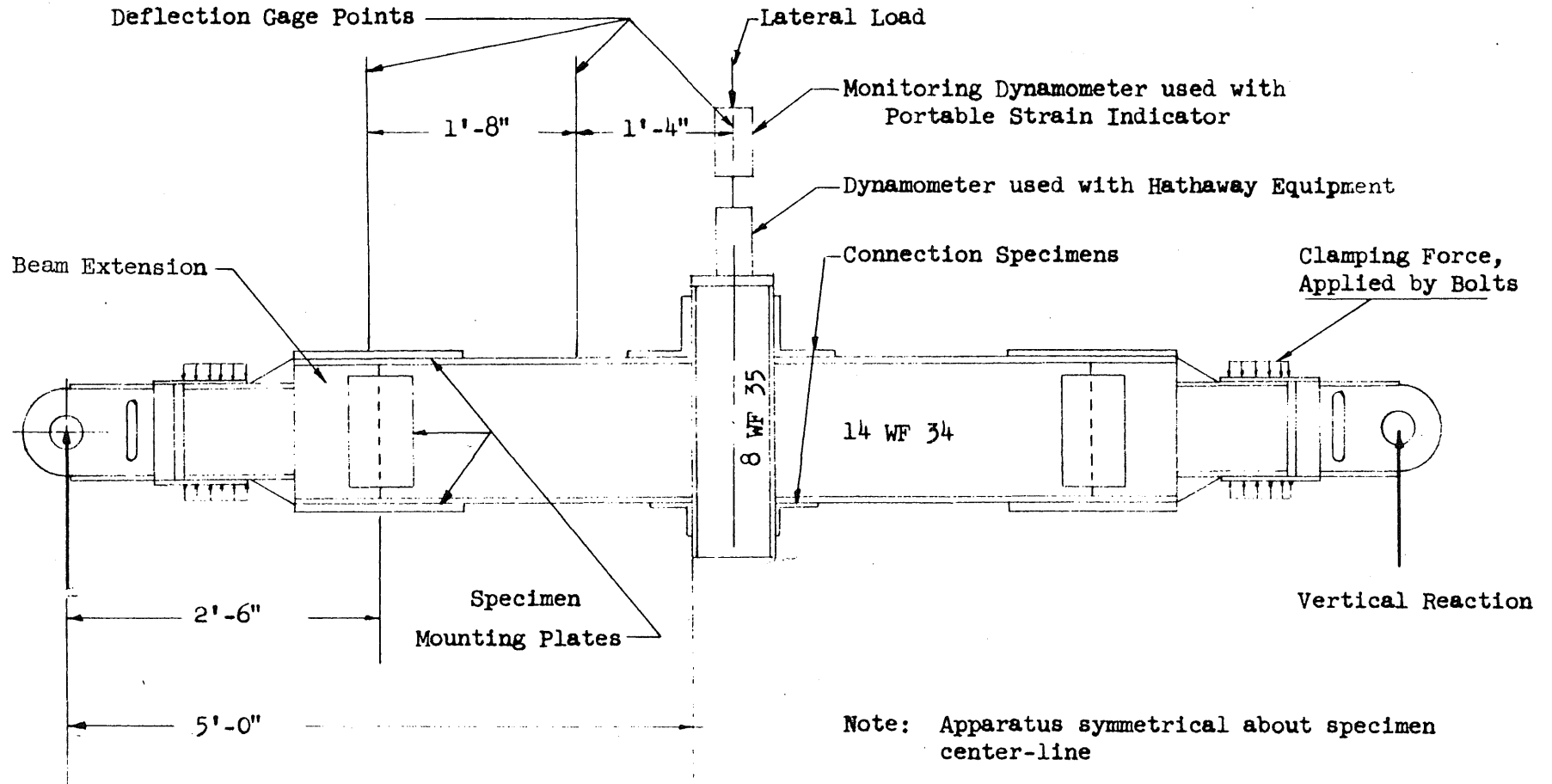
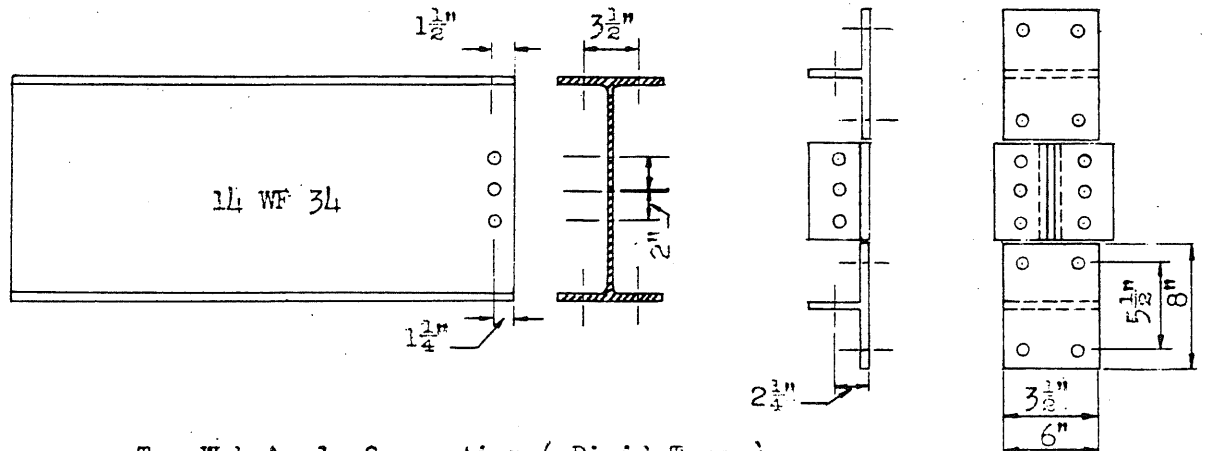
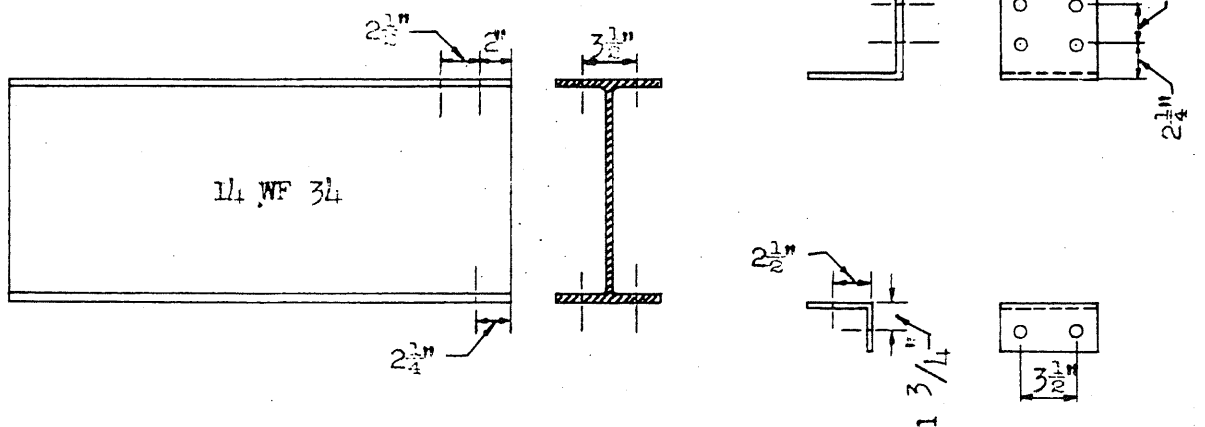


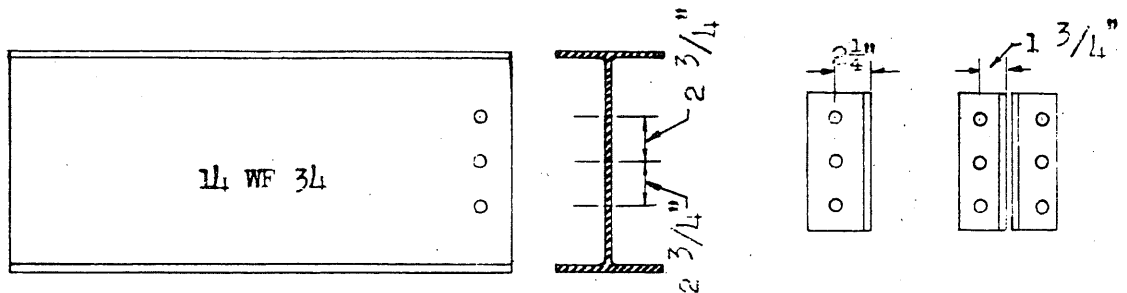
FIG. 9: SCHEMATIC DRAWING OF TESTING ARRANGEMENT FOR BEAM-TO-COLUMN CONNECTIONS



Tee Web Angle Connection (Rigid Type)



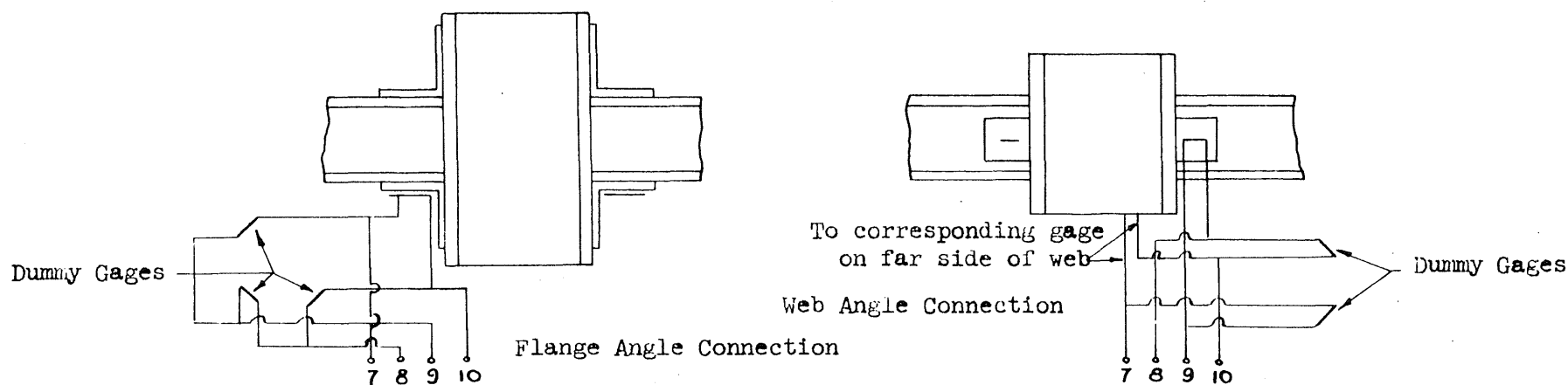
Top and Seat Angle Connection (Semi Rigid Type)



Web Angle Connection (Flexible Type)

Scale 1" = 1'-0"

Fig. 9a Details of Beam-To-Column Connections



No. 7 is ground.

All gages for each type of connection are wired similarly

Gage 1 is active, gages 2, 3, and 4 are dummies in flange-angle connection tests. Gages 1 and 3 are active, gages 2 and 4 are dummies in web-angle connection tests.

A total of 5 channels of strain equipment used:

- 2 for strain measurement
- 1 for lateral load measurement
- 2 for reaction measurements

Standard Hathaway MRC 18 unit modified to reduce cross-talk between channels and to provide carrier supply oscillator with approximately 0.01 per cent regulation.

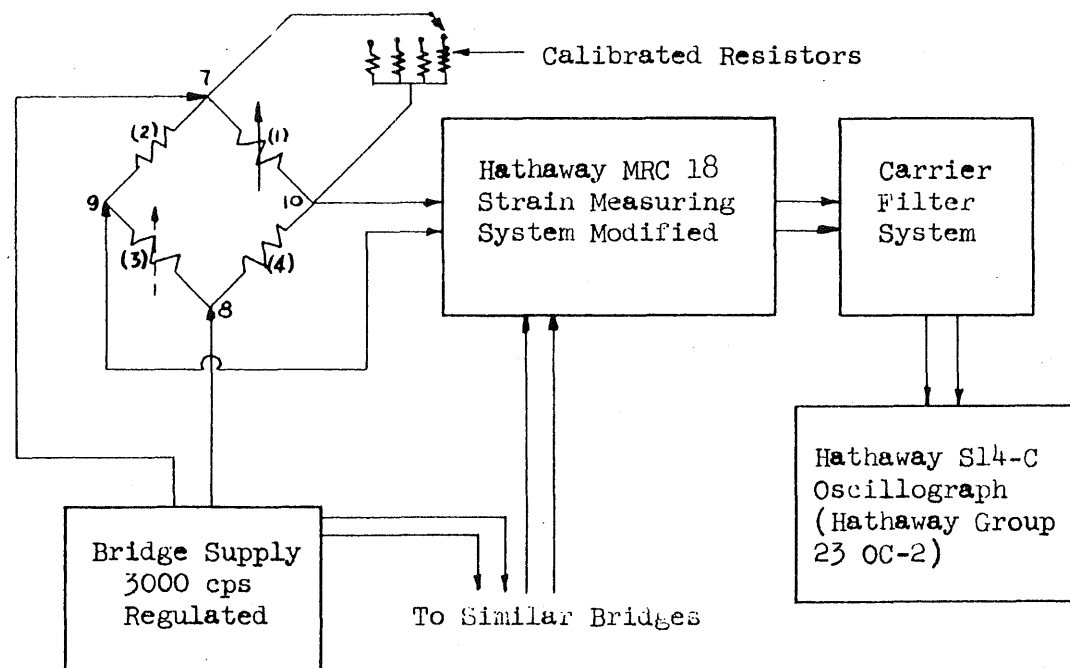


FIG. 10a: WIRING DIAGRAM FOR SR-4 STRAIN BRIDGES - COLUMN BASE CONNECTIONS

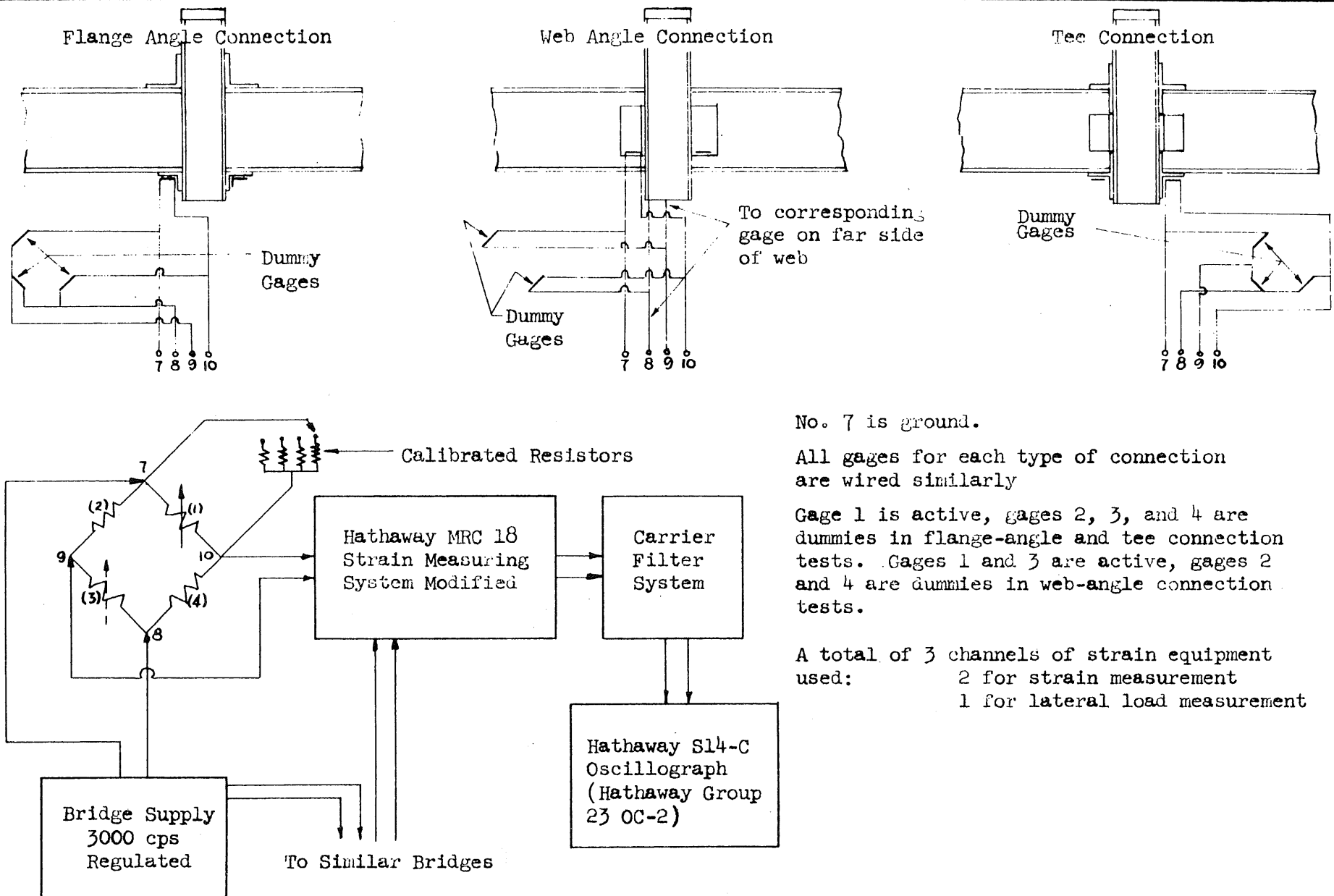
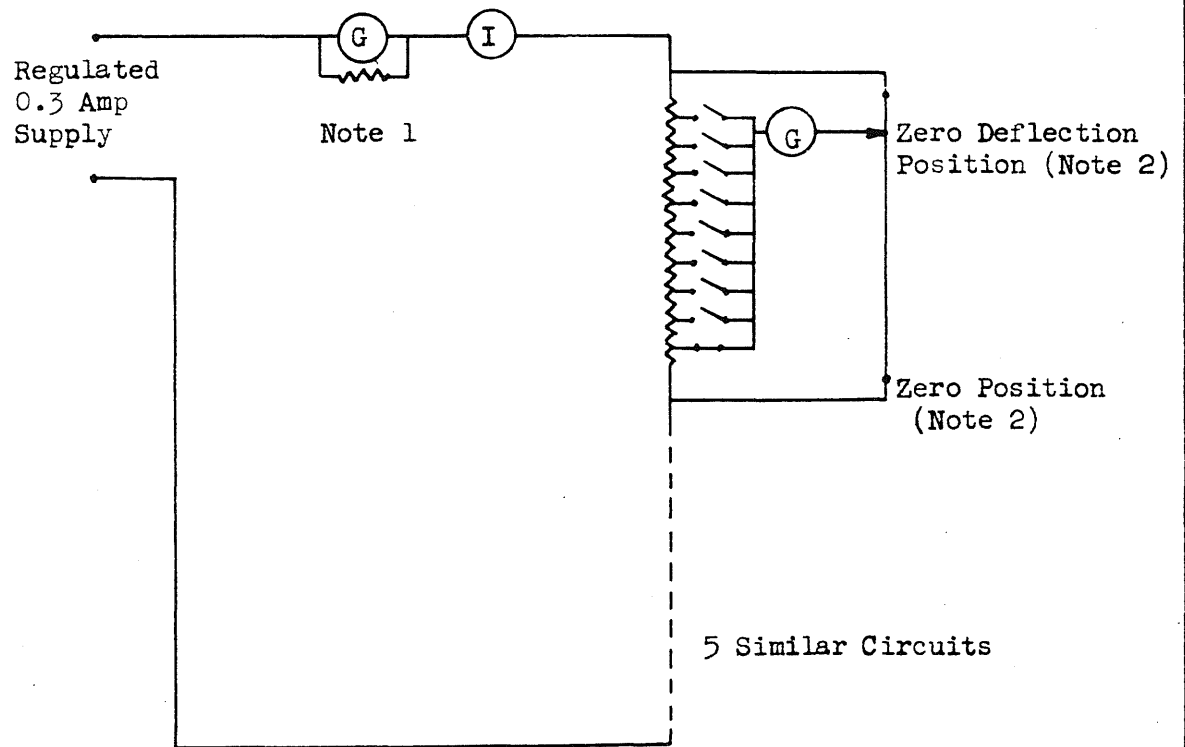


FIG. 10b: WIRING DIAGRAM FOR SR-4 STRAIN-BRIDGES - BEAM-TO-COLUMN CONNECTIONS



Notes

1. Gage current measured during test with visual ammeter and recorded on separate recording galvanometer.
2. Calibration switches roughly correspond to 2 in deflection increments. At zero deflection, bridge circuit had maximum unbalance. Both calibration switches and slide deflection move bridge toward balance.

FIG.11: WIRING DIAGRAM FOR DEFLECTION GAGE

Monitoring dynamometer used with portable strain indicator

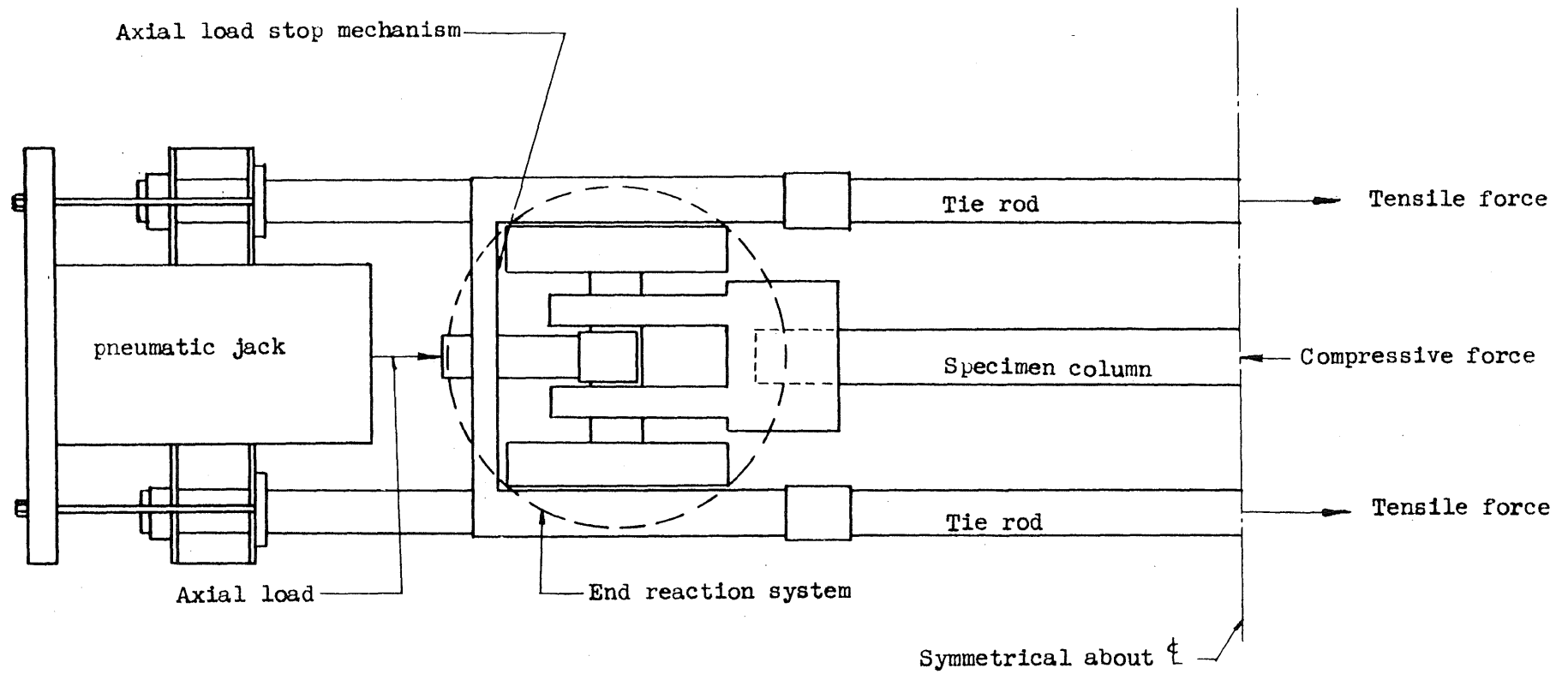


FIG. 12: SCHEMATIC DRAWING OF AXIAL LOAD TIE ROD SYSTEM

	Loading Data		Description of Specimens				Values of Phenomena Measured						
Test	Type of Loading	Testing Machine Used	Type of Connection	Connection Angle Section, AISC Designation	Type of Fastener	Type of Loading Stub	Rise Time to Maximum Lateral Load, sec.	Maximum Lateral Load, Kip	Nominal Axial Thrust, Kip	Maximum Load Point Acceleration, g.	Maximum Load Point Deflection, in.	Maximum Angle Strain, in./in.	Mode of Failure
CB1	Slow	Hydraulic Jack	Flange angle	6X6X1/2	Rivet 3/4"	Concrete	320	13.7	40	--	6.59	.0057	Brittle Fracture in connection angle
CB2-1	Rapid	Loading unit**	Flange angle	6X6X1/2	Rivet 3/4"	Concrete	0.022	14.4	34	21.7	2.5	.0029	No failure Reloaded (CB2-2)
CB2-2	Rapid	Loading unit**	Flange angle	6X6X1/2	Rivet 3/4"	Concrete	0.031	20.9	32	34.7	9.94	.0044	Tensile fracture in anchor bolt
CB3	Slow	Hydraulic jack	Flange angle	6X6X1/2	HTS bolt 3/4"	Metal	178	13.1	-	-	8.53	.0069	Specimen *** bottomed
CB4	Rapid	Loading unit**	Flange angle	6X6X1/2	HTS bolt 3/4"	Metal	0.023	18.9	32	38.6	9.00	.0019	Tensile fracture in anchor bolt
CB5	Slow	Hydraulic jack	Web angle	6X6X1/2	Rivet 3/4"	Concrete	60	8.4	43	-	-	.0056	Brittle Fracture in connection angle No defl. data
CB6	Rapid	Loading unit**	Web angle	6X6X1/2	Rivet 3/4"	Concrete	0.021	12.4	39	51.2	8.98	.0009	Nut sheared off of anchor bolt
CB7	Slow	Hydraulic jack	Web angle	6X4X1/2	HTS bolt 3/4"	Metal	219	8.7	38	-	8.25	.0020	Specimen *** bottomed
CB8	Rapid	Loading unit**	Web angle	6X4X1/2	HTS bolt 3/4"	Metal	0.019	12.6	44	44.9	8.80	.0005	Specimen *** bottomed

All columns were 8WF35; anchor bolts 1" ϕ

*Same specimen subjected to two loadings

**60 kip pulse loading unit

***Struck bottom of frame without failure

TABLE 2. SUMMARY OF COLUMN-BASE CONNECTION TESTS

Test	Loading Data		Description of Specimens				Values of Phenomena Measured					Mode of Failure
	Type of Loading	Testing Machine Used	Type of Connection	Connection Section, AISC Designation	Type of Fastener	Column Section AISC Designation	Rise Time to Maximum Lateral Load, secs.	Maximum Lateral Load, kip	Maximum Load Point Acceleration, g.	Maximum Load Point Deflection, ins.	Maximum Angle Strain, in./in.	
CTBS	Slow	Hydraulic jack	Tee + Web Angle	4 T 17.5 4x3 $\frac{1}{2}$ x $\frac{3}{8}$	HTS Bolt 3/4"	8 WF 35	346	37.1	—	7.32	0.0206	Specimen bottomed *
CTRS	Slow	Hydraulic jack	Tee + Web Angle	4 T 17.5 4x3 $\frac{1}{2}$ x $\frac{3}{8}$	Rivet 3/4"	8 WF 35	168	34.0	—	6.40	0.0032	Rivet sheared, web of top tee
CFBS	Slow	Hydraulic jack	Top and Seat Angle	6x6x $\frac{1}{2}$ 4x3x $\frac{3}{8}$	HTS Bolt 3/4"	8 WF 35	220	23.2	—	4.93	0.0254	Brittle fracture, bottom angle
CFRS	Slow	Hydraulic jack	Top and Seat Angle	6x6x $\frac{1}{2}$ 4x3x $\frac{3}{8}$	Rivet 3/4"	8 WF 35	156	18.6	—	4.15	0.0260	Ductile tension failure in rivet
CWBS	Slow	Hydraulic jack	Web Angle	4x3x $\frac{3}{8}$	HTS Bolt 3/4"	8 WF 35	396	20.2	—	6.91	0.0242	Jack reached full stroke
CWRS	Slow	Hydraulic jack	Web Angle	4x3x $\frac{3}{8}$	Rivet 3/4"	8 WF 35	256	18.6	—	7.32	0.0124	Jack reached full stroke

All beams were 14 WF 34 Sections

* Struck bottom of frame without failure

TABLE 3a: SUMMARY OF BEAM-TO-COLUMN CONNECTION TEST RESULTS

Test	Loading Data		Description of Specimens				Values of Phenomena Measured					Mode of Failure
	Type of Loading	Testing Machine Used	Type of Connection	Connection Section, AISC Designation	Type of Fastener	Column Section, AISC Designation	Rise Time to Maximum Lateral Load, secs.	Maximum Lateral Load, kips	Maximum Load Point Acceleration, G.	Maximum Loc. Point Deflection, ins.	Maximum Angle Strain, in./in.	
CTBR	Rapid	Loading unit **	Tee + web angle	4 T 17.5 4x4x $\frac{3}{8}$	HTS bolt 3/4"	8 WF 35	0.022	45.5	157.0	7.47	0.0205	Specimen bottomed *
CTRR	Rapid	Loading unit **	Tee + web angle	4 T 17.5 4x4x $\frac{3}{8}$	Rivet 3/4"	8 WF 35	0.021	45.5	161.5	4.11	0.0090	Beam rivets sheared in web and bottom tee
CFBR	Rapid	Loading unit **	Top and Seat angle	6x6x $\frac{1}{2}$ 4x3x $\frac{3}{8}$	HTS bolt 3/4"	8 WF 35	0.040	25.5	105.9	8.48	0.0226	Brittle fracture, bottom angle
CFRR	Rapid	Loading unit **	Top and Seat angle	6x6x $\frac{1}{2}$ 4x3x $\frac{3}{8}$	Rivet 3/4"	8 WF 35	0.011	25.9	97.0	8.95	0.0355	Ductile tension failure in rivet
CWBR	Rapid	Loading unit **	Web angle	4x3x $\frac{3}{8}$	HTS bolt 3/4"	8 WF 35	0.024	22.6	89.8	6.92	0.0255	Specimen bottomed *
CWRR	Rapid	Loading unit **	Web angle	4x3x $\frac{3}{8}$	Rivet 3/4"	8 WF 35	0.022	22.2	171.8	8.56	0.0234	Specimen bottomed

All beams were 14 WF 34 Sections

* Struck bottom of frame without failure
 ** 60 kip pulse loading unit

TABLE 3b. SUMMARY OF BEAM-TO-COLUMN CONNECTION TEST RESULTS

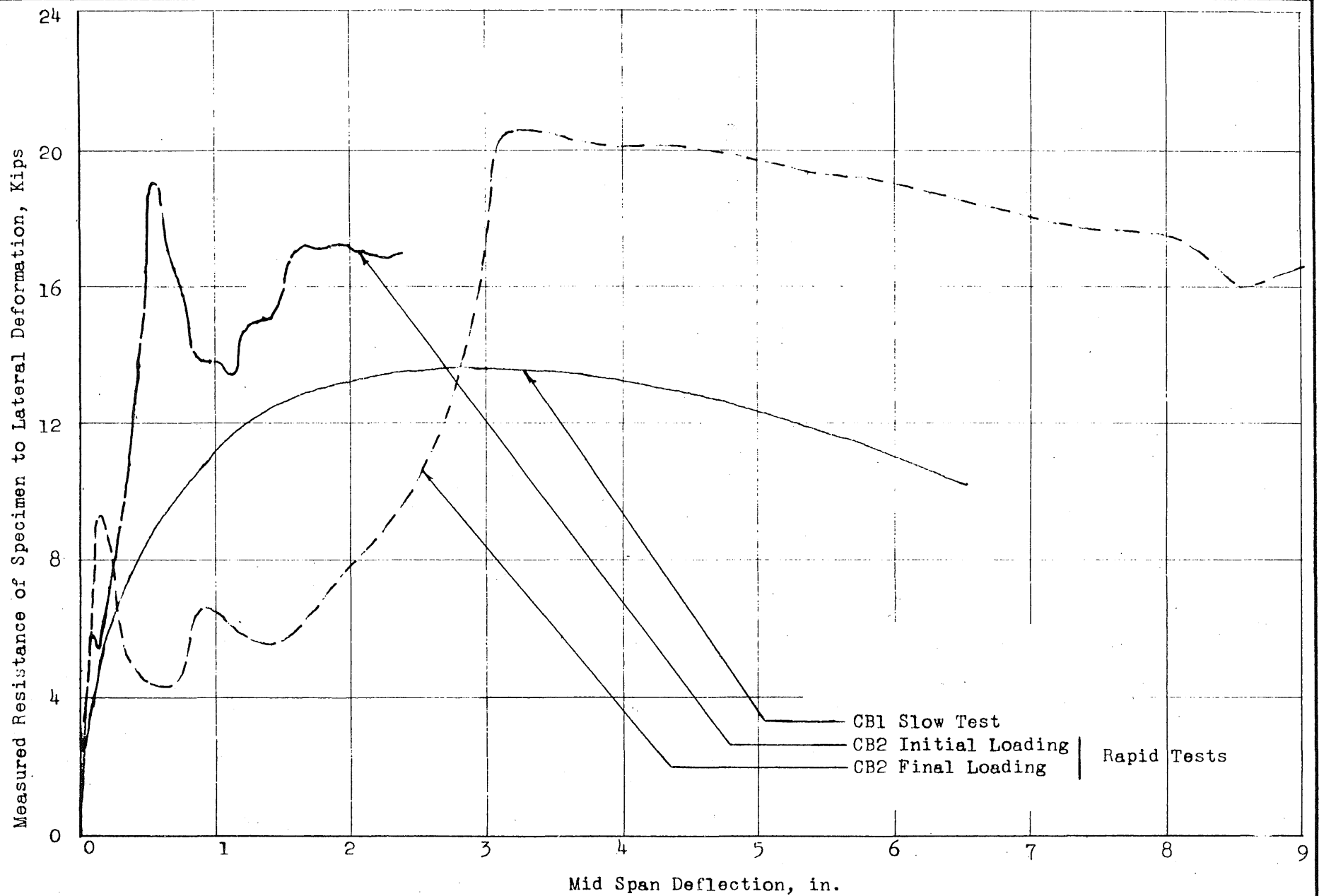


FIG. 13 MEASURED RESISTANCE VERSUS MID SPAN DEFLECTION OF COLUMN-BASE SPECIMENS: CB1, CB2

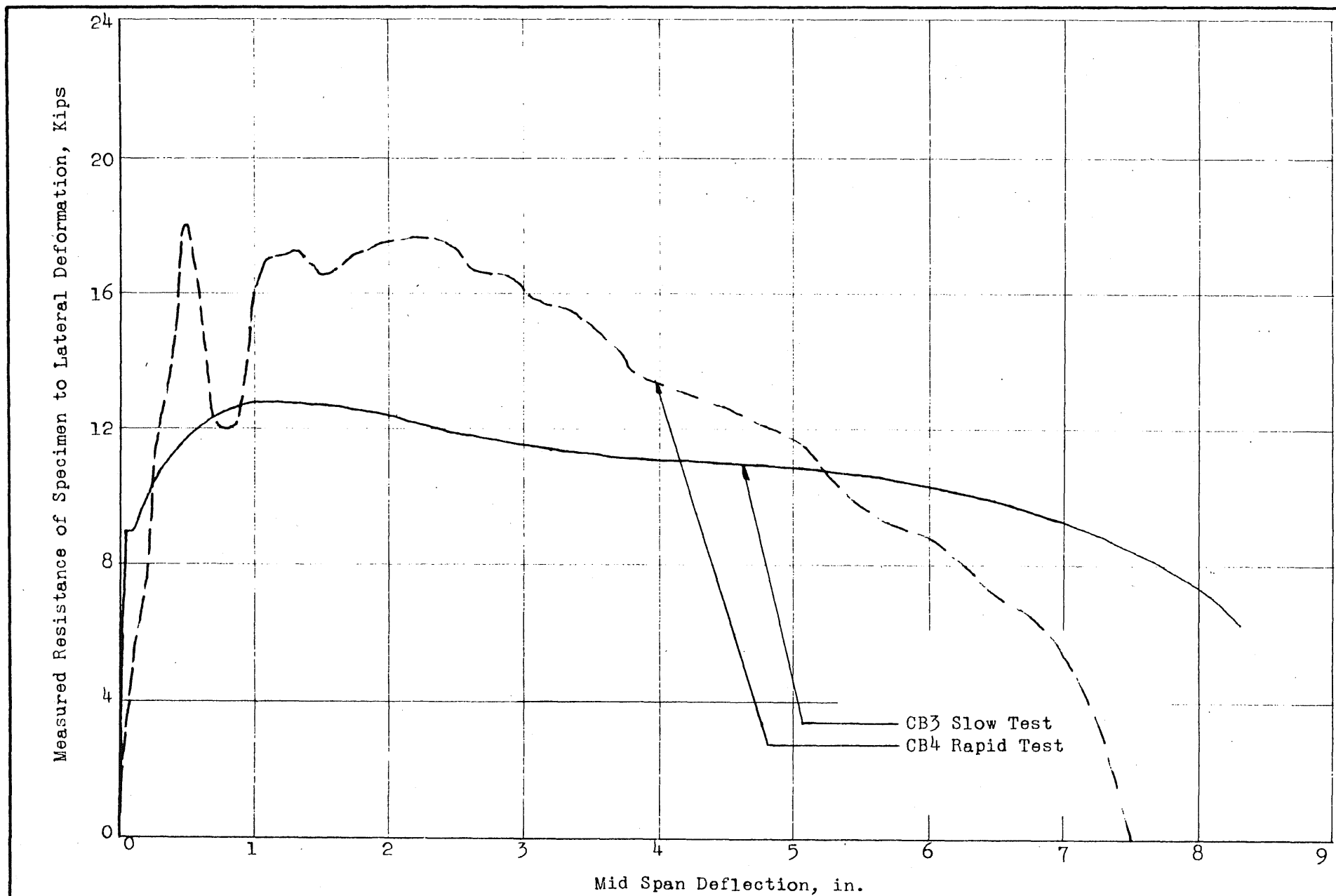


FIG. 14 MEASURED RESISTANCE VERSUS MID SPAN DEFLECTION OF COLUMN-BASE SPECIMENS; CB3, CB4

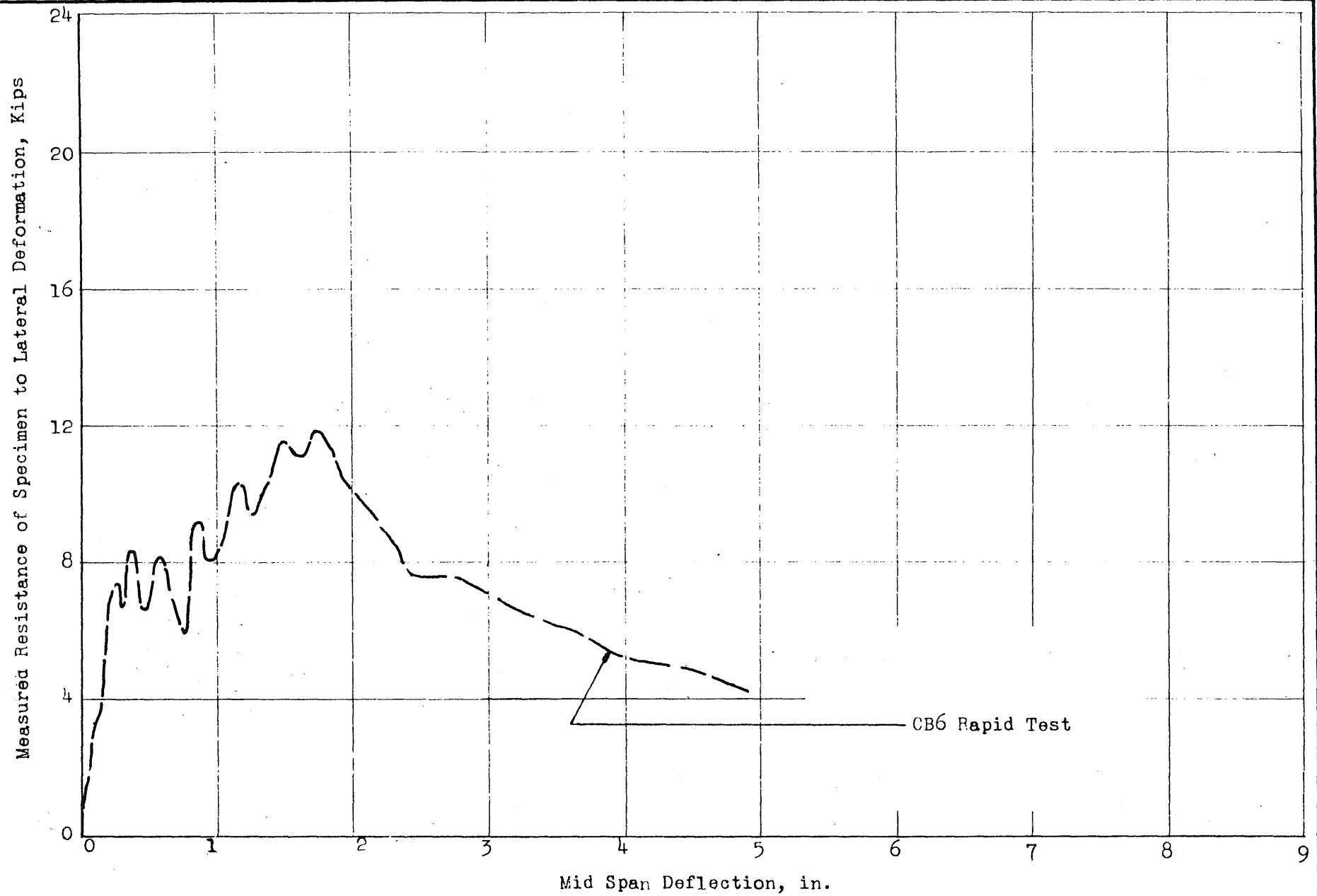


FIG. 15 MEASURED RESISTANCE VERSUS MID SPAN DEFLECTION OF COLUMN-BASE SPECIMEN; CB6

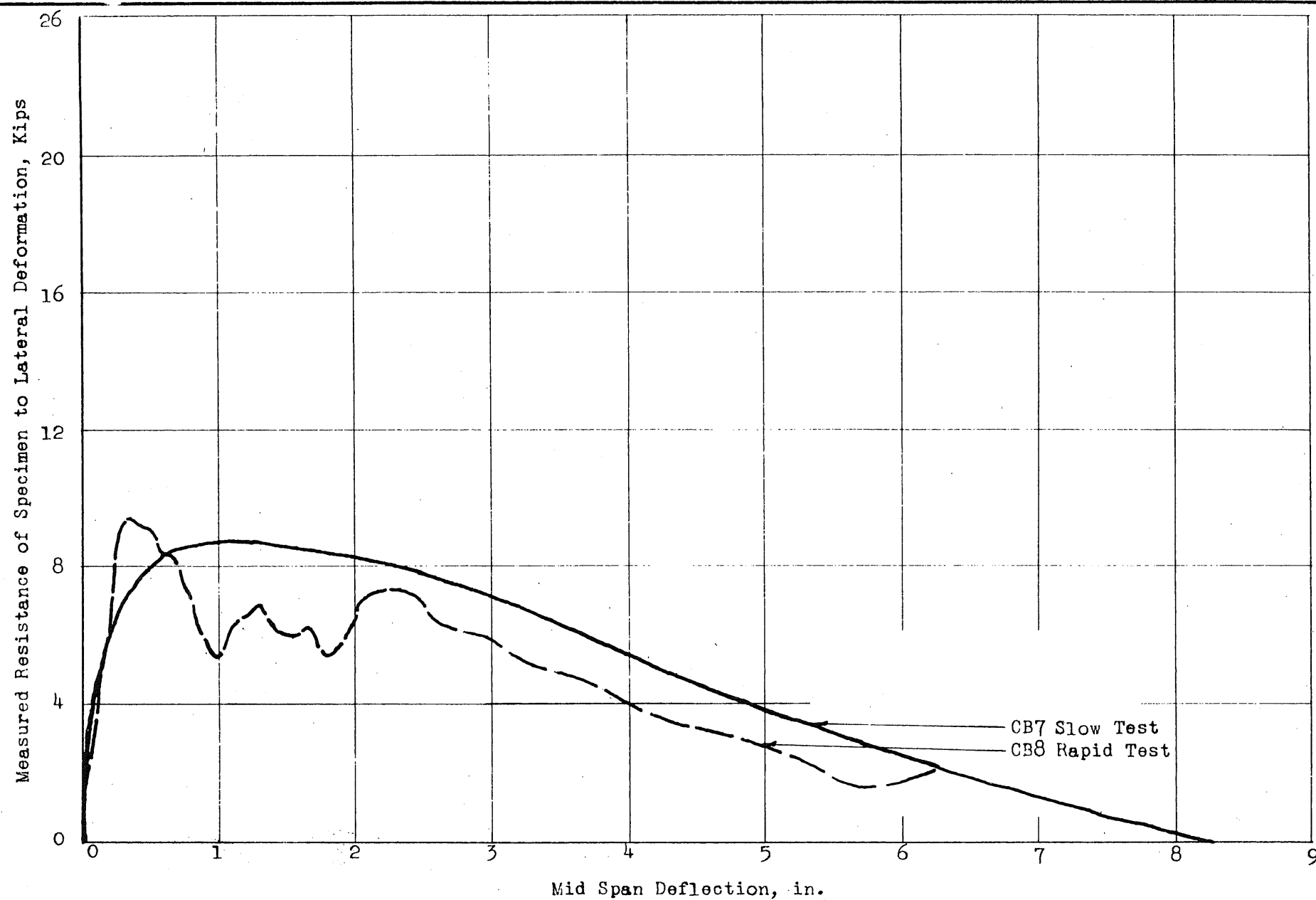


FIG. 16 MEASURED RESISTANCE VERSUS MID SPAN DEFLECTION OF COLUMN-BASE SPECIMENS; CB7, CB8

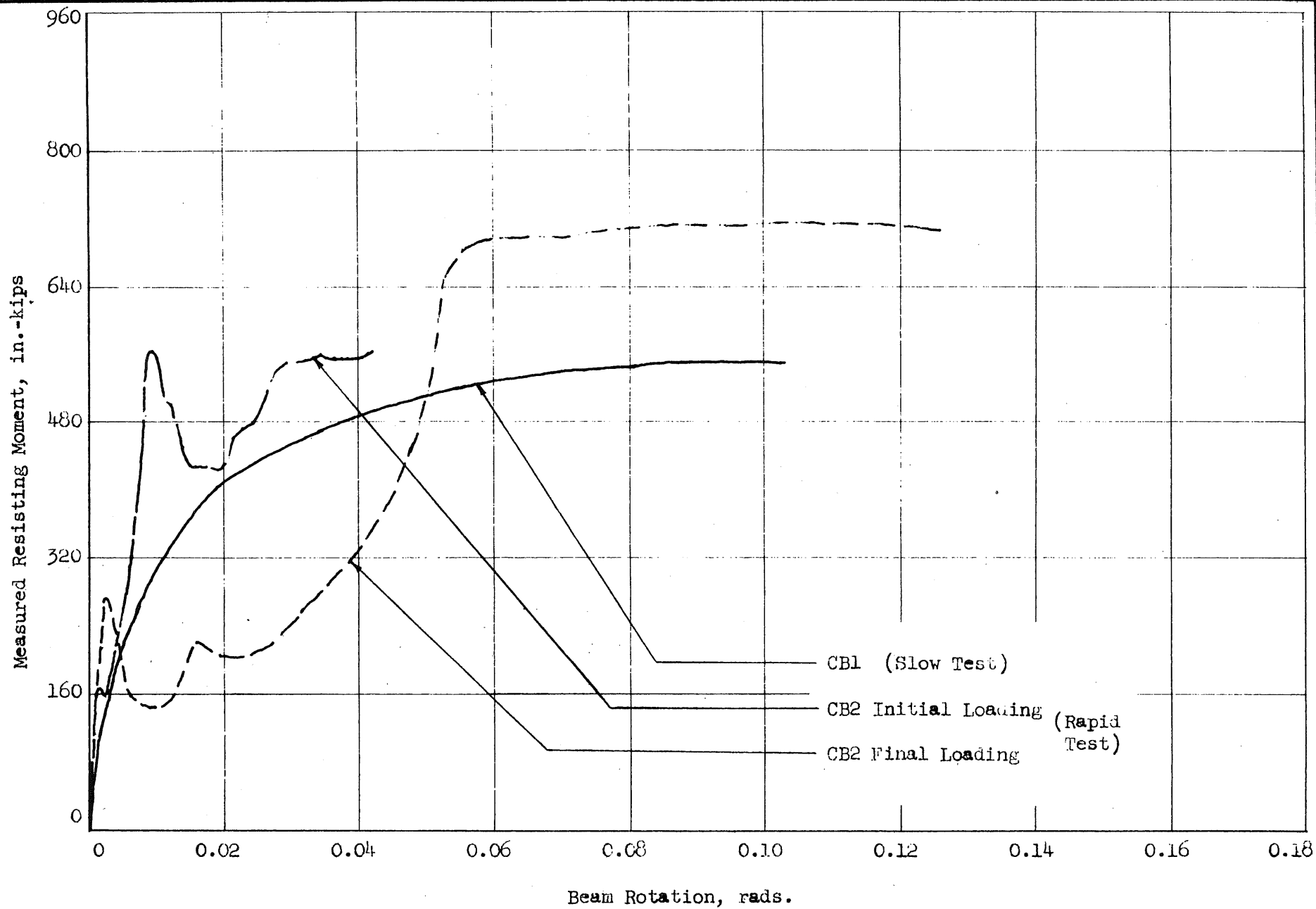


FIG. 17: MEASURED RESISTING MOMENT OF CONNECTION VERSUS COLUMN ROTATION; CB1, CB2

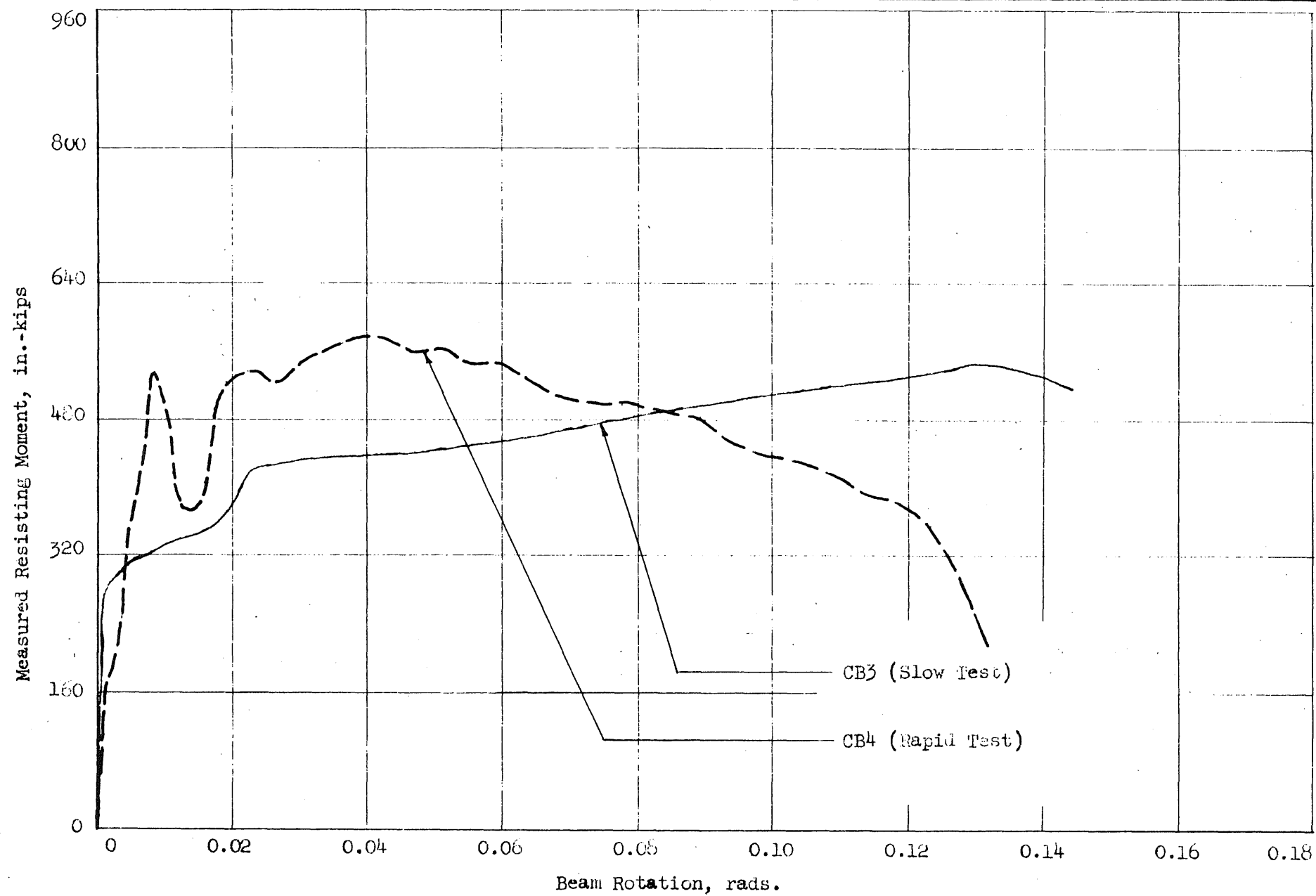


FIG. 18: MEASURED RESISTING MOMENT OF CONNECTION VERSUS COLUMN ROTATION; CB3, CB4

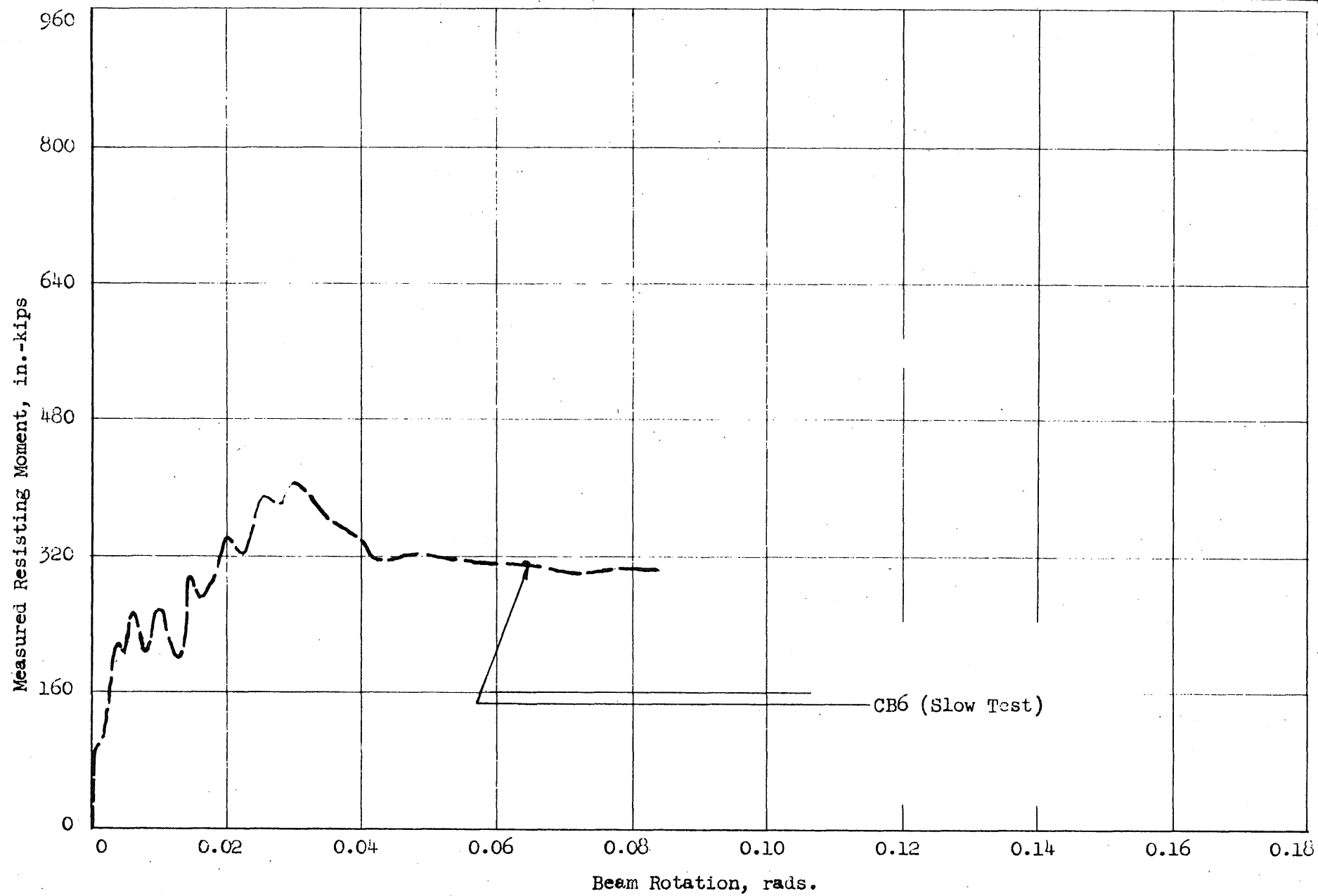


FIG. 19: MEASURED RESISTING MOMENT OF CONNECTION VERSUS COLUMN ROTATION; CB6

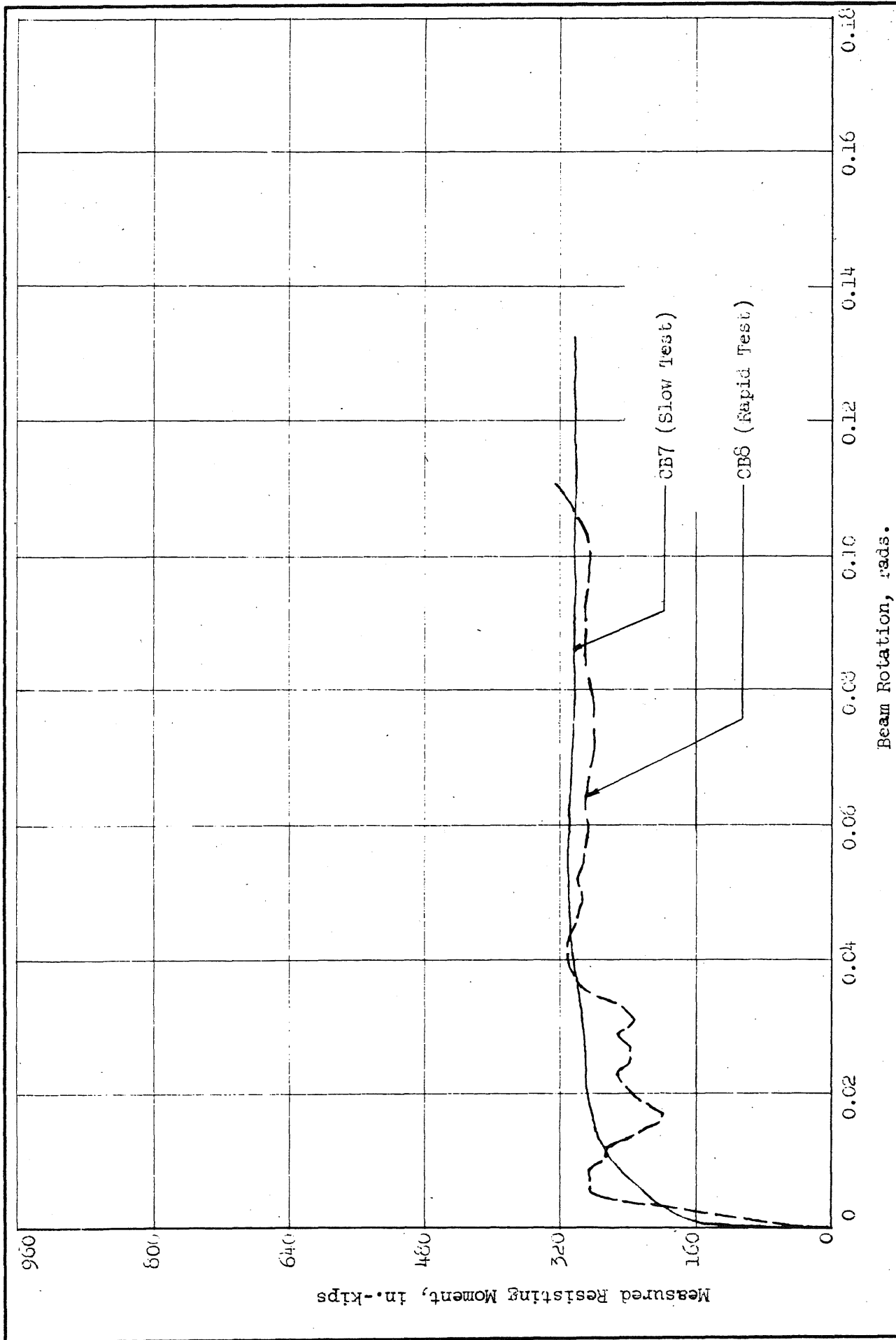


FIG. 2C: MEASURED RESISTING MOMENT OF CONNECTION VERSUS COLUMN ROTATION; CB7, CB8

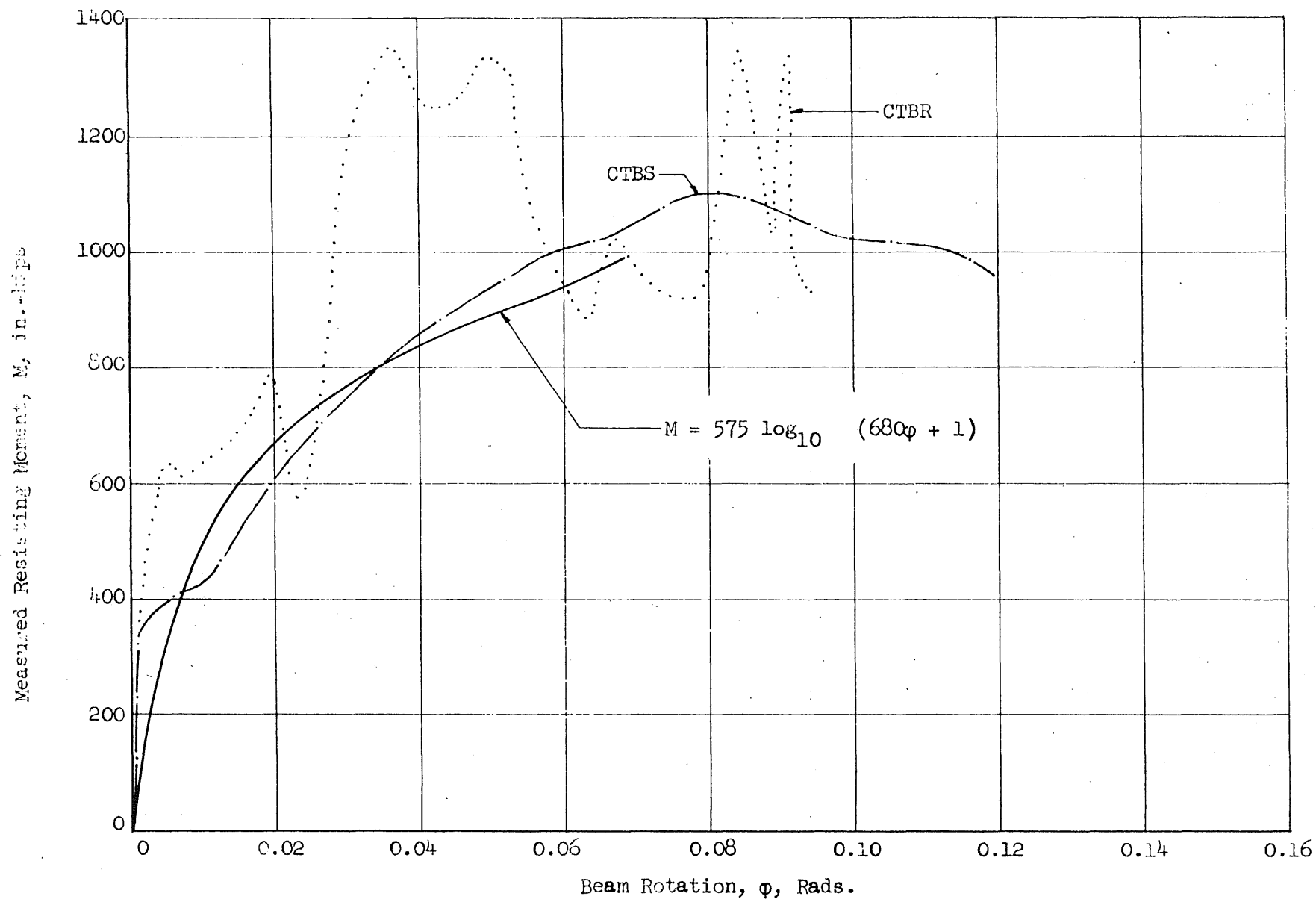


FIG. 21: MEASURED RESISTING MOMENT OF CONNECTION VERSUS BEAM ROTATION; CTBS, CTBR

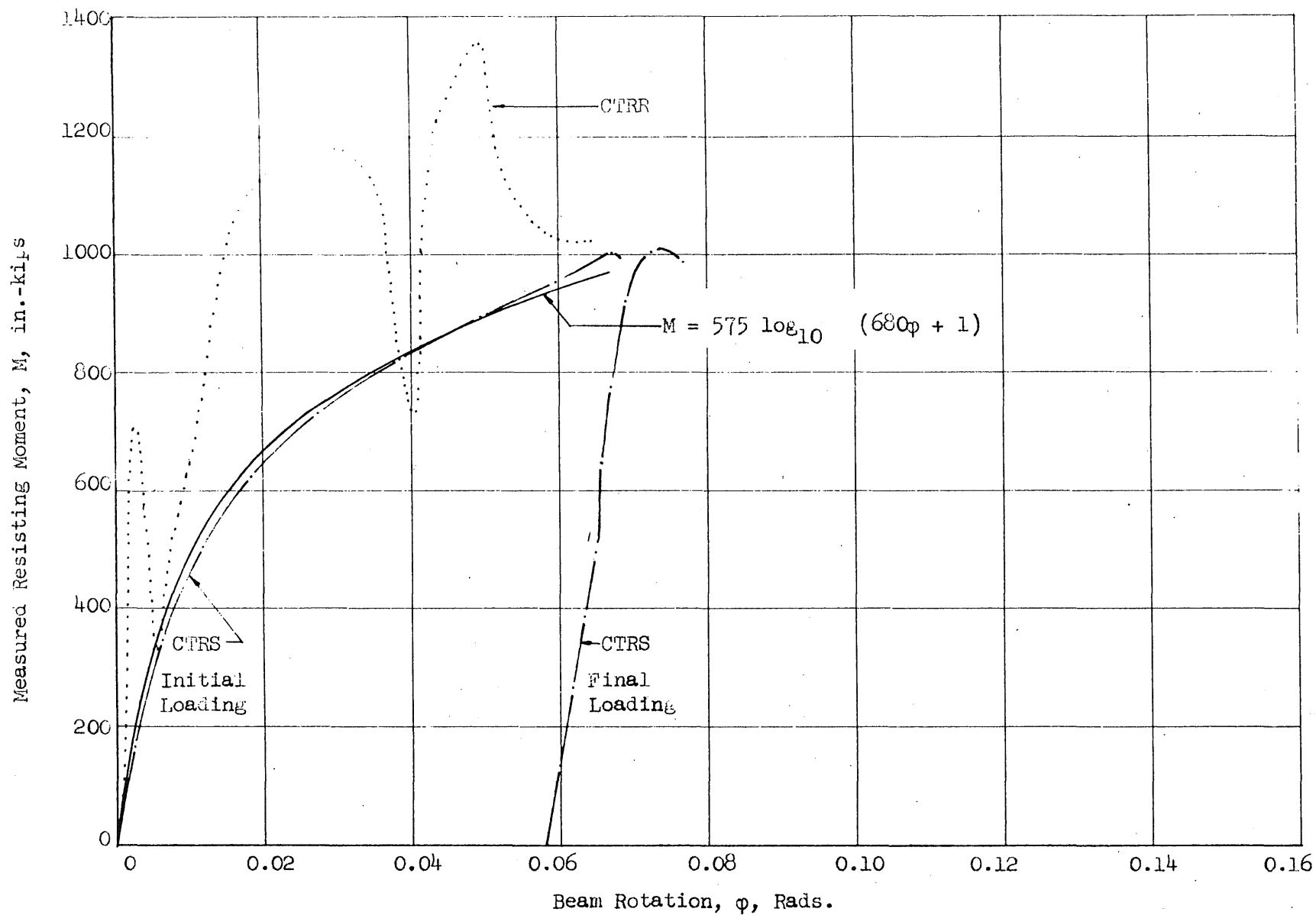


FIG. 22: MEASURED RESISTING MOMENT OF CONNECTION VERSUS BEAM ROTATION; CTRS, CTRR

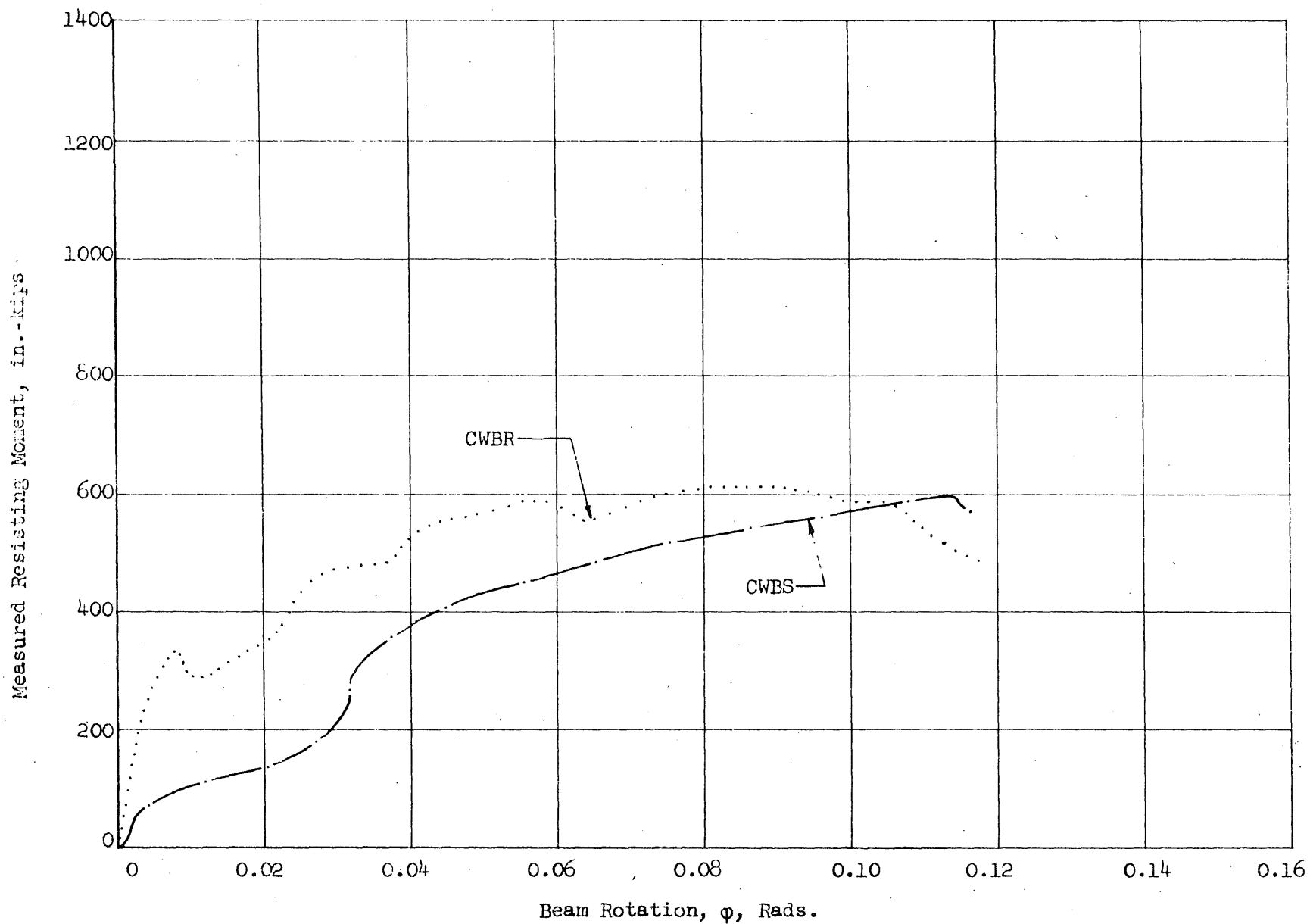


FIG. 23: MEASURED RESISTING MOMENT OF CONNECTION VERSUS BEAM ROTATION; CWBS, CWBA

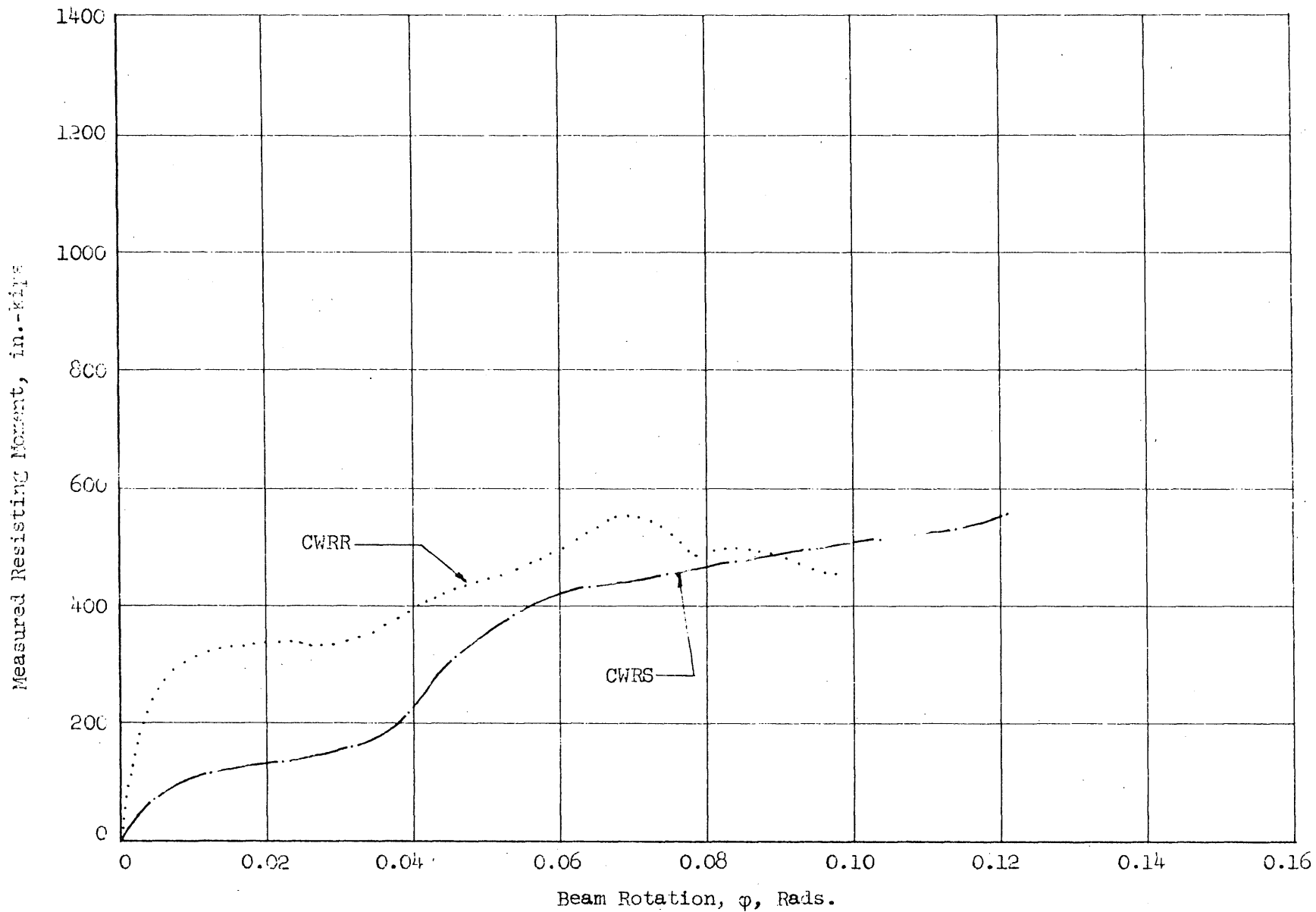


FIG. 24: MEASURED RESISTING MOMENT OF CONNECTION VERSUS BEAM ROTATION; CWRS, CWRR

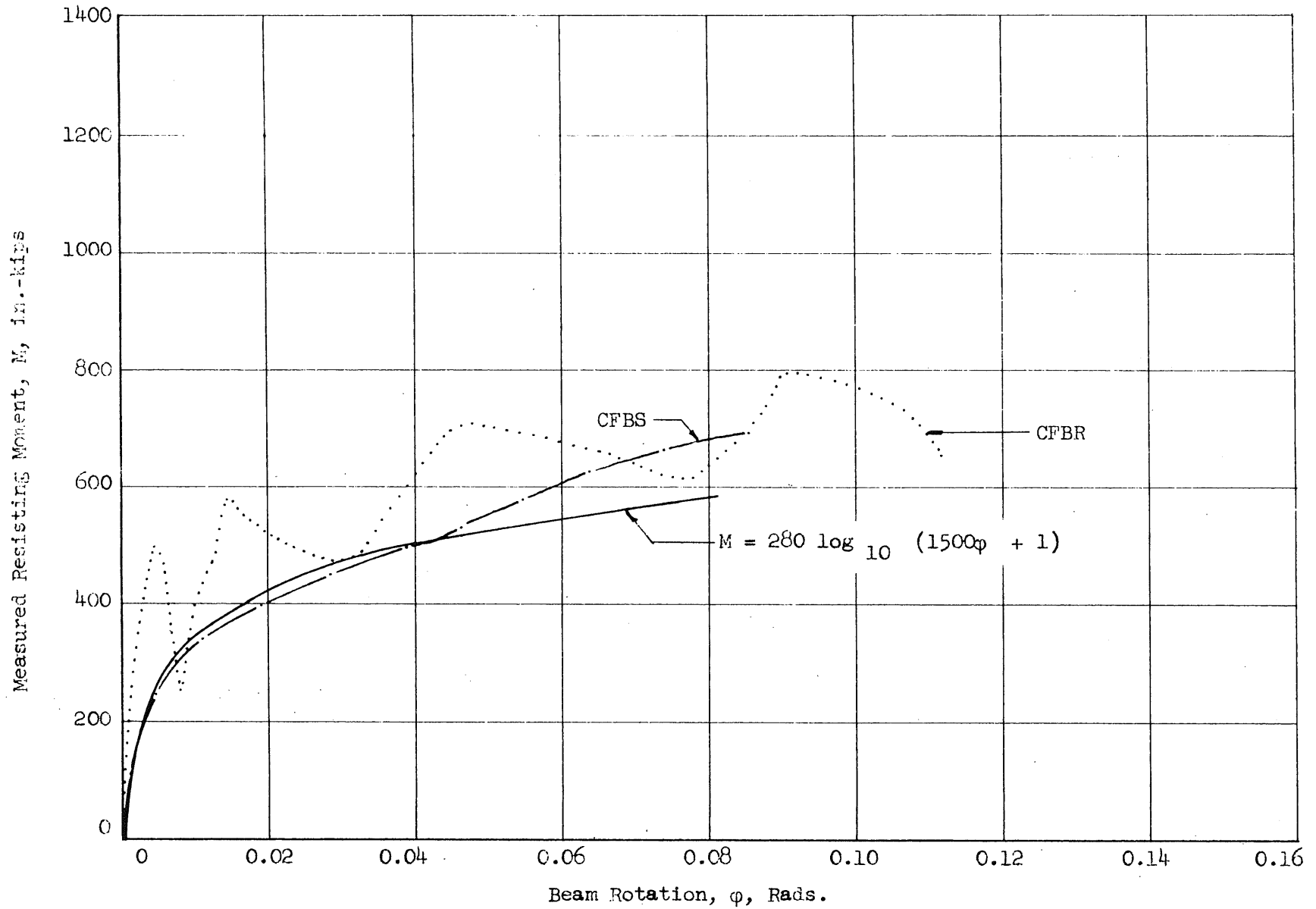


FIG. 25: MEASURED RESISTING MOMENT OF CONNECTION VERSUS BEAM ROTATION; CFBS, CFBR

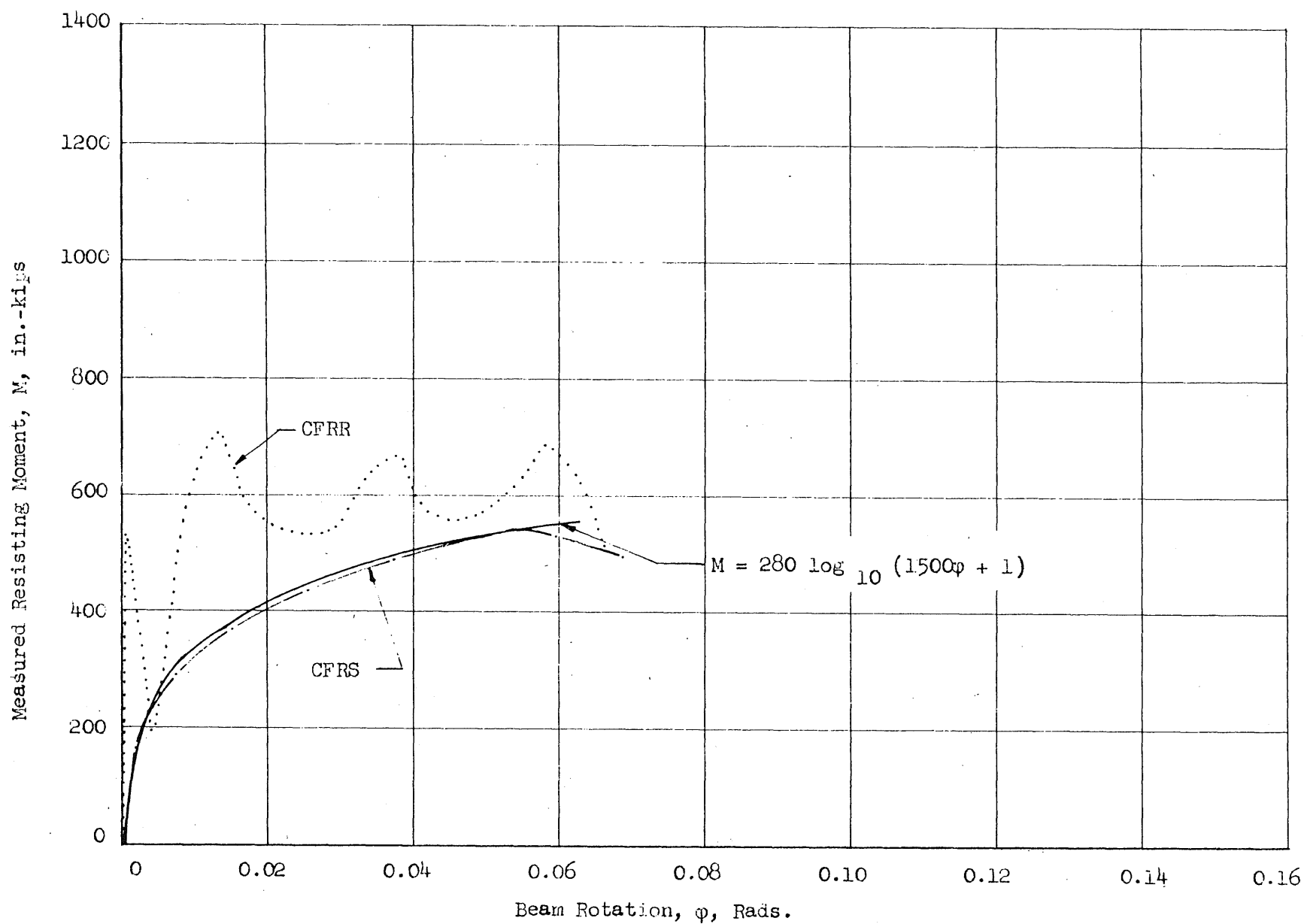


FIG. 26: MEASURED RESISTING MOMENT OF CONNECTION VERSUS BEAM ROTATION; CFRS, CFRR

APPENDIX A
RECORDED DATA FROM CONNECTION TESTS

<u>Figure</u>		<u>Page</u>
A1	Recorded Data from Test CB1	77
A2	Recorded Data from Test CB2	80
A3	Recorded Data from Test CB3	86
A4	Recorded Data from Test CB4	89
A5	Recorded Data from Test CB5	92
A6	Recorded Data from Test CB6	94
A7	Recorded Data from Test CB7	97
A8	Recorded Data from Test CB8	100
A9	Recorded Data from Test CTBS.	103
A10	Recorded Data from Test CTRS.	105
A11	Recorded Data from Test CFBS.	107
A12	Recorded Data from Test CFRS.	109
A13	Recorded Data from Test CWBS.	111
A14	Recorded Data from Test CWRS.	113
A15	Recorded Data from Test CTBR.	115
A16	Recorded Data from Test CTRR.	117
A17	Recorded Data from Test CFBR.	119
A18	Recorded Data from Test CFRR.	121
A19	Recorded Data from Test CWBR.	123
A20	Recorded Data from Test CWRR.	125

Loads and Forces, Kips

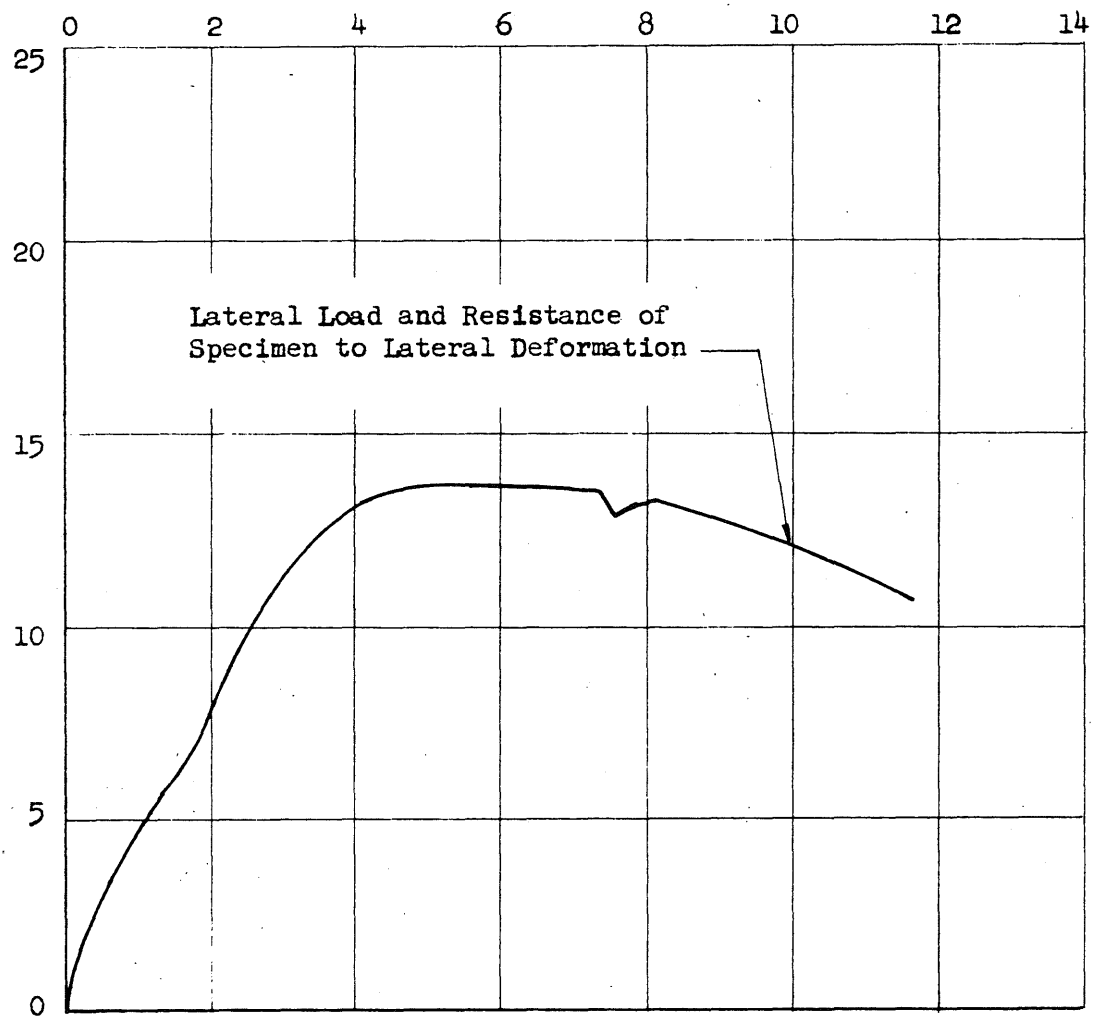
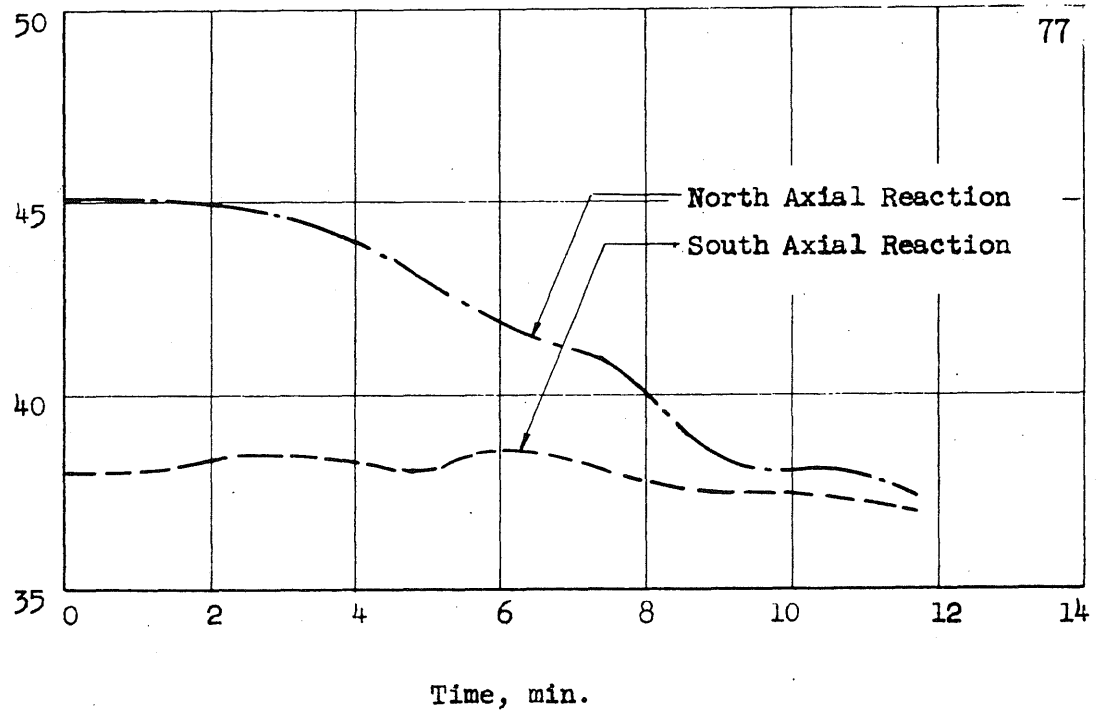


FIG. A1a: RECORDED DATA FROM TEST CB1

Deflection, in.

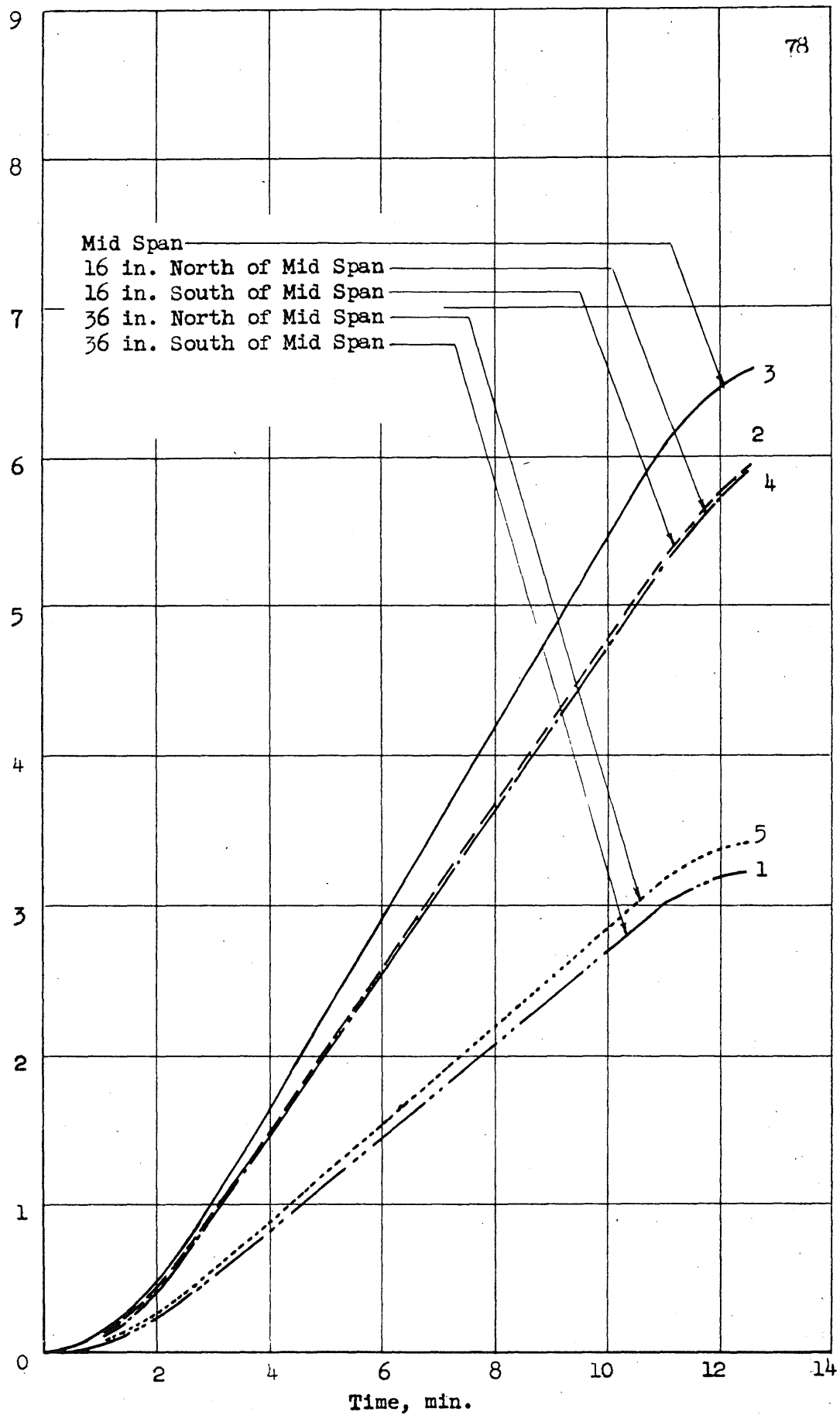


FIG. A1b: RECORDED DATA FROM TEST CB1

Strain in Connection Angle, in./in.

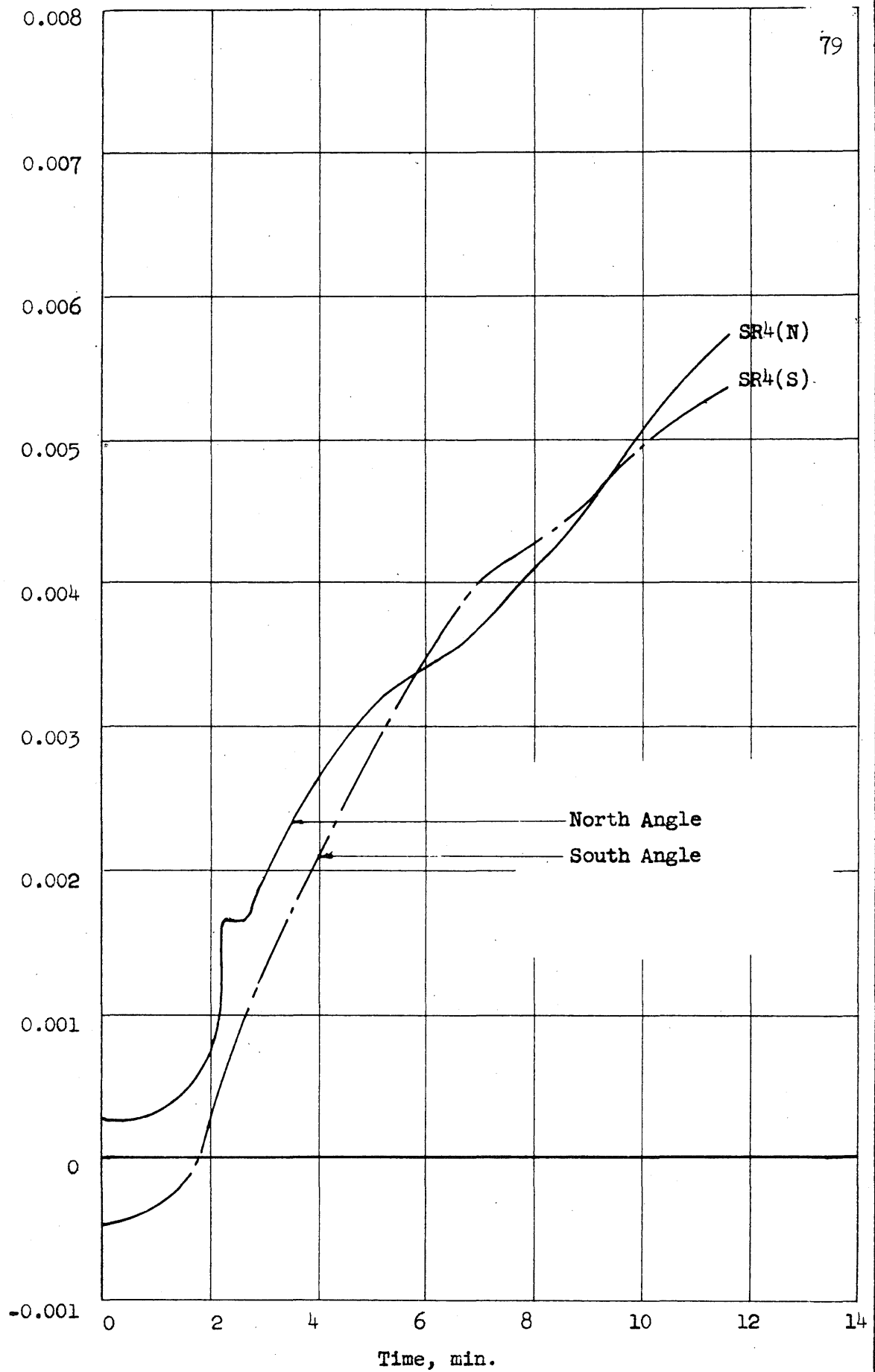


FIG. 1. Also: RECORDED DATA FROM TEST CB1

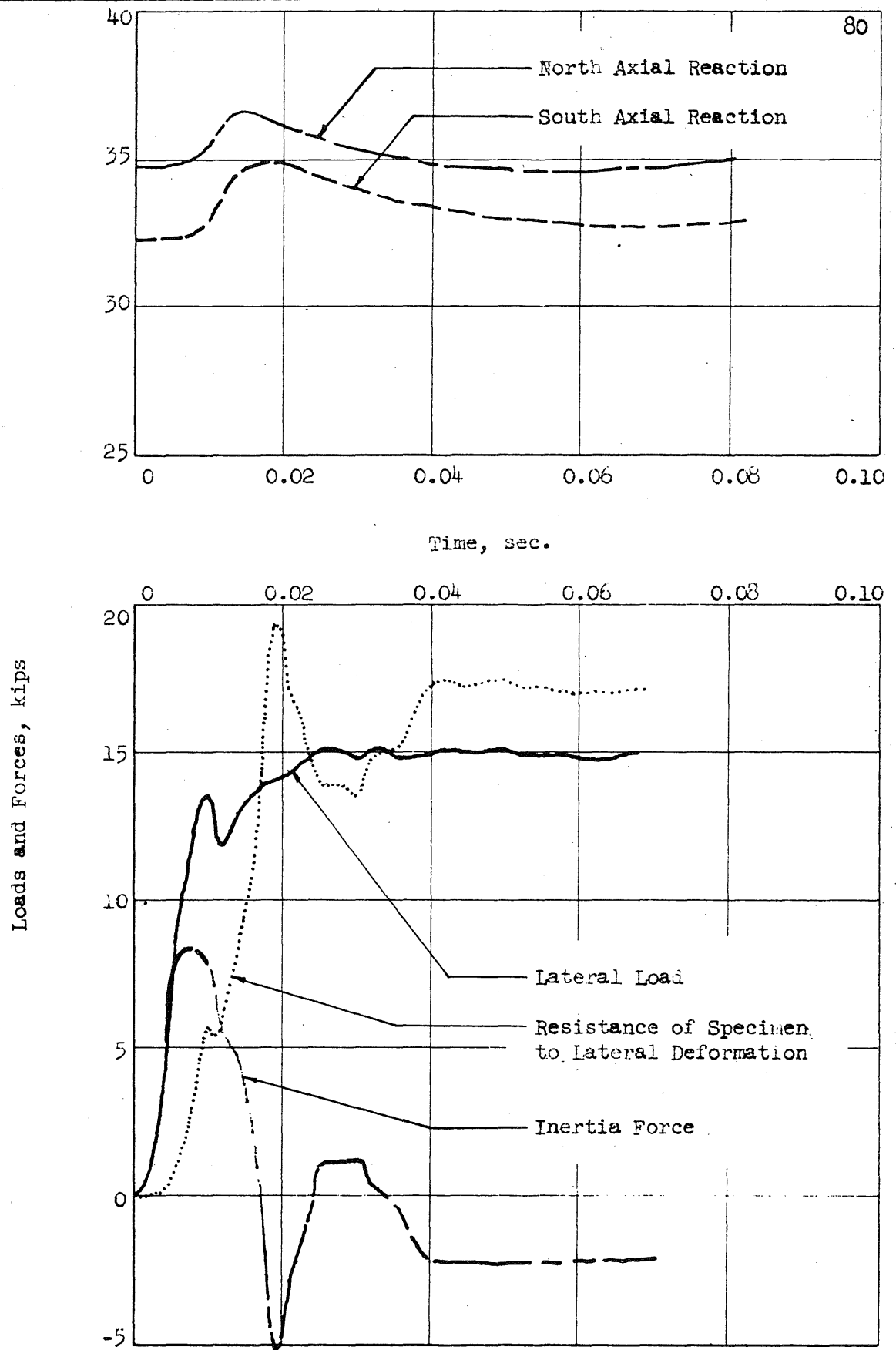


FIG. A2a: RECORDED DATA FROM TEST CB21 (INITIAL LOADING)

Deflection, in.

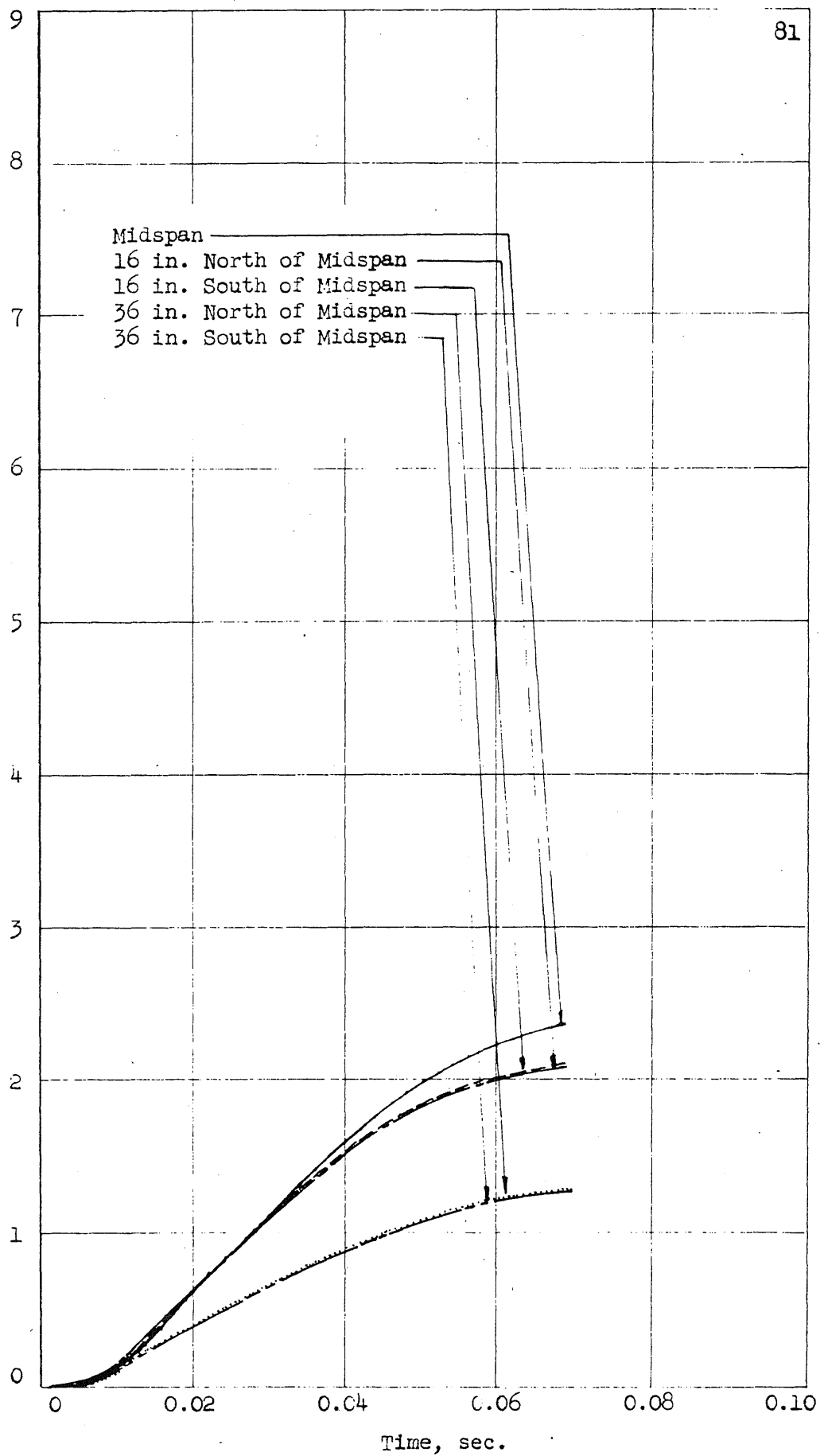


FIG. A2b: RECORDED DATA FROM TEST CB2-1 (INITIAL LOADING)

Strain in Connection Angle, in./in.

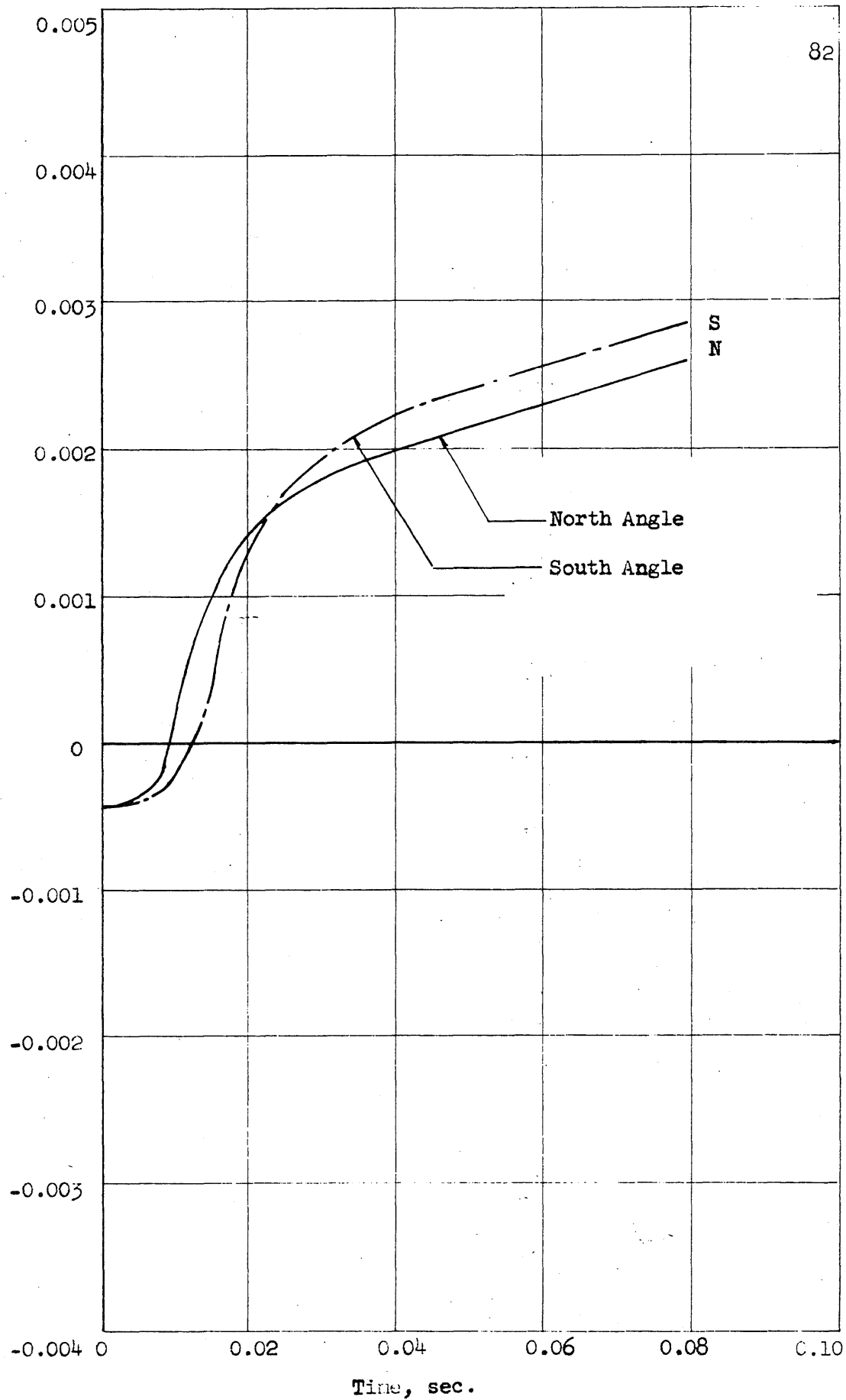


FIG. 12c: RECORDED DATA FROM TEST CB2-1 (INITIAL LOADING)

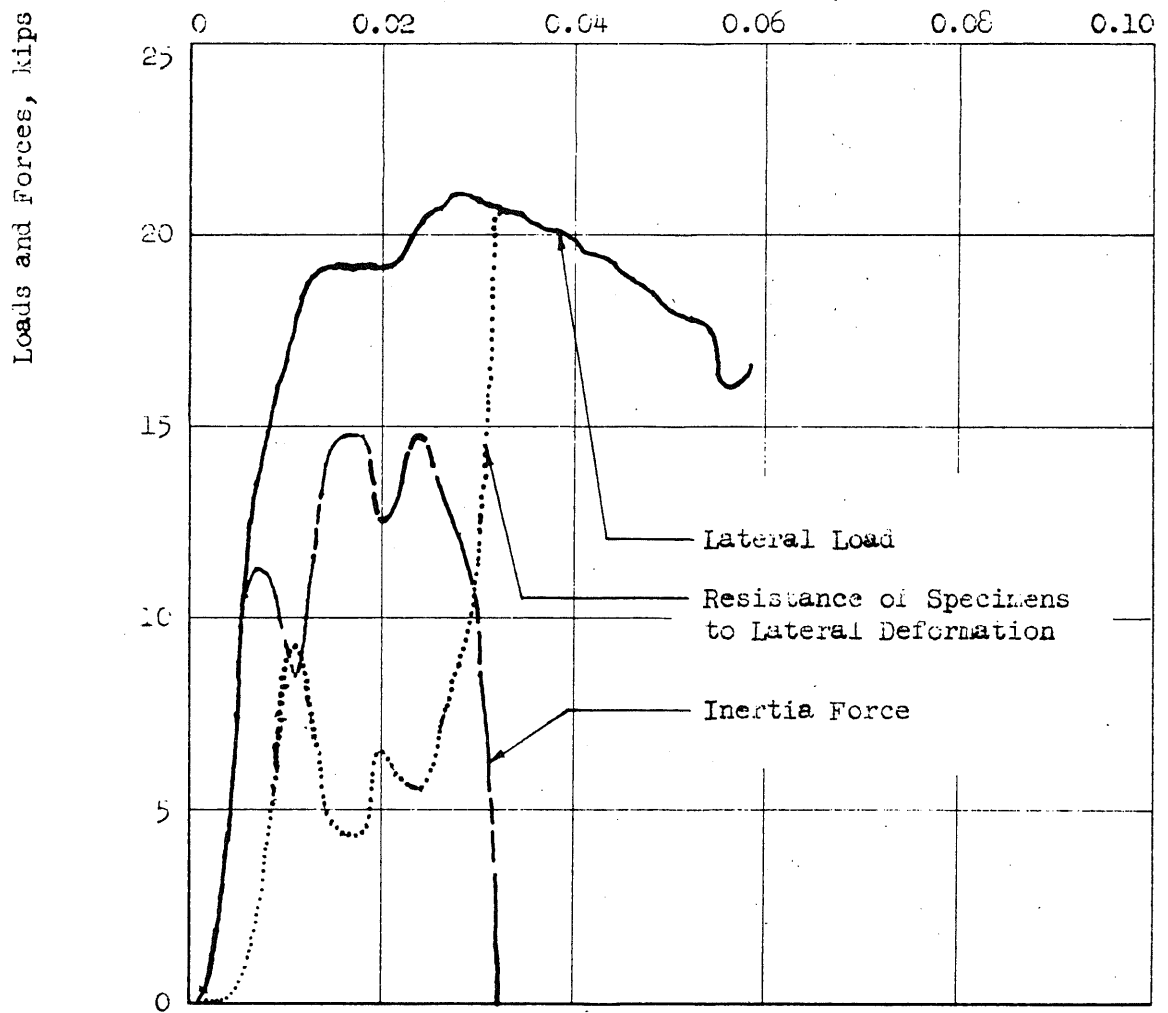
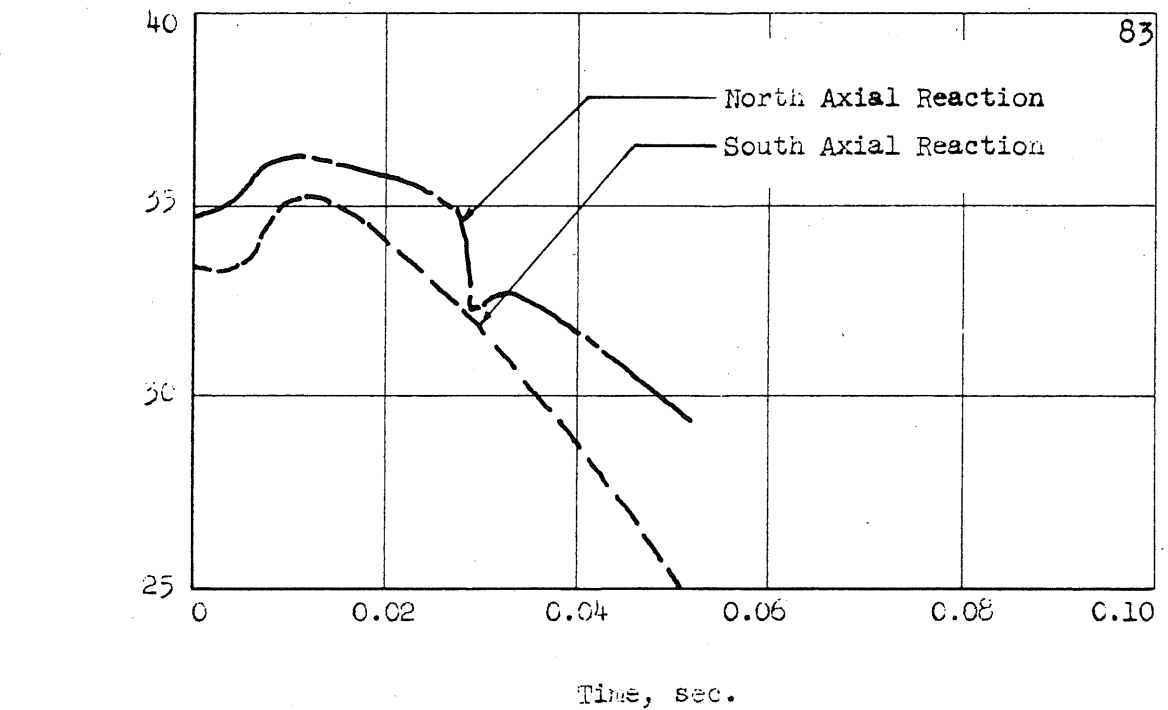


FIG. A2d: RECORDED DATA FROM TEST CB2-2(FINAL LOADING)

Deflection, in.

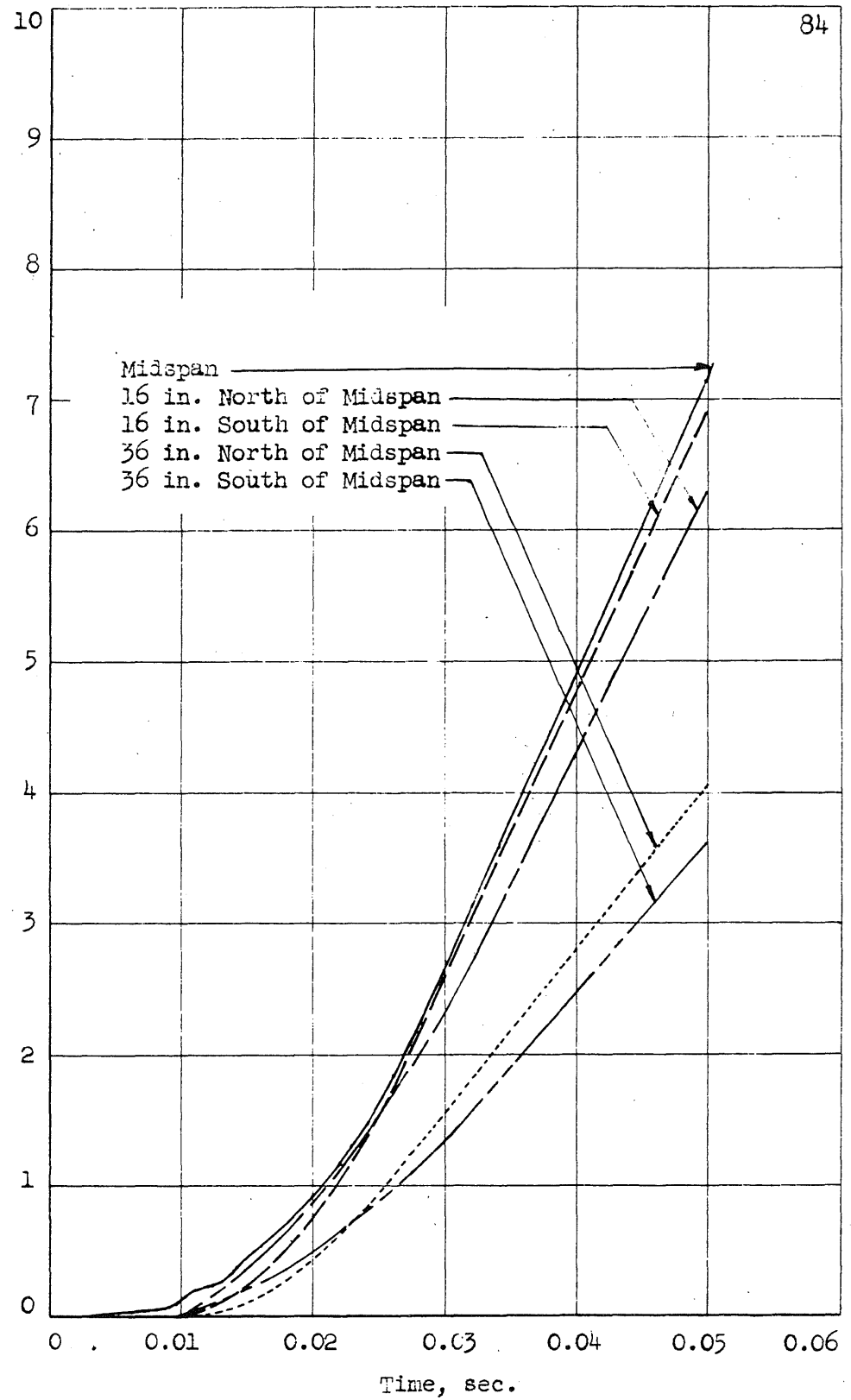


FIG. A2e: RECORDED DATA FROM TEST CB22(FINAL LOADING)

Strain in Connection Angle, in/in.

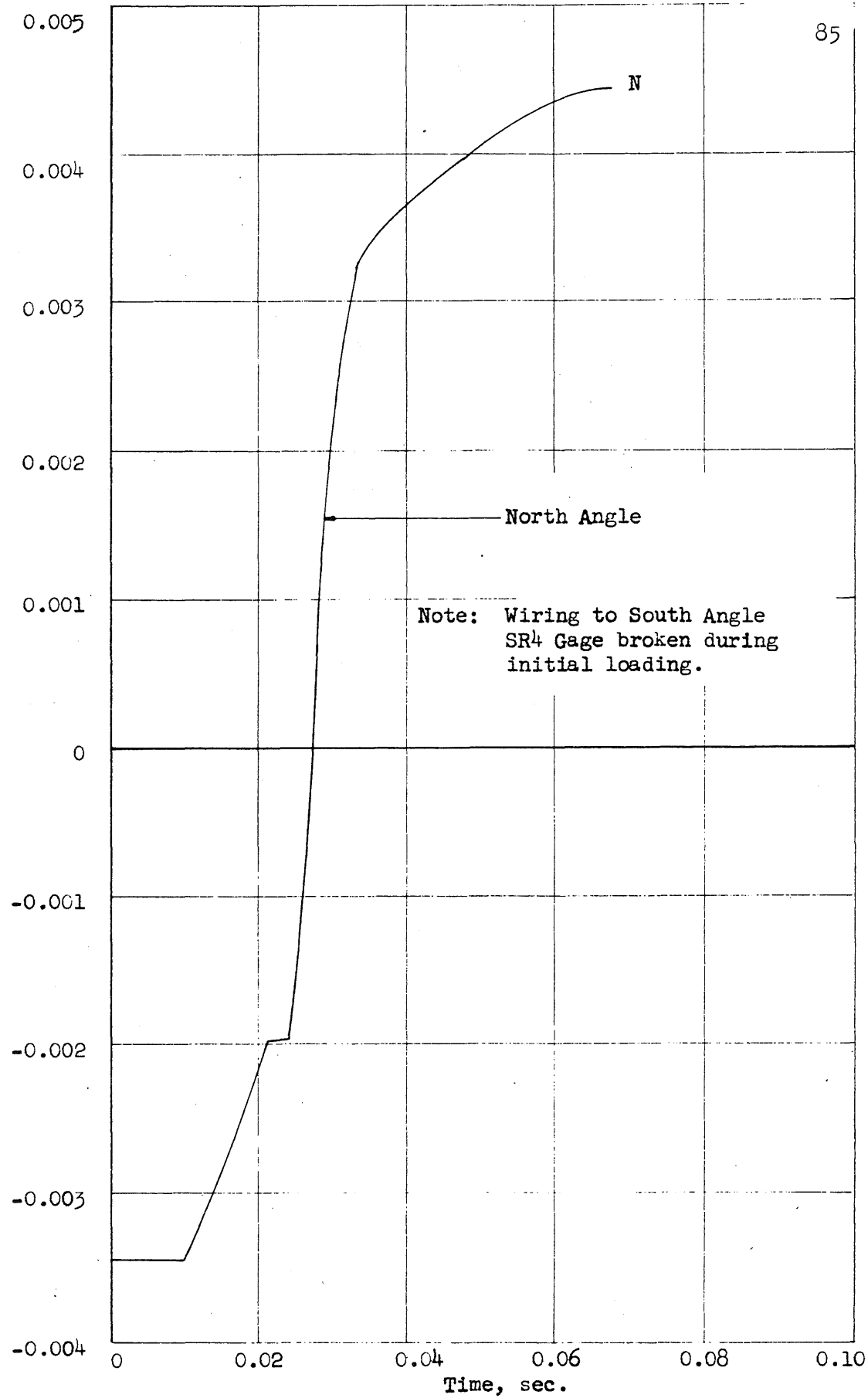


FIG. A2f: RECORDED DATA FROM TEST CB2-2(FINAL LOADING)

Note: Axial Reaction
Records Erratic

Time, min.

Loads and Forces, Kips

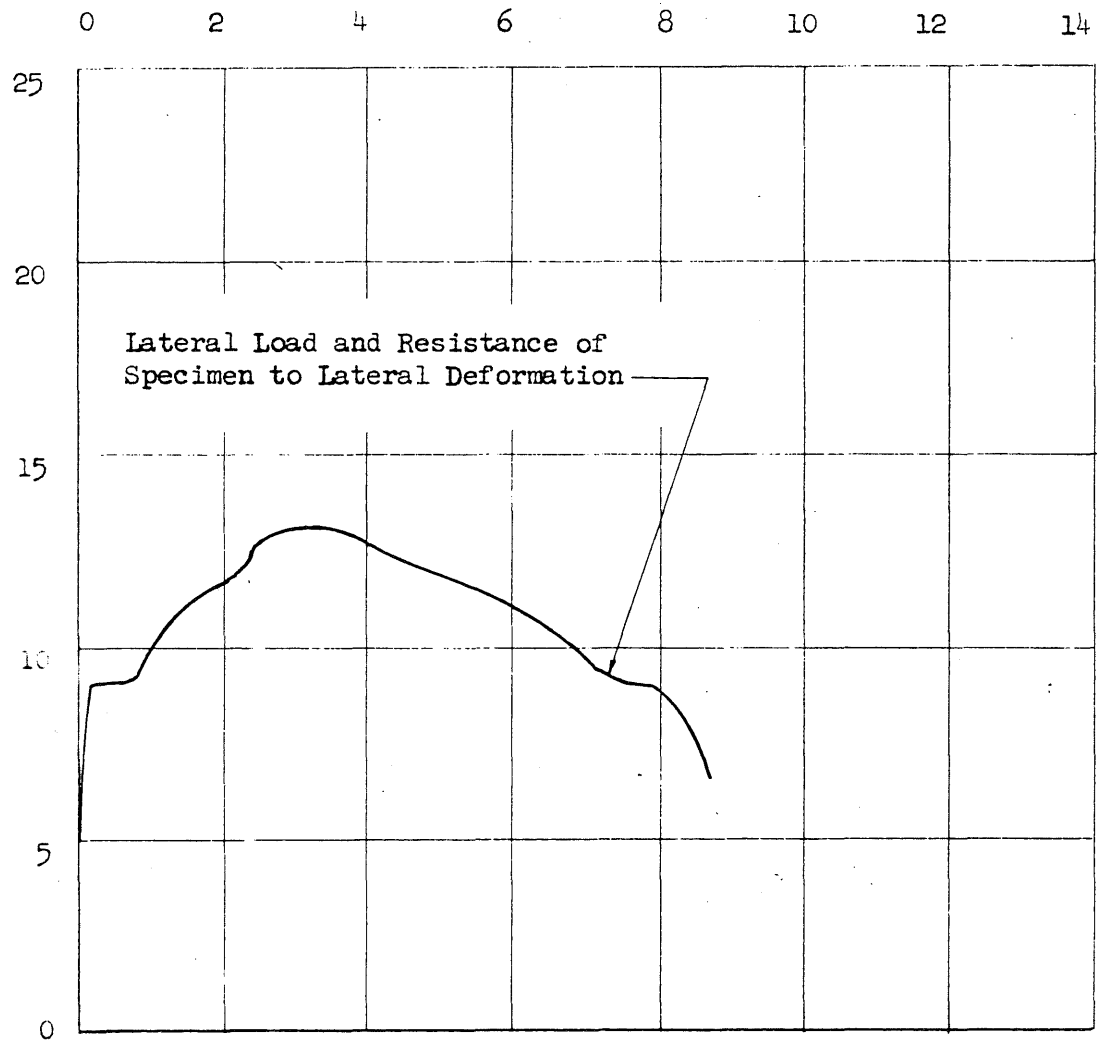


FIG. A-1: RECORDED DATA FROM TEST CB3

Deflection, in.

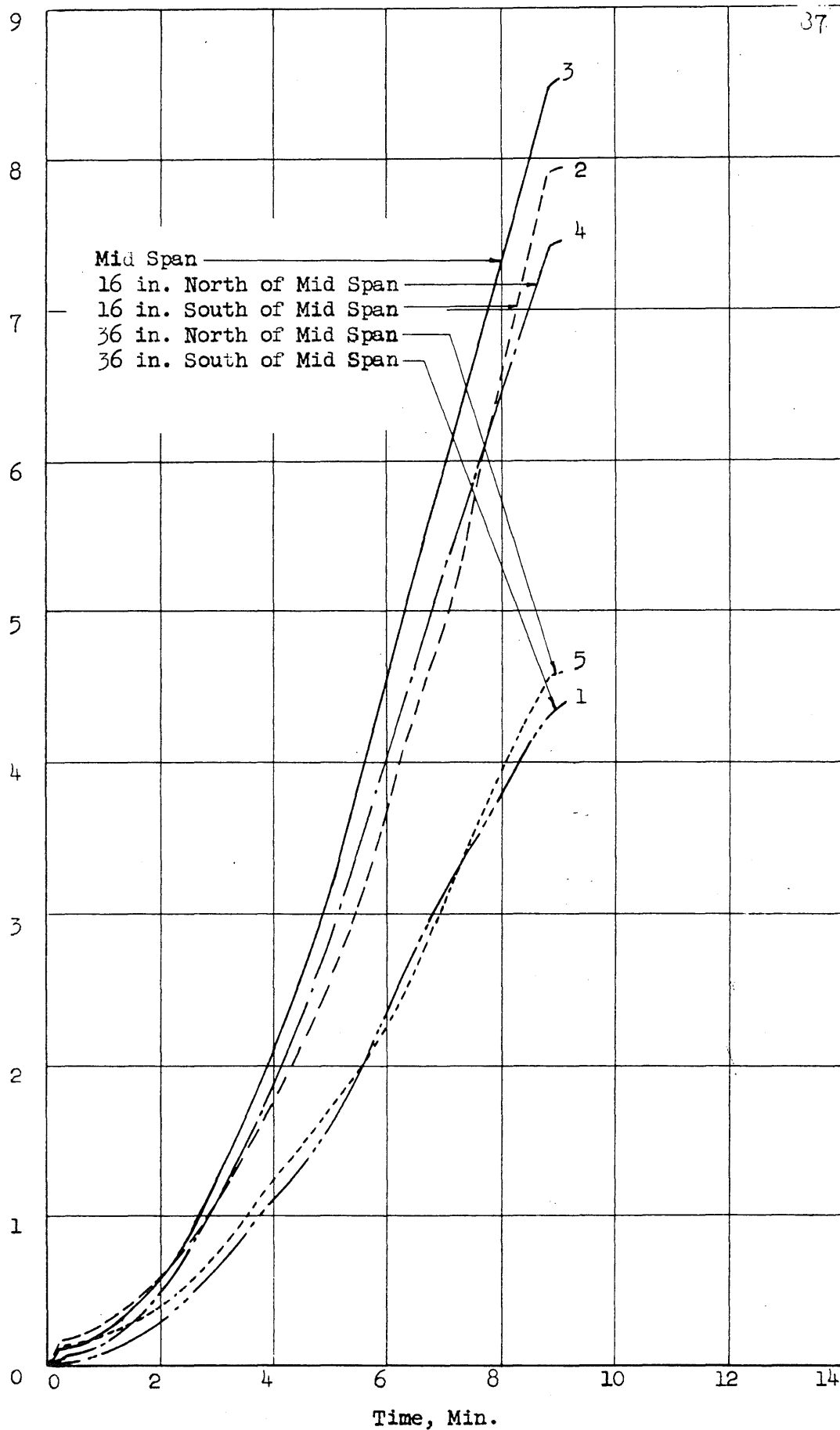


FIG. A(b): RECORDED DATA FROM TEST CB3

Strain in Connection Angle, in./in.

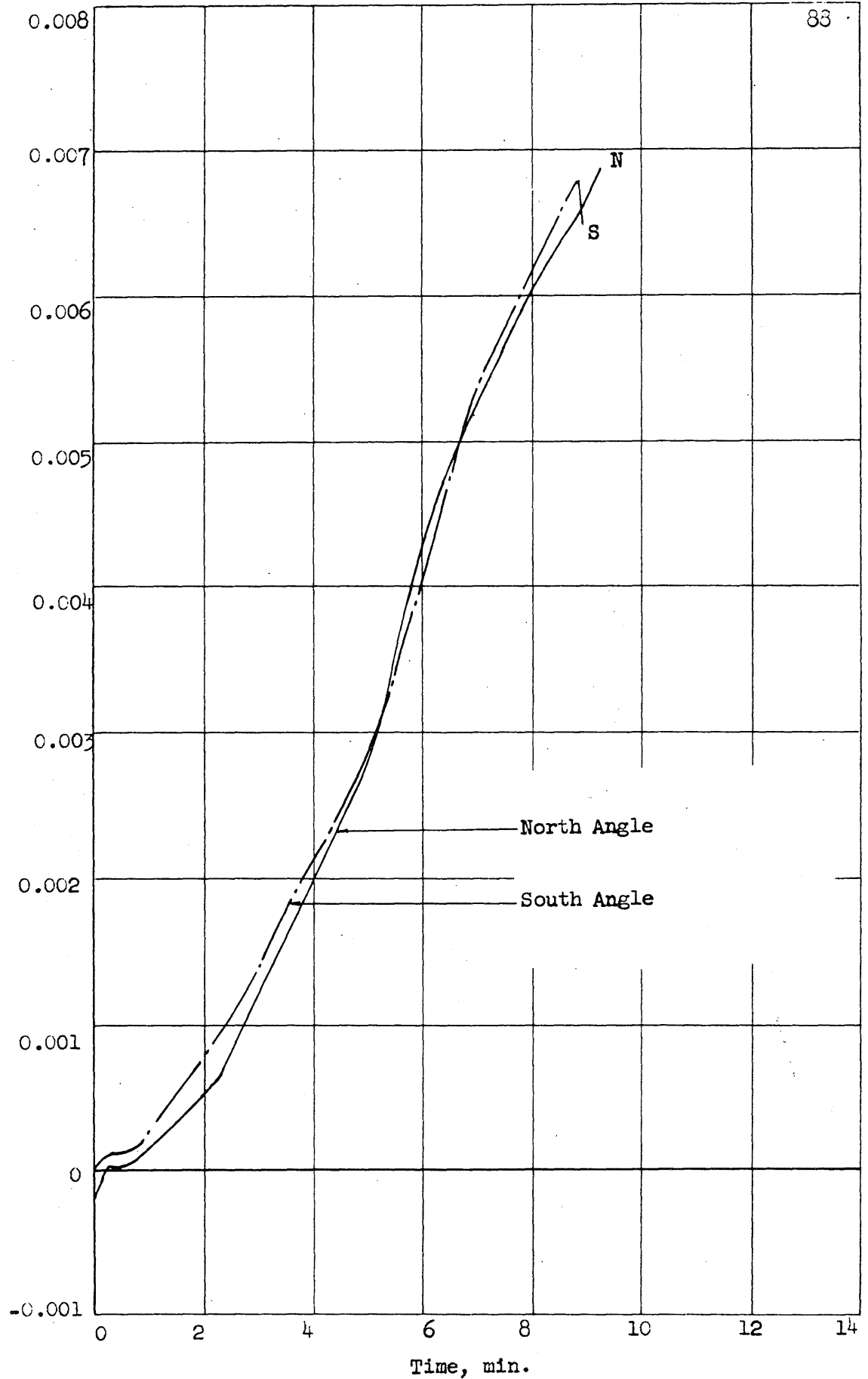


FIG. A30: RECORDED DATA FROM TEST CB3

Loads and forces, kips

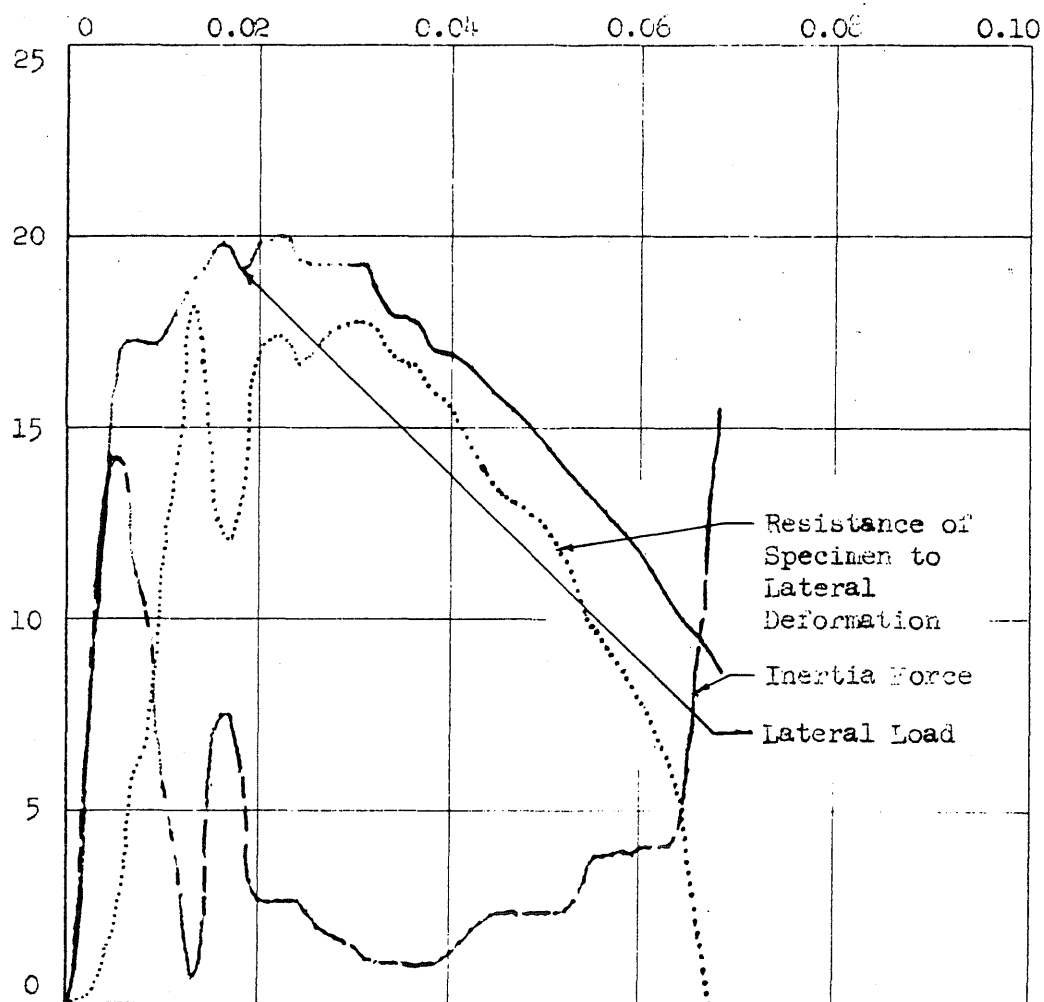
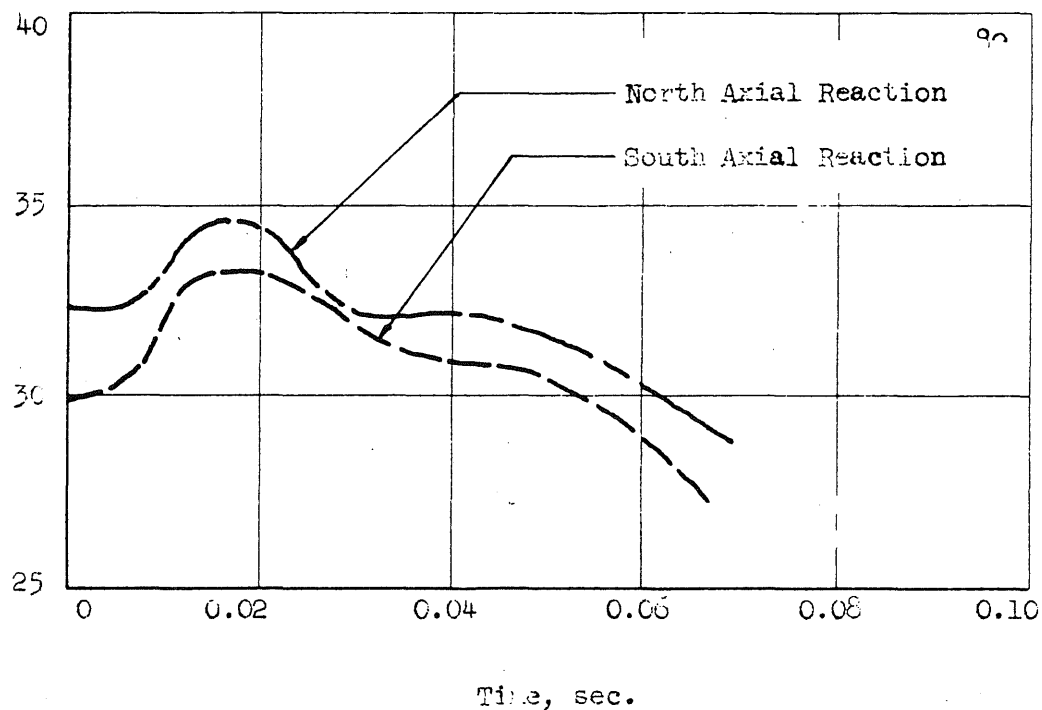


FIG. A4a: RECORDED DATA FROM TEST CB4

Deflection, in.

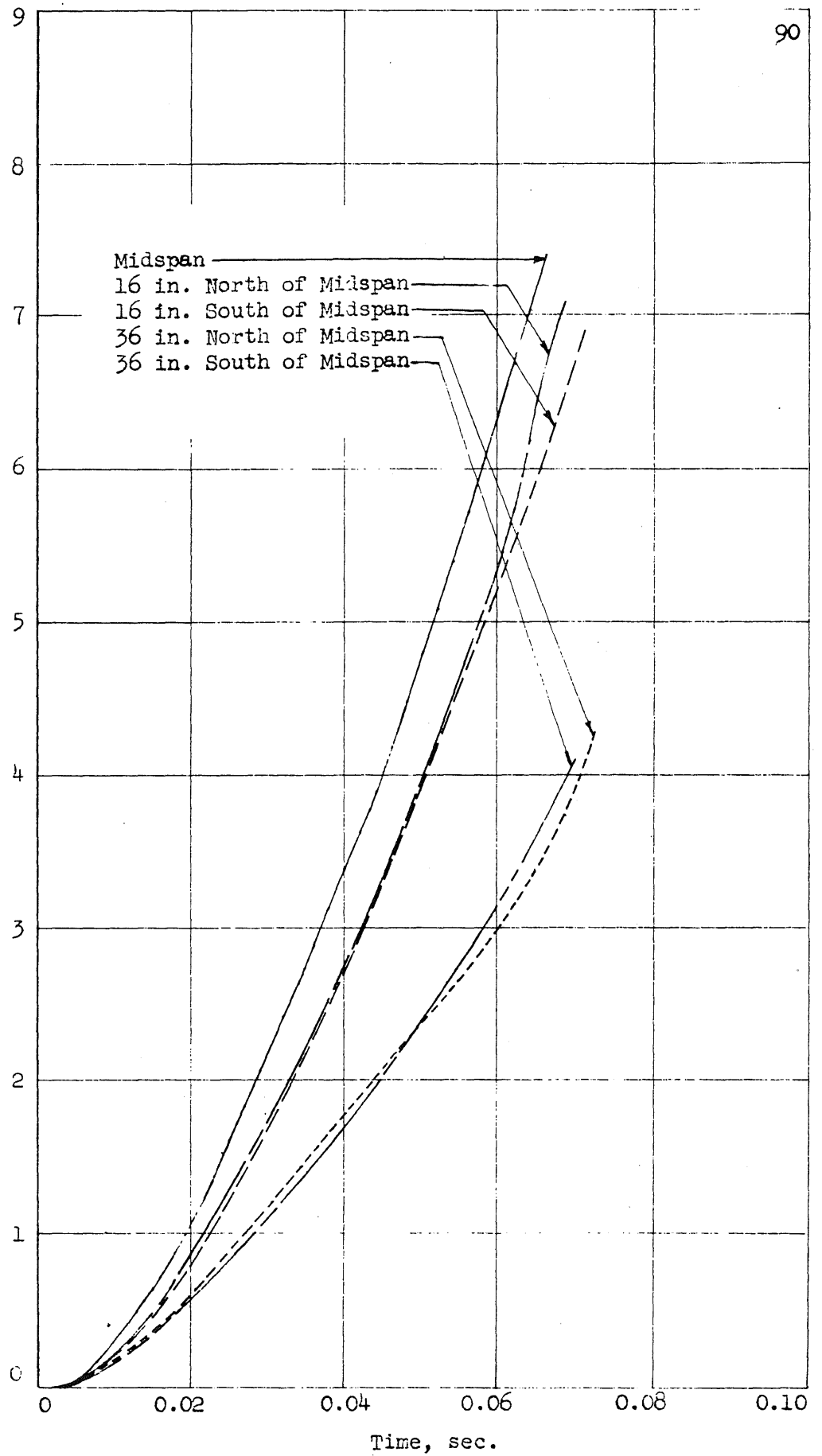


FIG. A4b: RECORDED DATA FROM TEST CB4

Strain in Connection Angle, in./in.

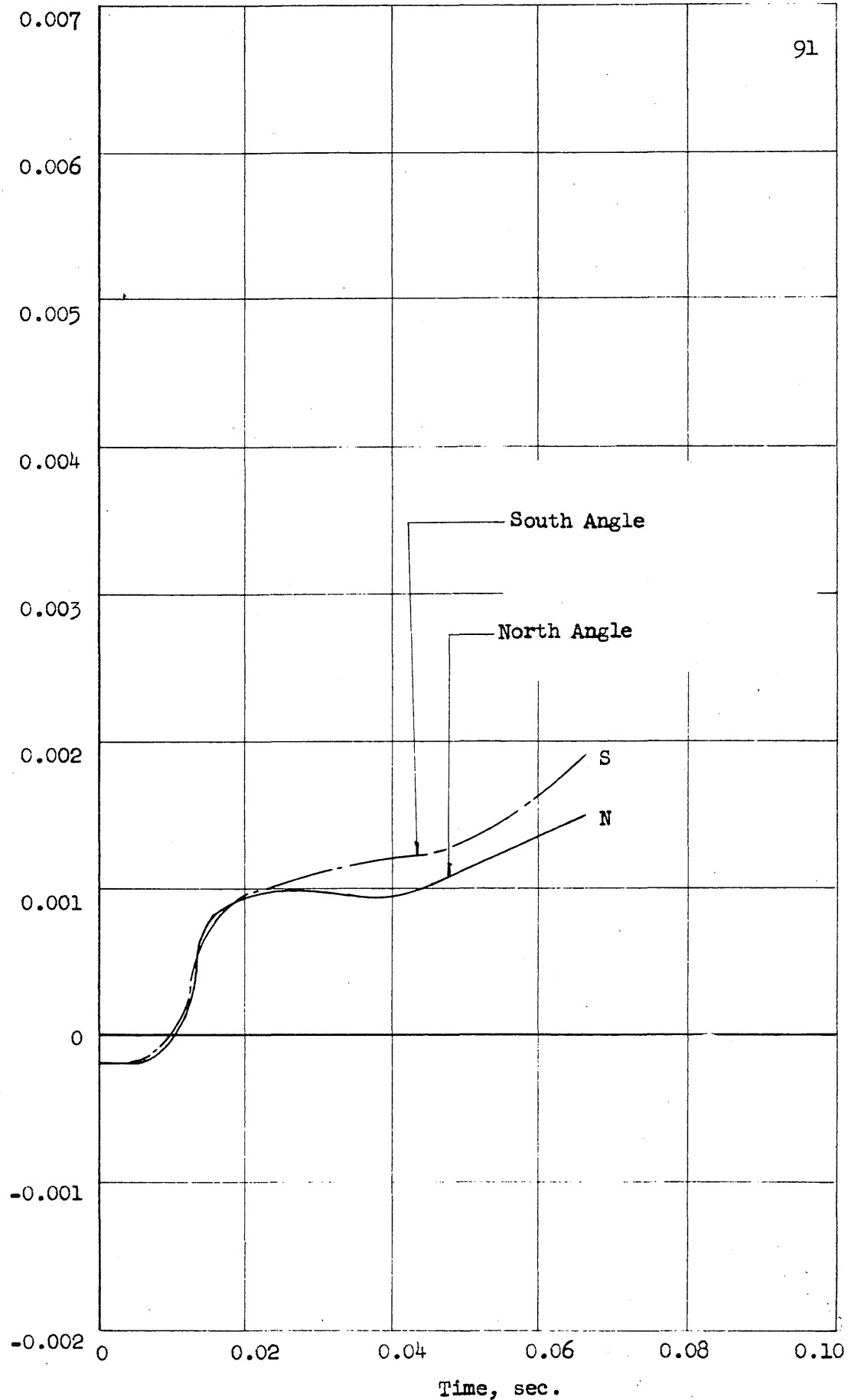


FIG. A+c. RECORDED DATA FROM TEST CB4

Loads and Forces, Kips

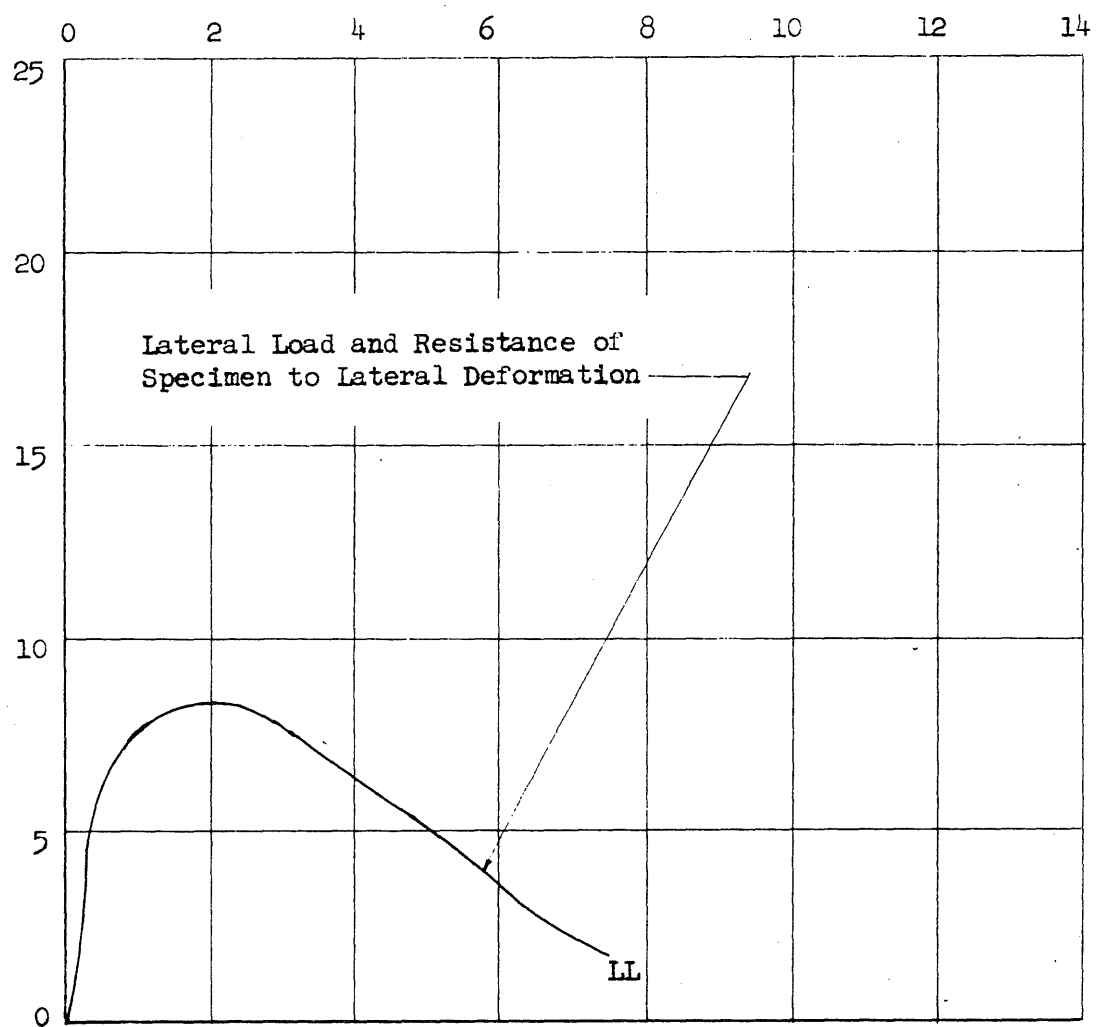
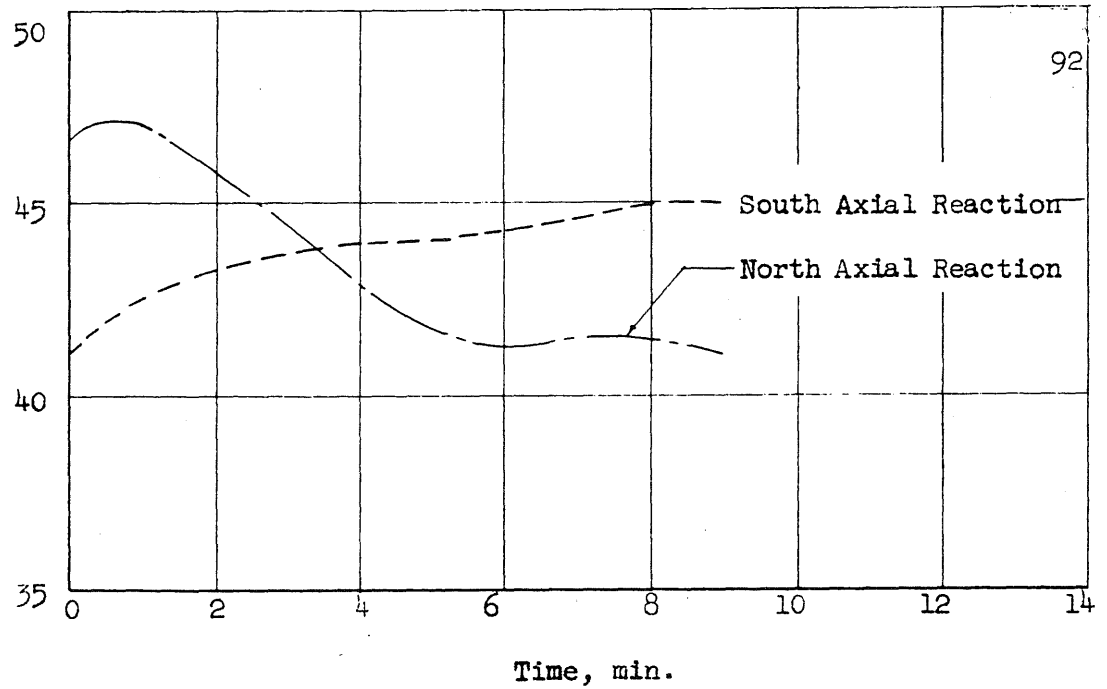


FIG. A5a: RECORDED DATA FROM TEST CB5

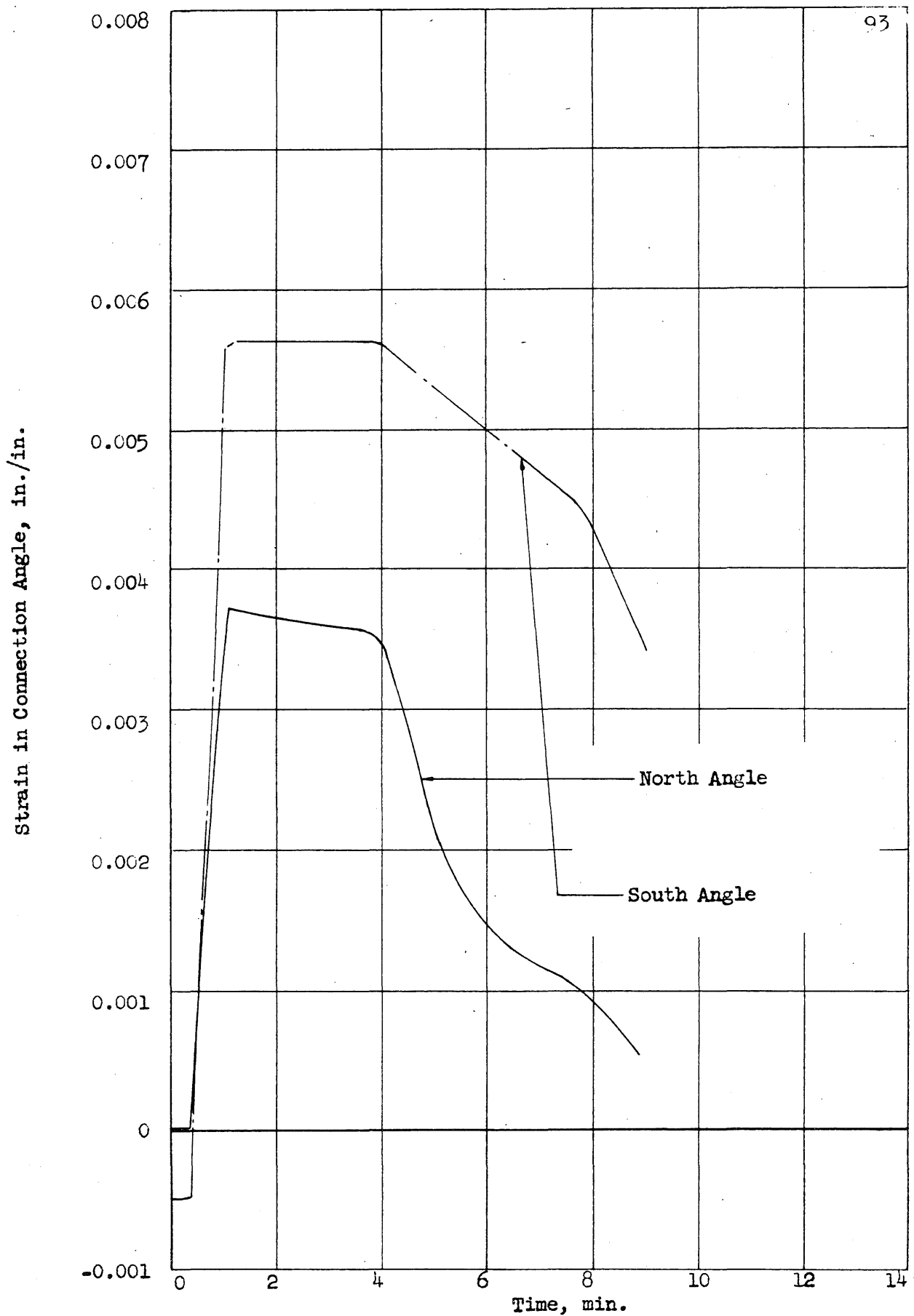


FIG. A5b: RECORDED DATA FROM TEST CB5

Loads and Forces, kips

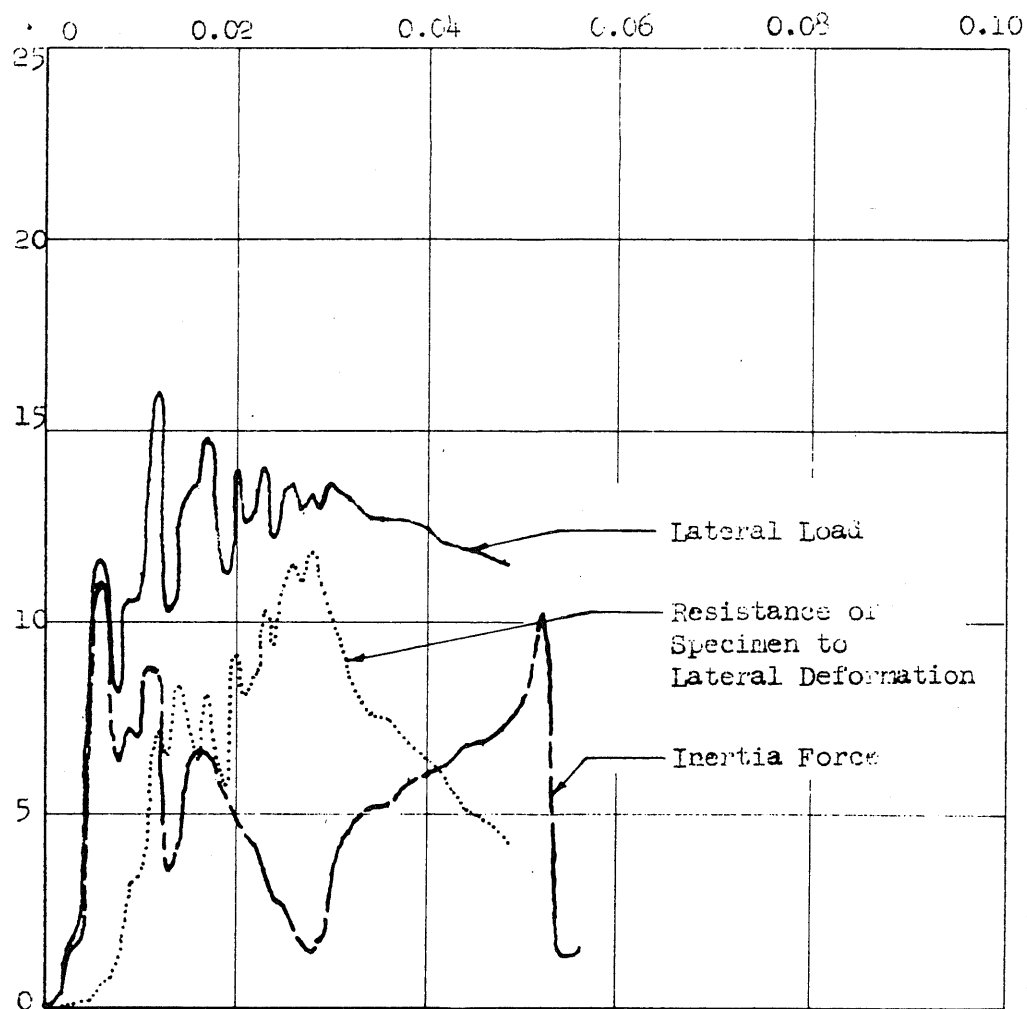
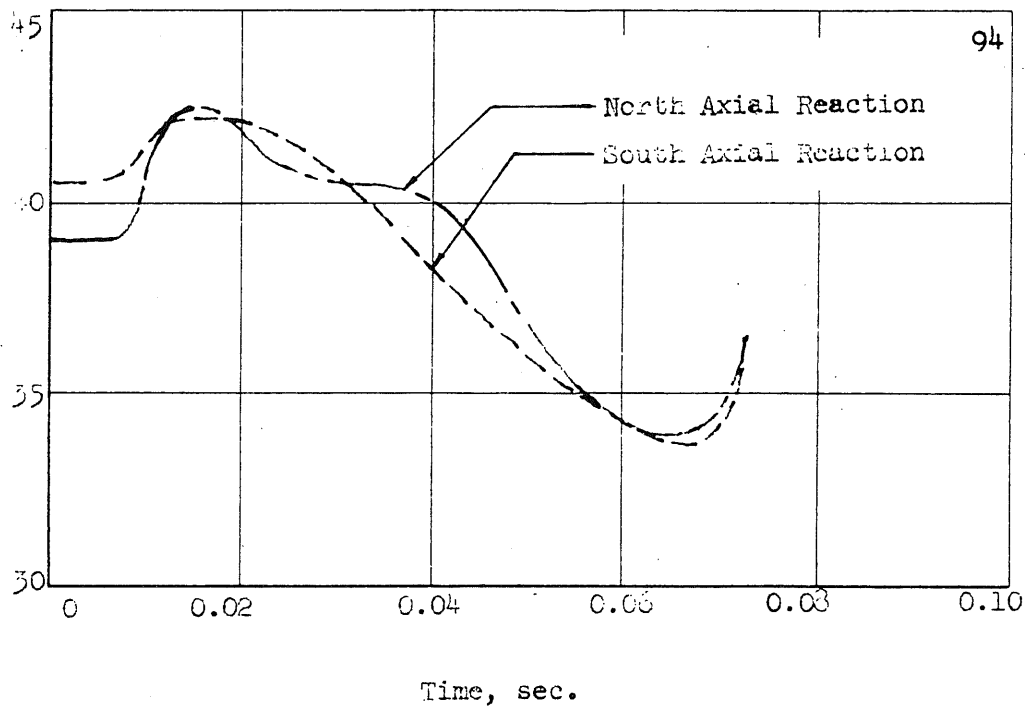


FIG. A6a: RECORDED DATA FROM TEST CB6

Deflection, in.

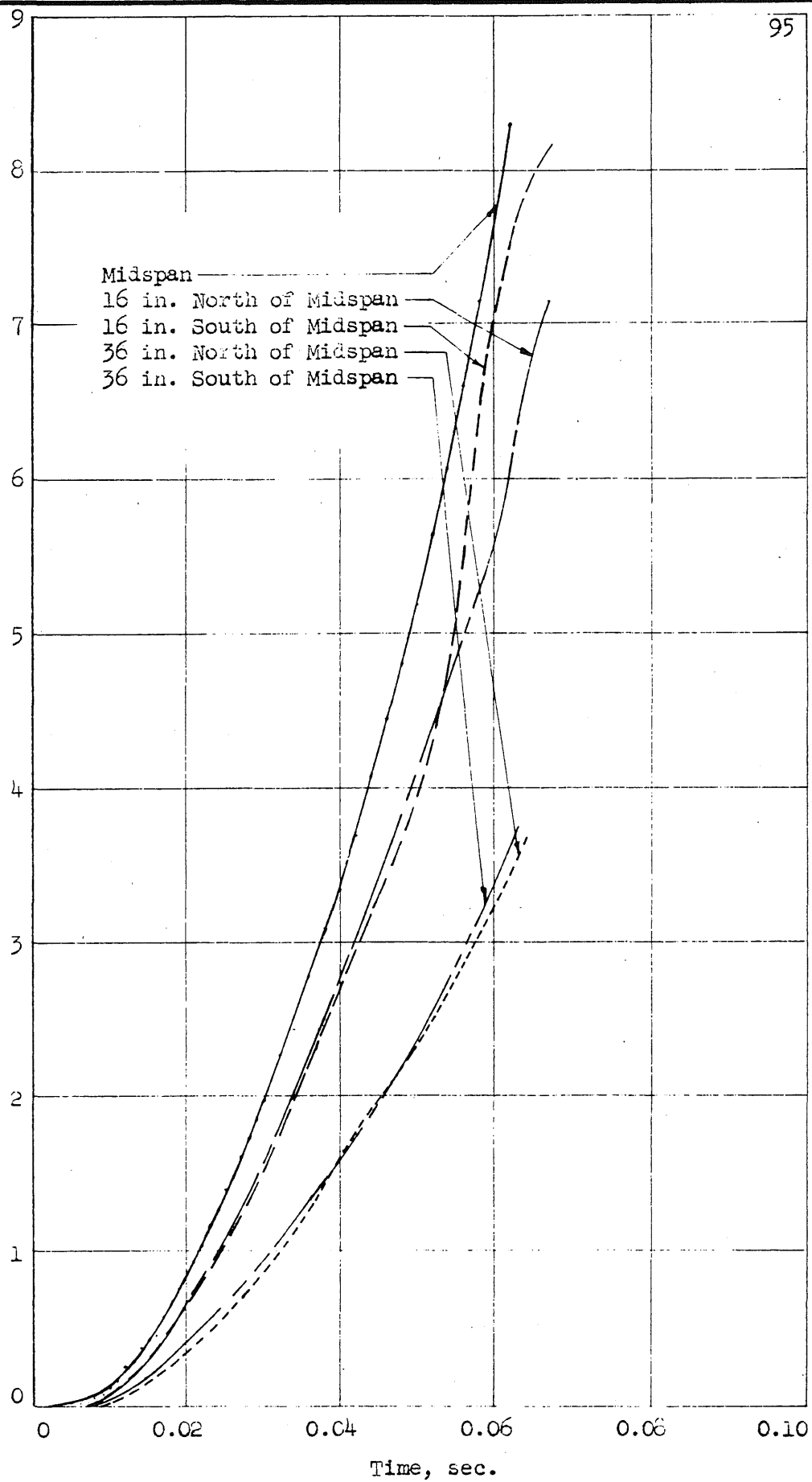


FIG. A6b: RECORDED DATA FROM TEST CB6

Strain in Connection Angle, in./in.

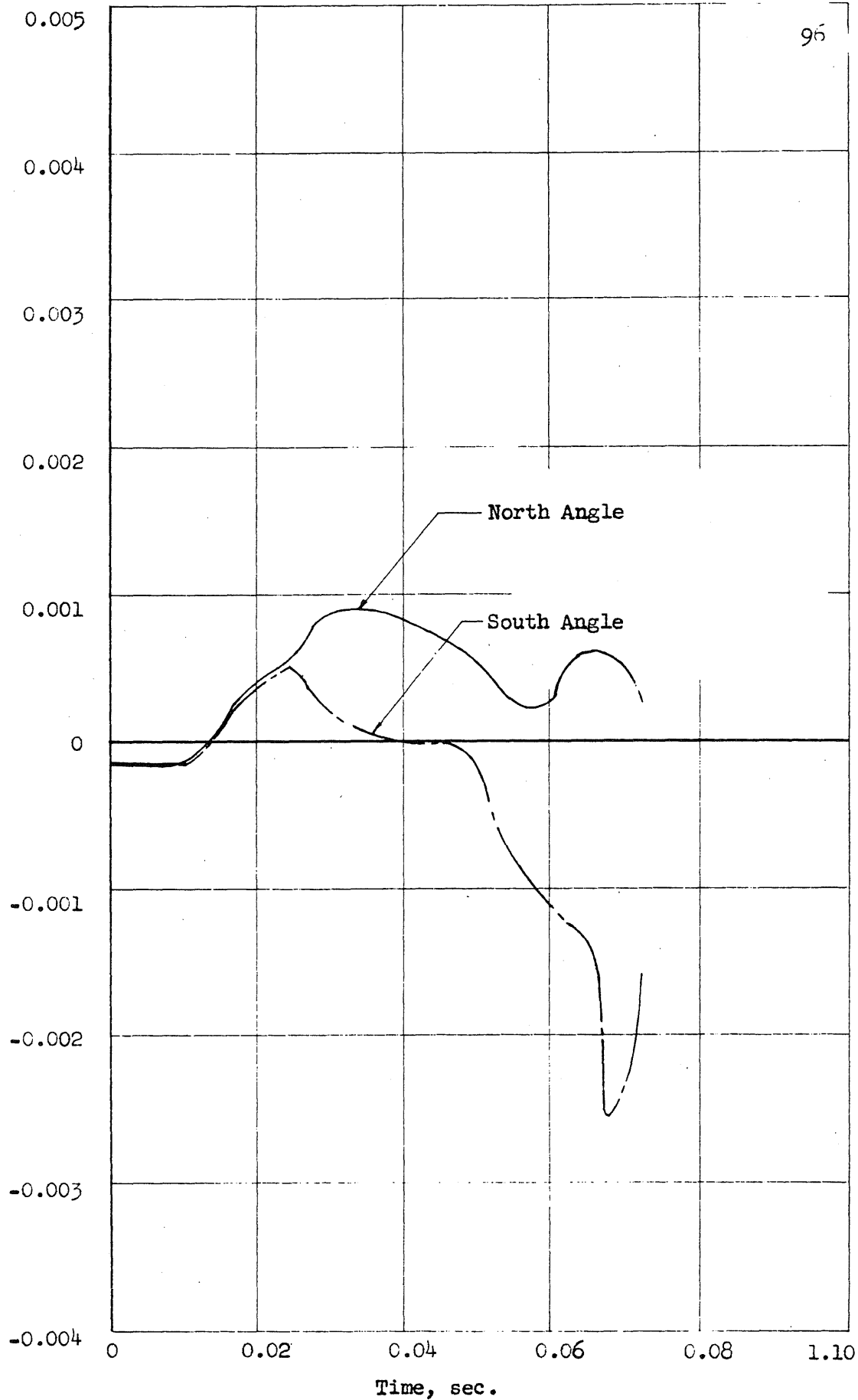


FIG. A66; RECORDED DATA FROM TEST CB6

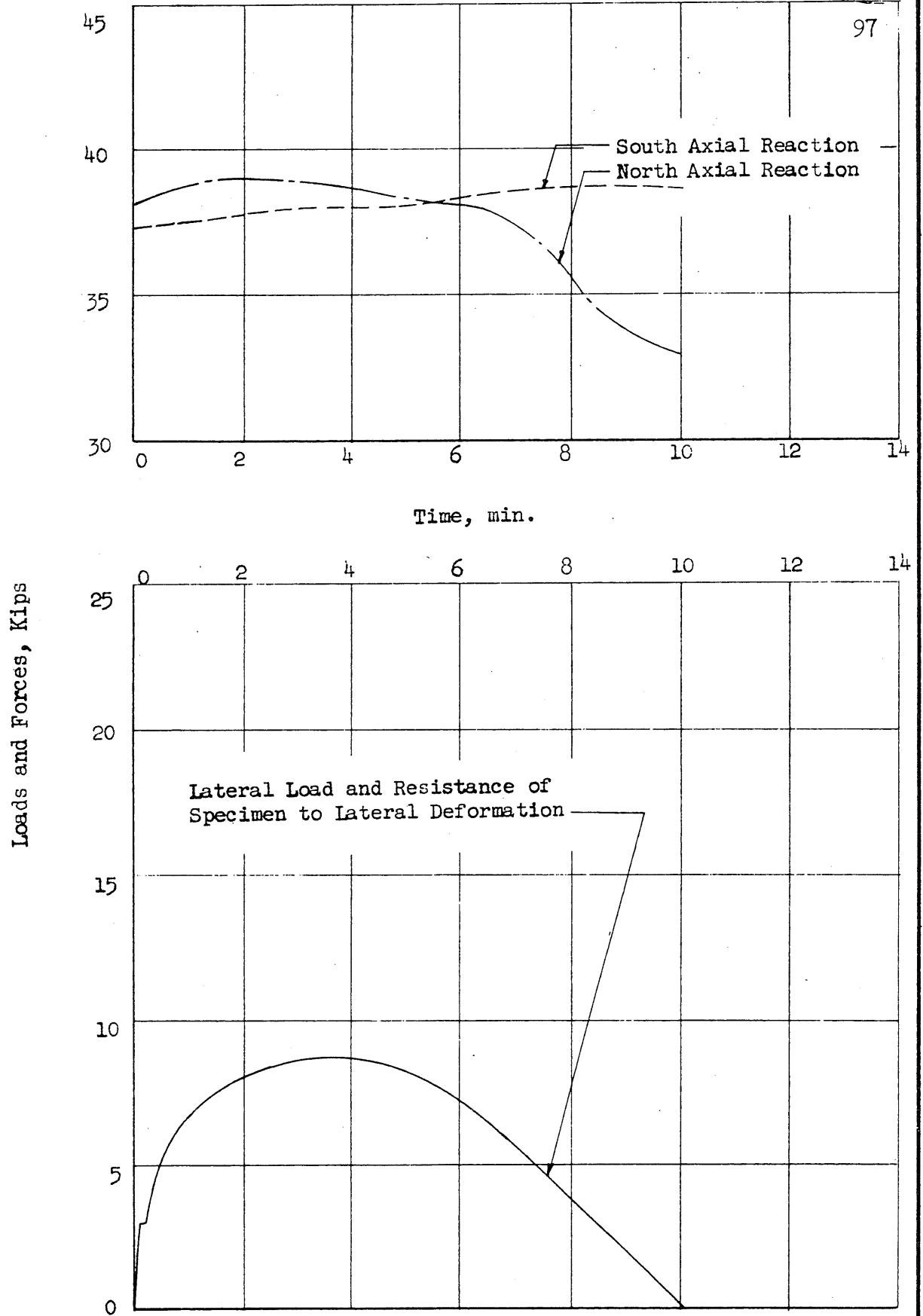


FIG. A1a: RECORDED DATA FROM TEST CB7

Deflection, in.

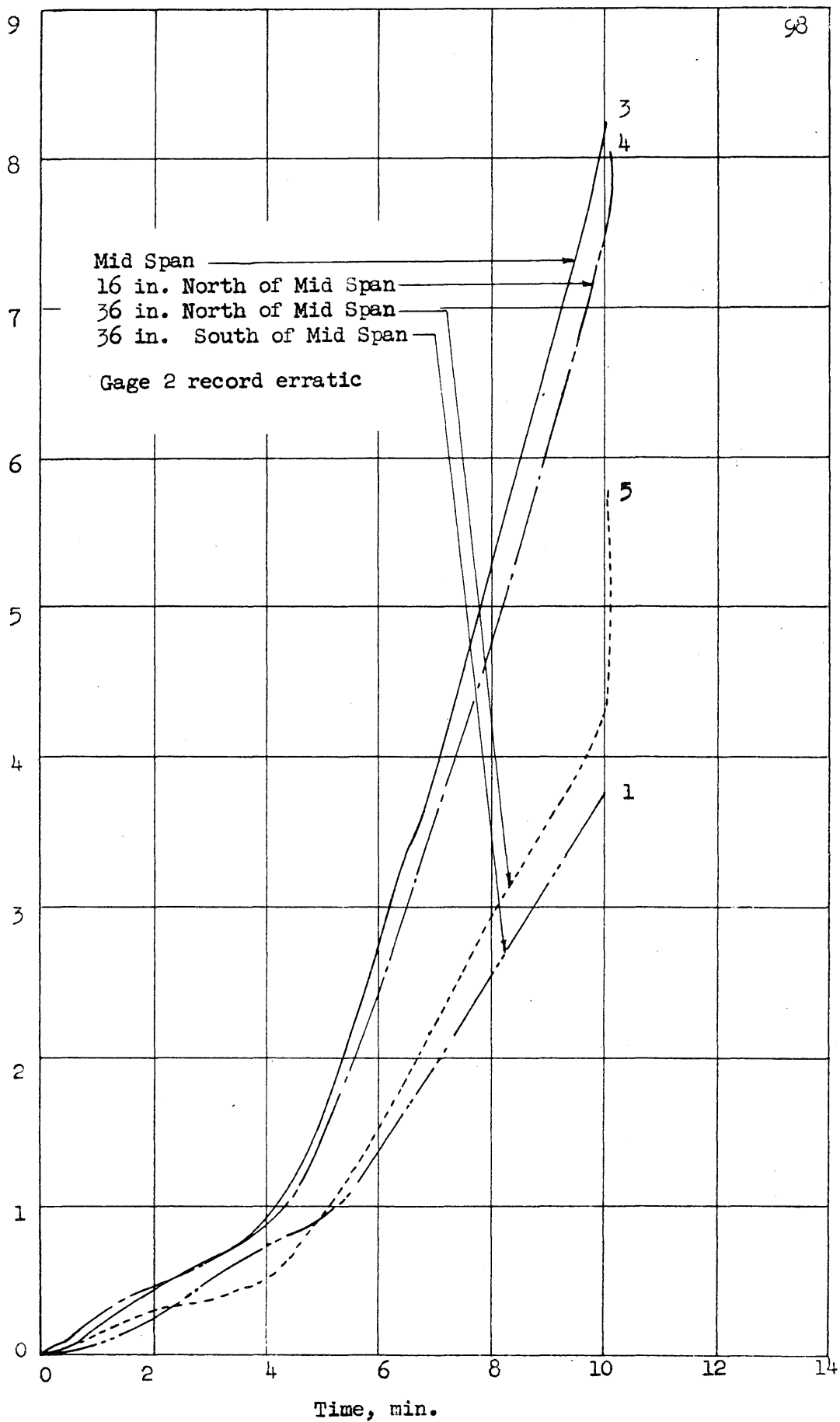


FIG. A7b: RECORDED DATA FROM TEST CB7

Strain in Connection Angle, in./in.

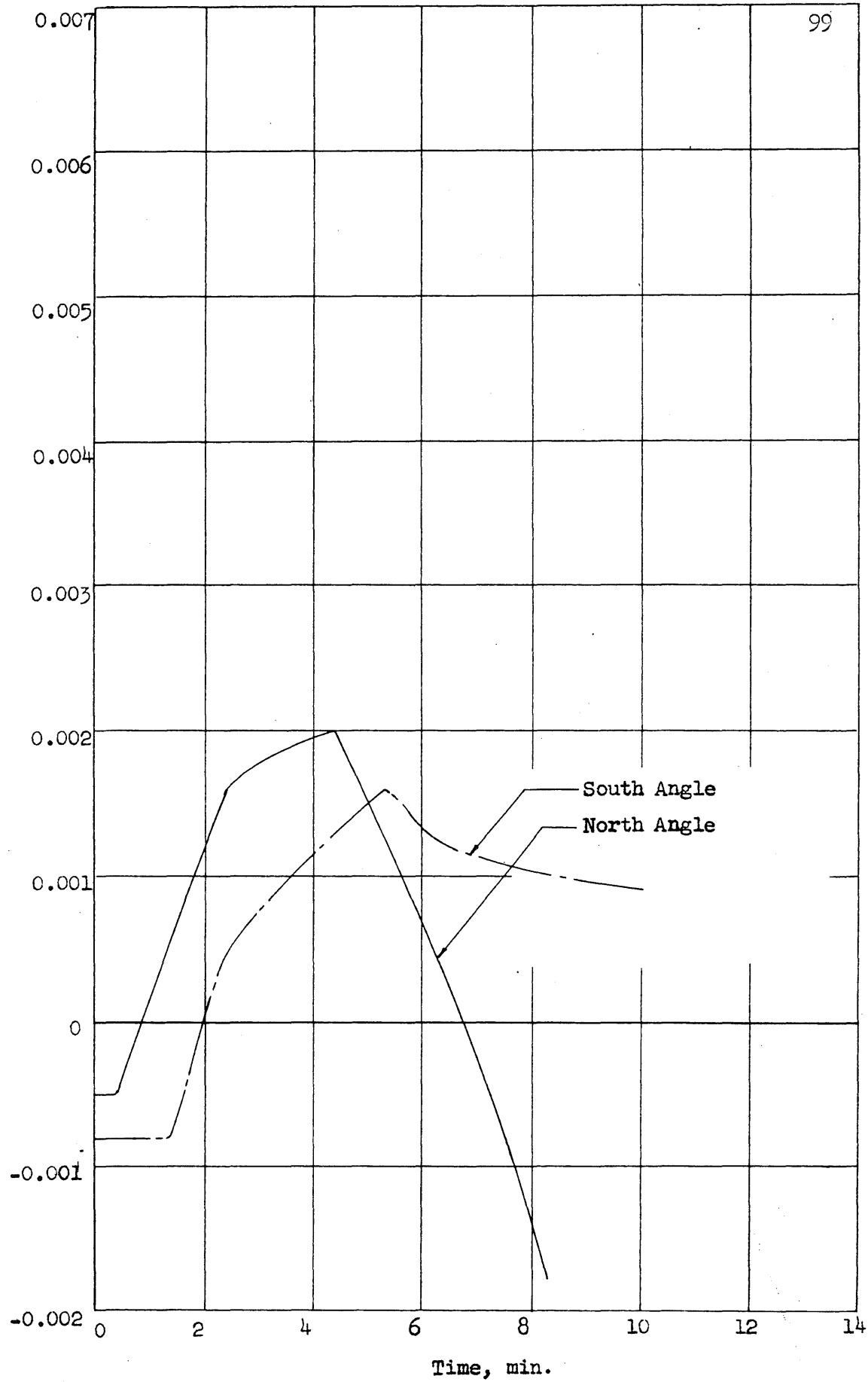
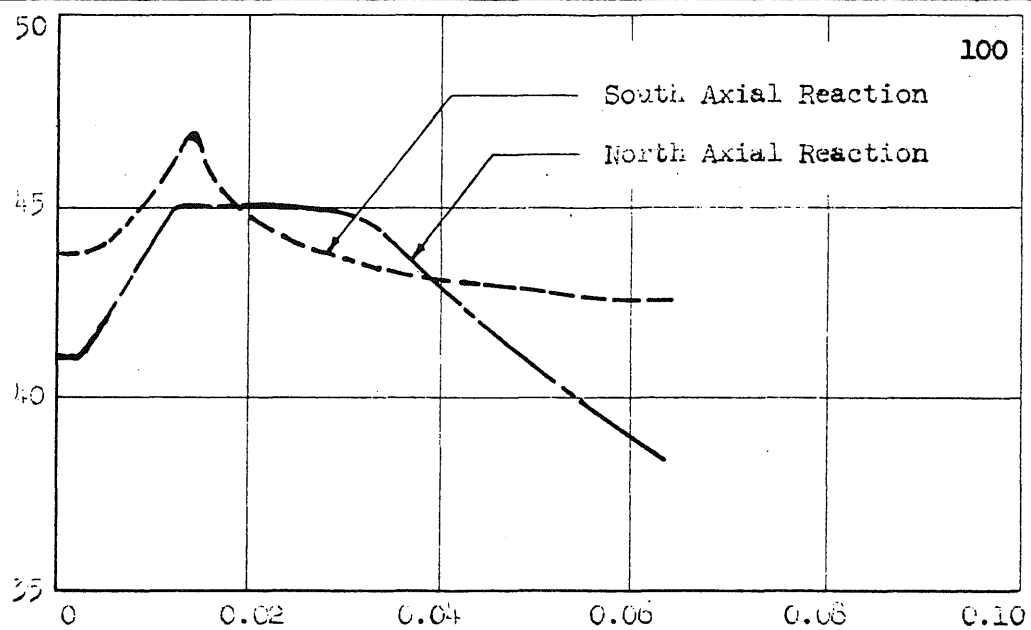


FIG. A7c: RECORDED DATA FROM TEST CB7

Loads and Forces, kips



Time, sec.

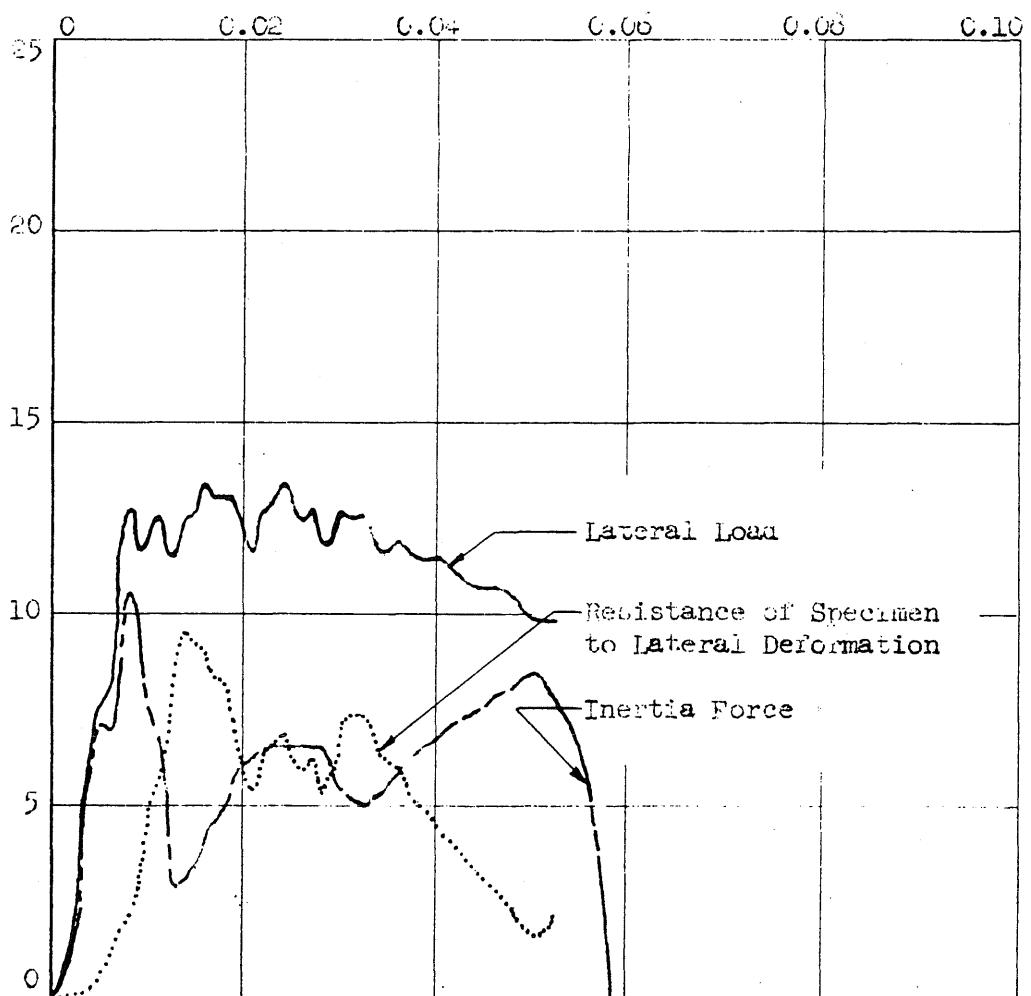


FIG. A8a: RECORDED DATA FROM TEST CB8

Deflection, in.

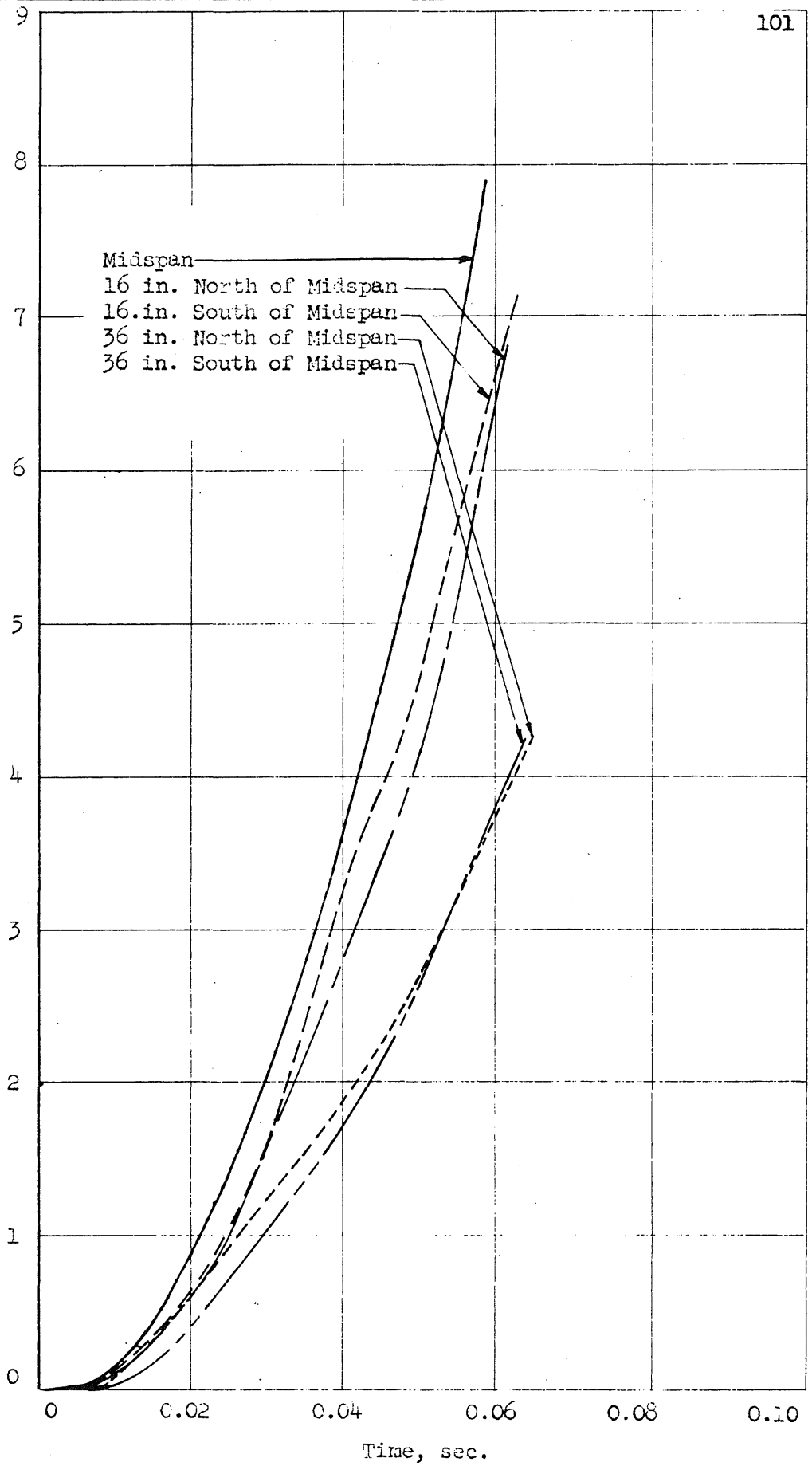


FIG. A8b: RECORDED DATA FROM TEST CB8

Strain in Connection Angle in./in.

0.005

0.004

0.003

0.002

0.001

0.

-0.001

-0.002

-0.003

-0.004

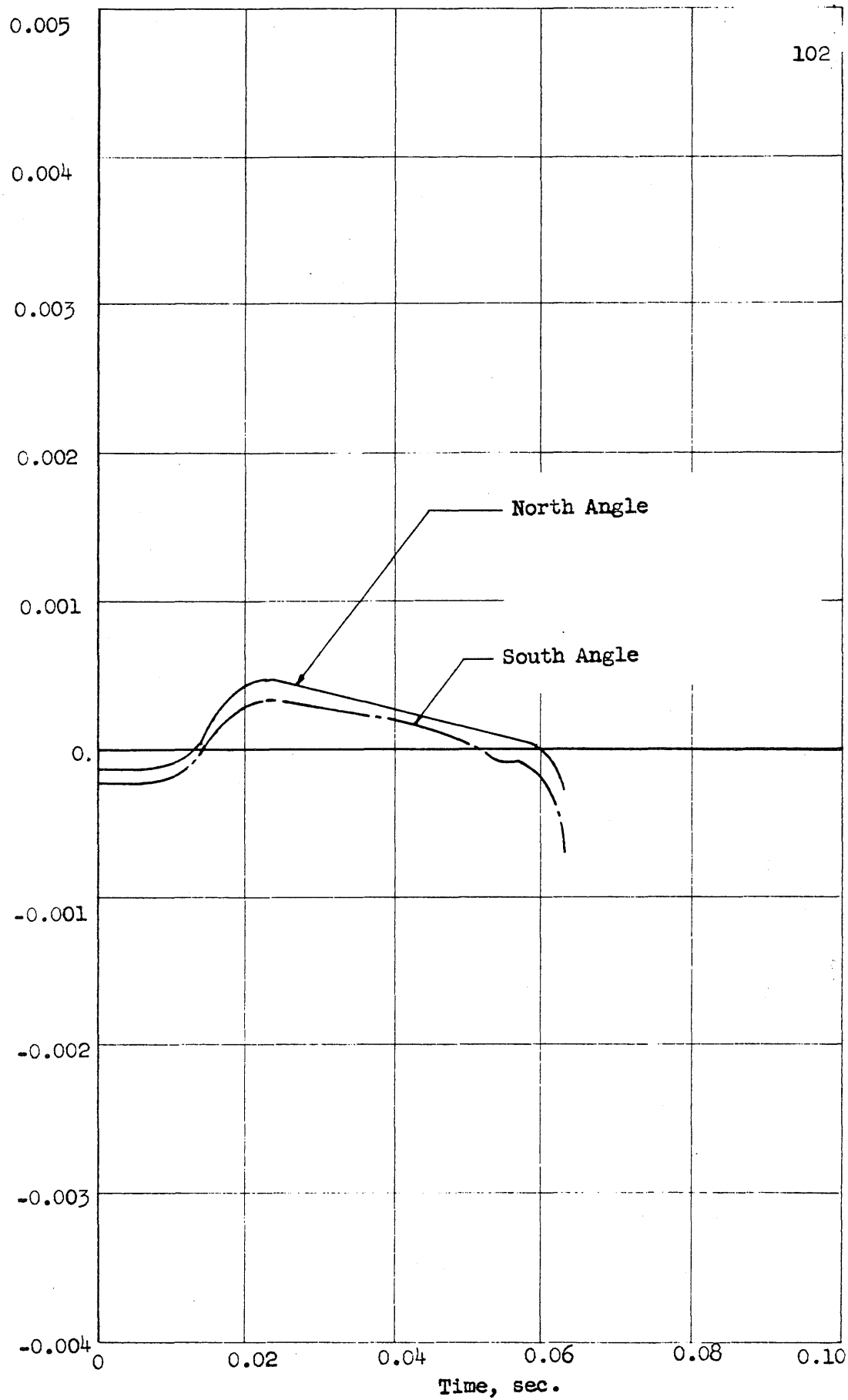
102

North Angle

South Angle

Time, sec.

FIG. A86: RECORDED DATA FROM TEST CB8



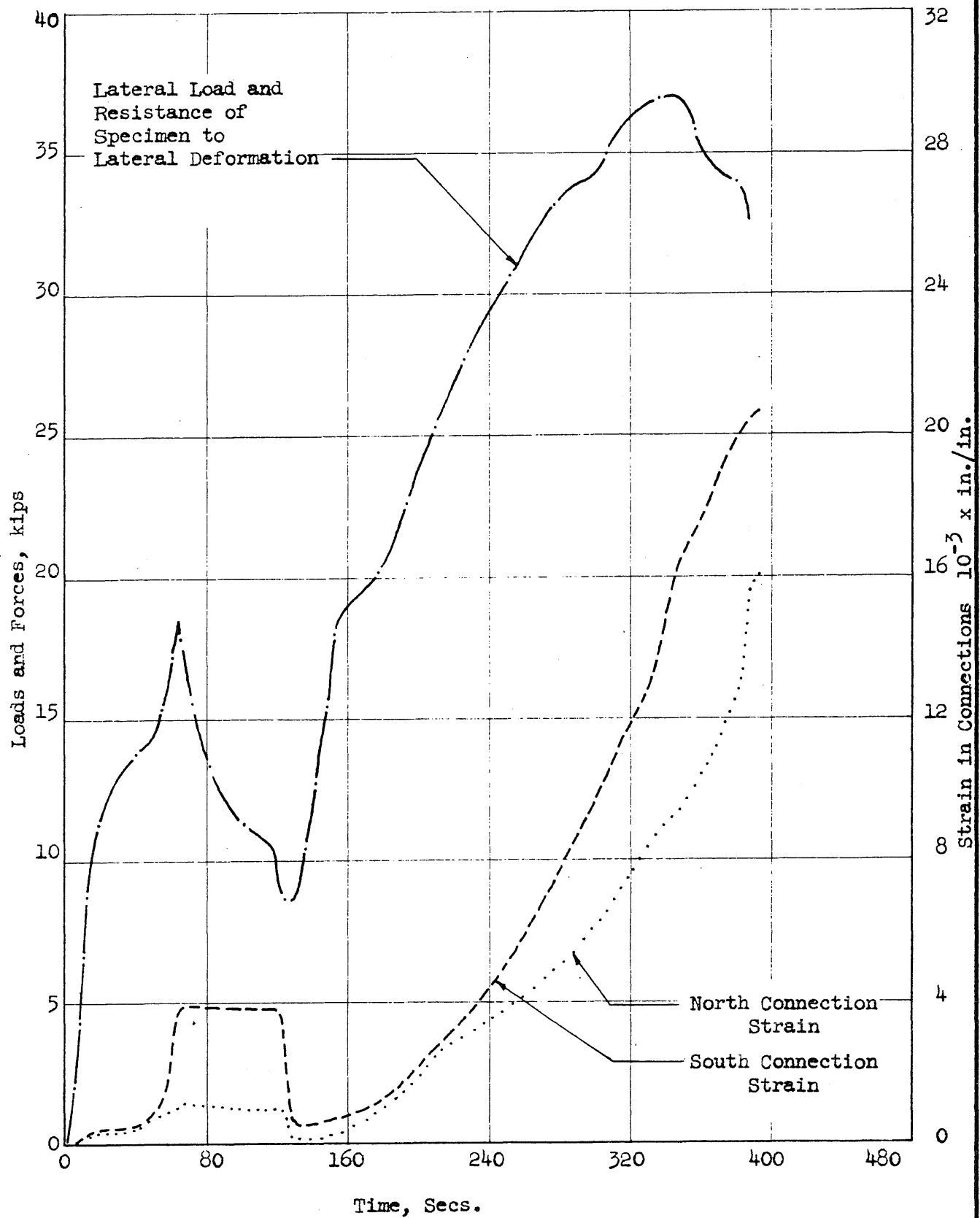


FIG. A9a: RECORDED DATA FROM TEST CTBS

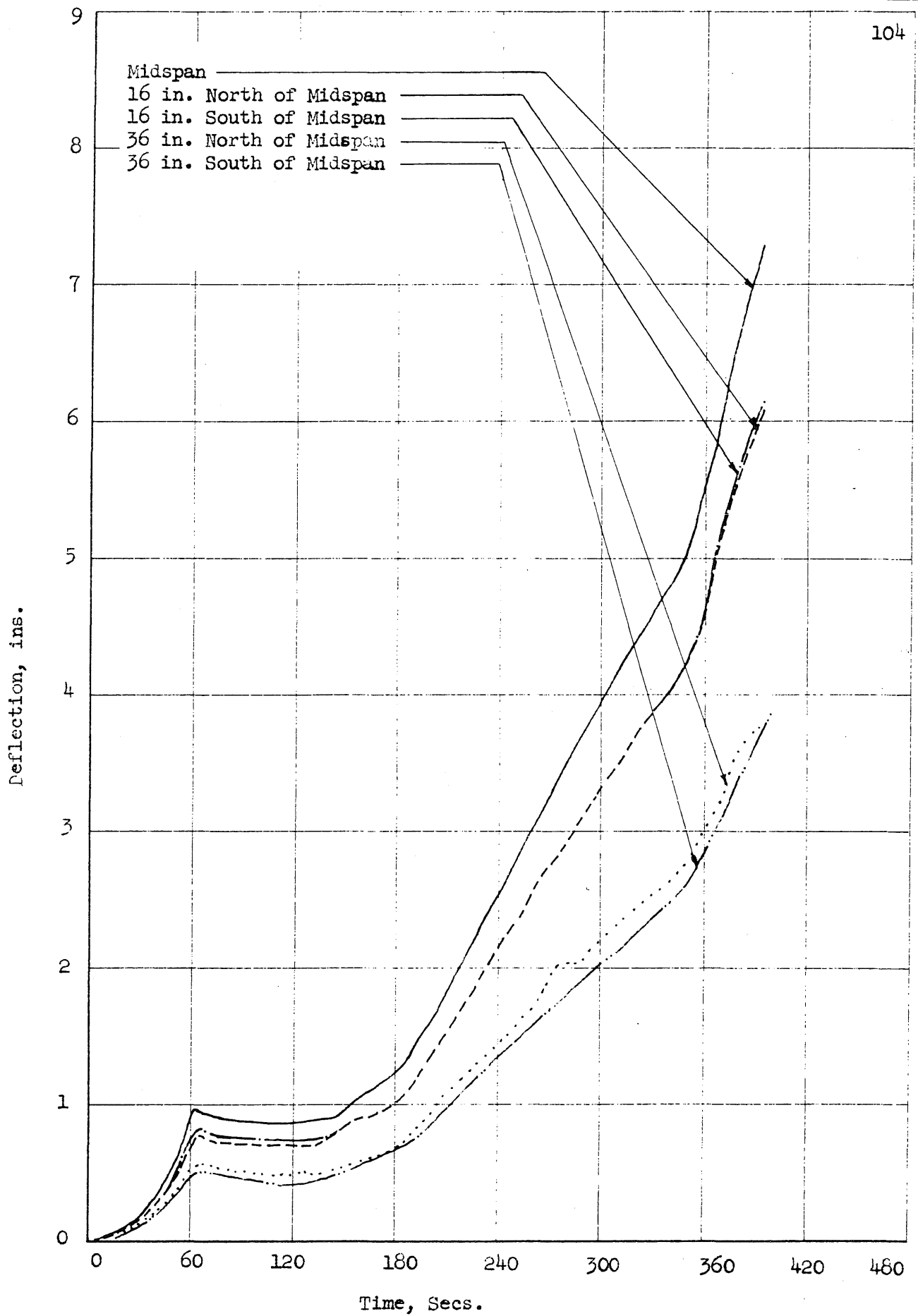


FIG. A9b: RECORDED DATA FROM TEST CTBS

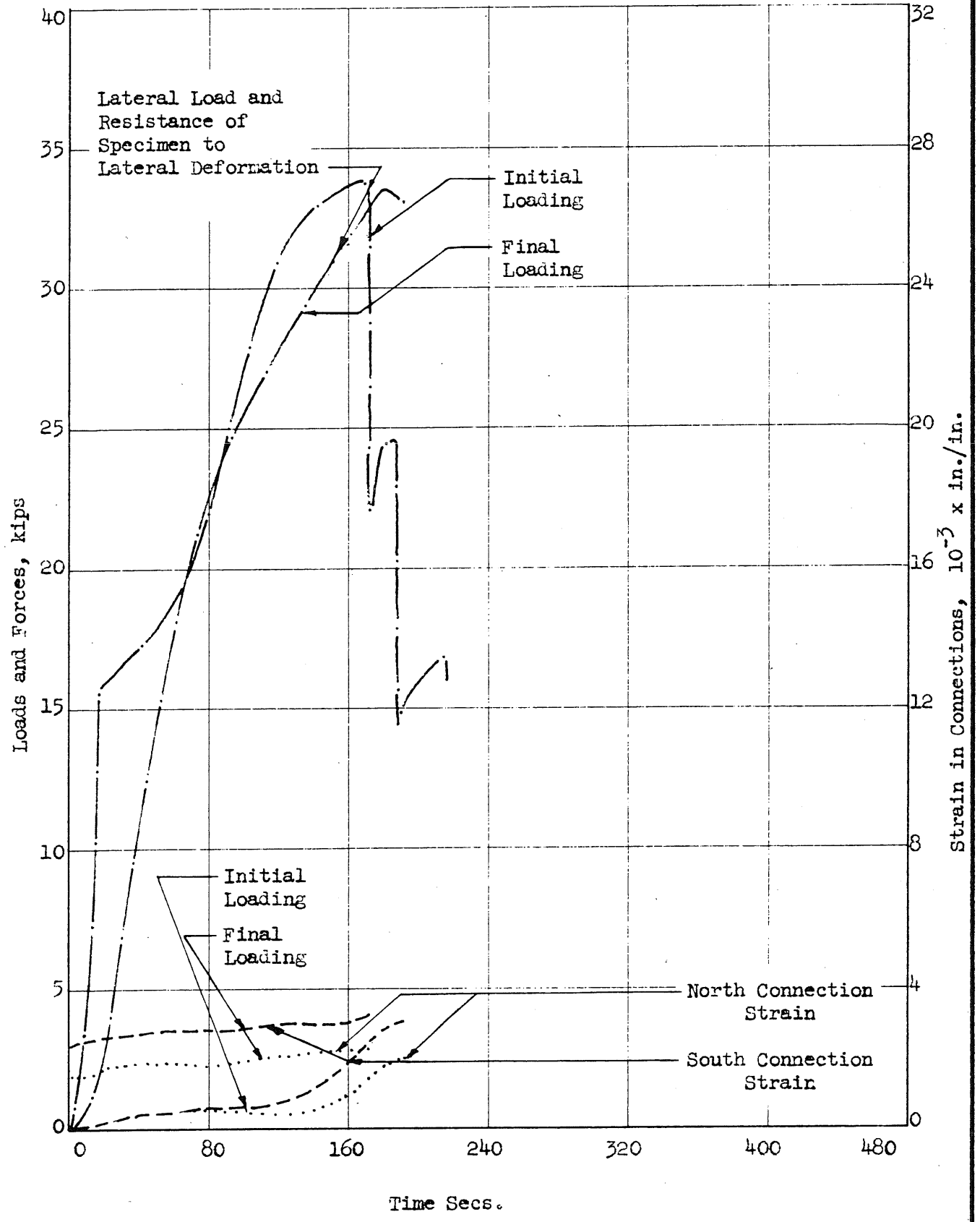


FIG. A10a: RECORDED DATA FROM TEST CTRS

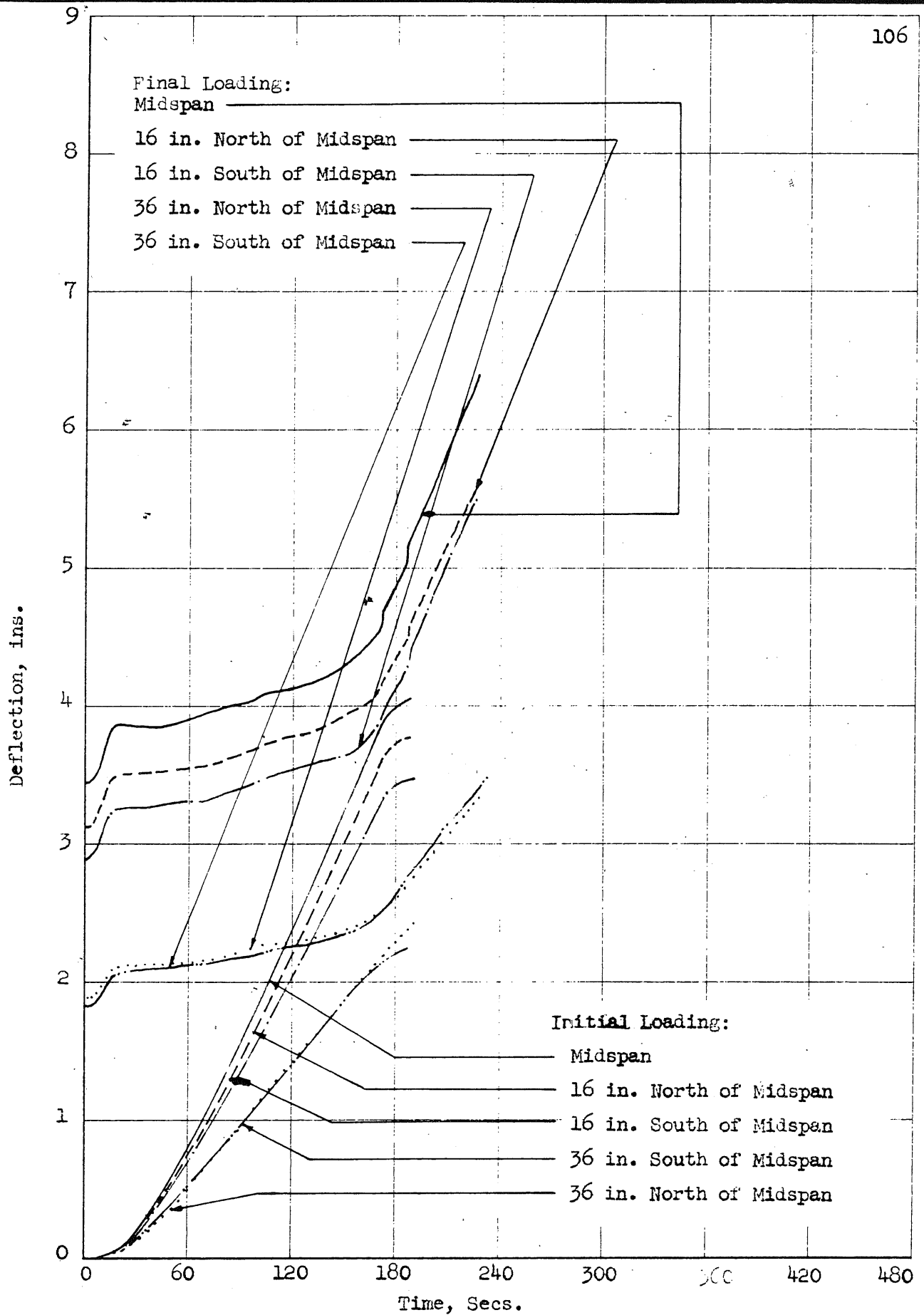


FIG. A10b: RECORDED DATA FROM TEST CTRS

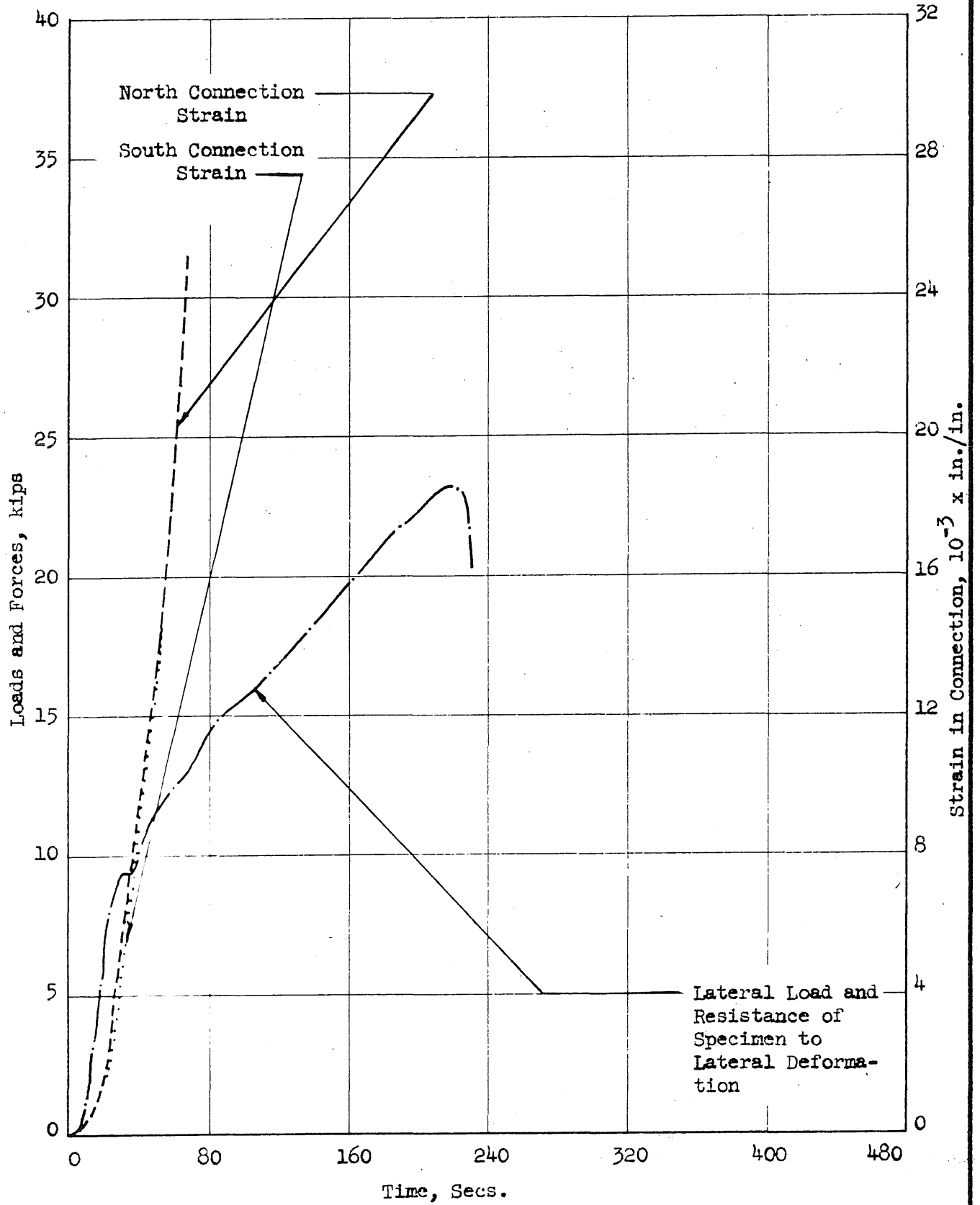


FIG. Alla: RECORDED DATA FROM TEST CFBS

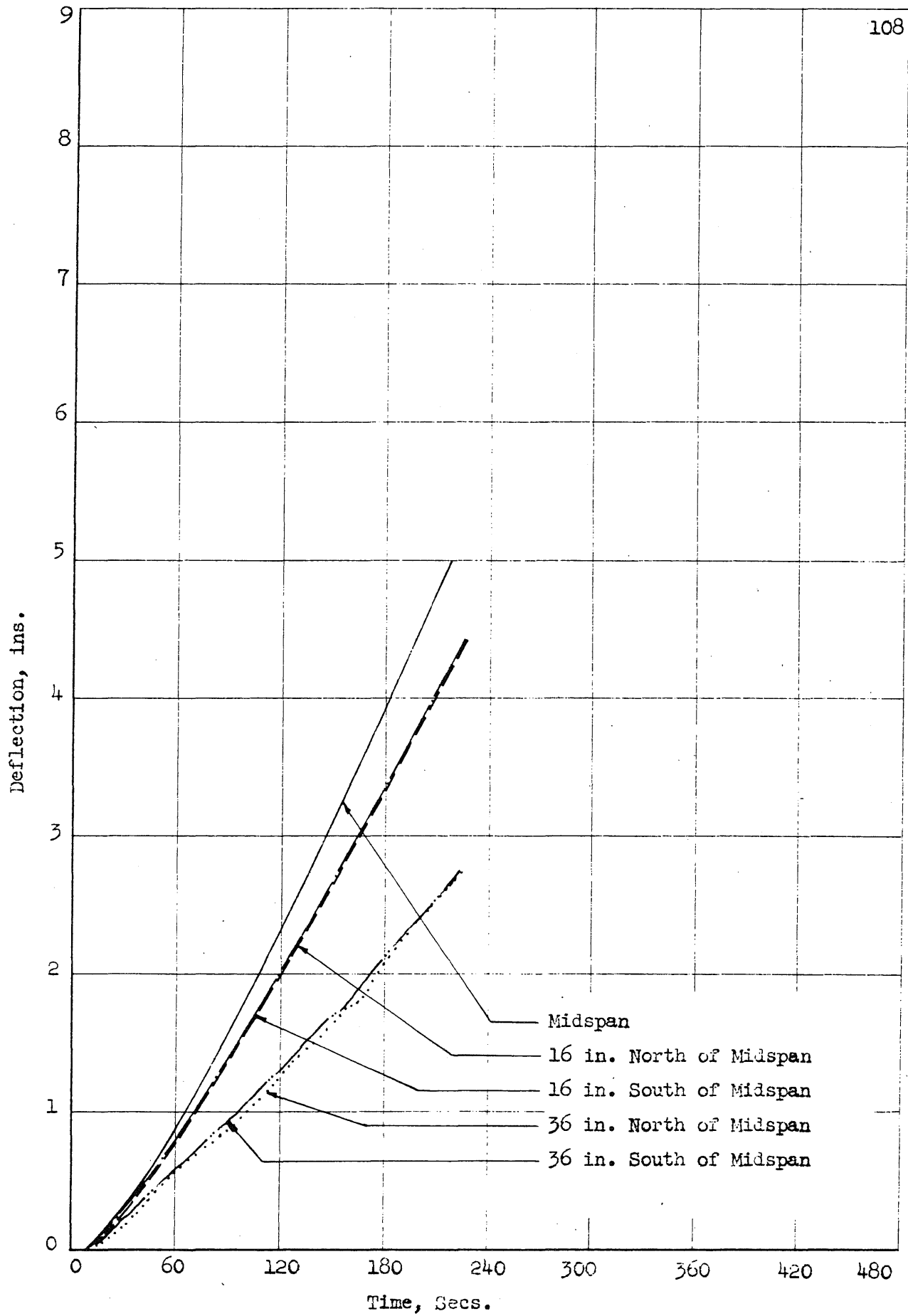


FIG. Allb: RECORDED DATA FROM TEST CFBS

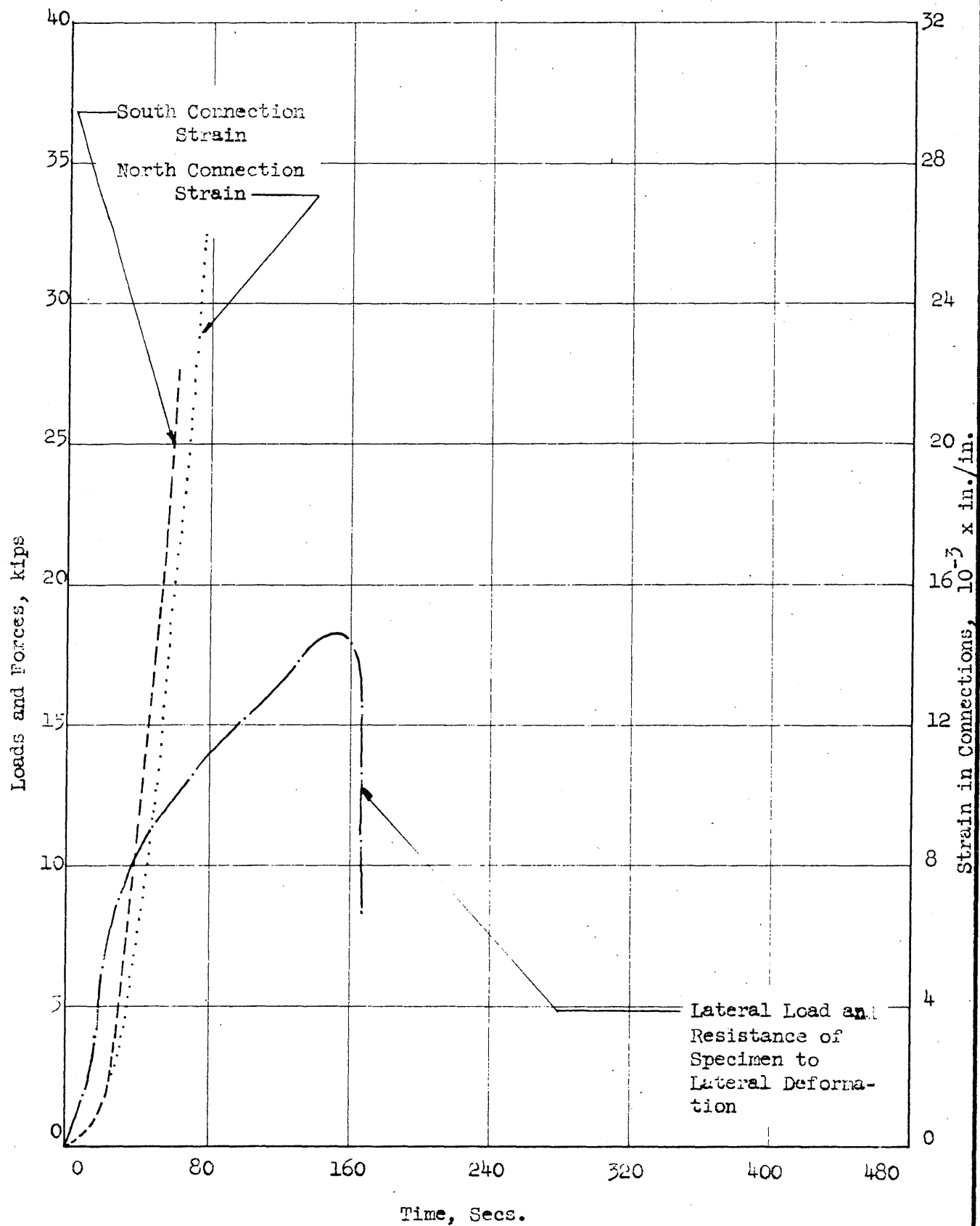


FIG. A12a: RECORDED DATA FROM TEST CFRS

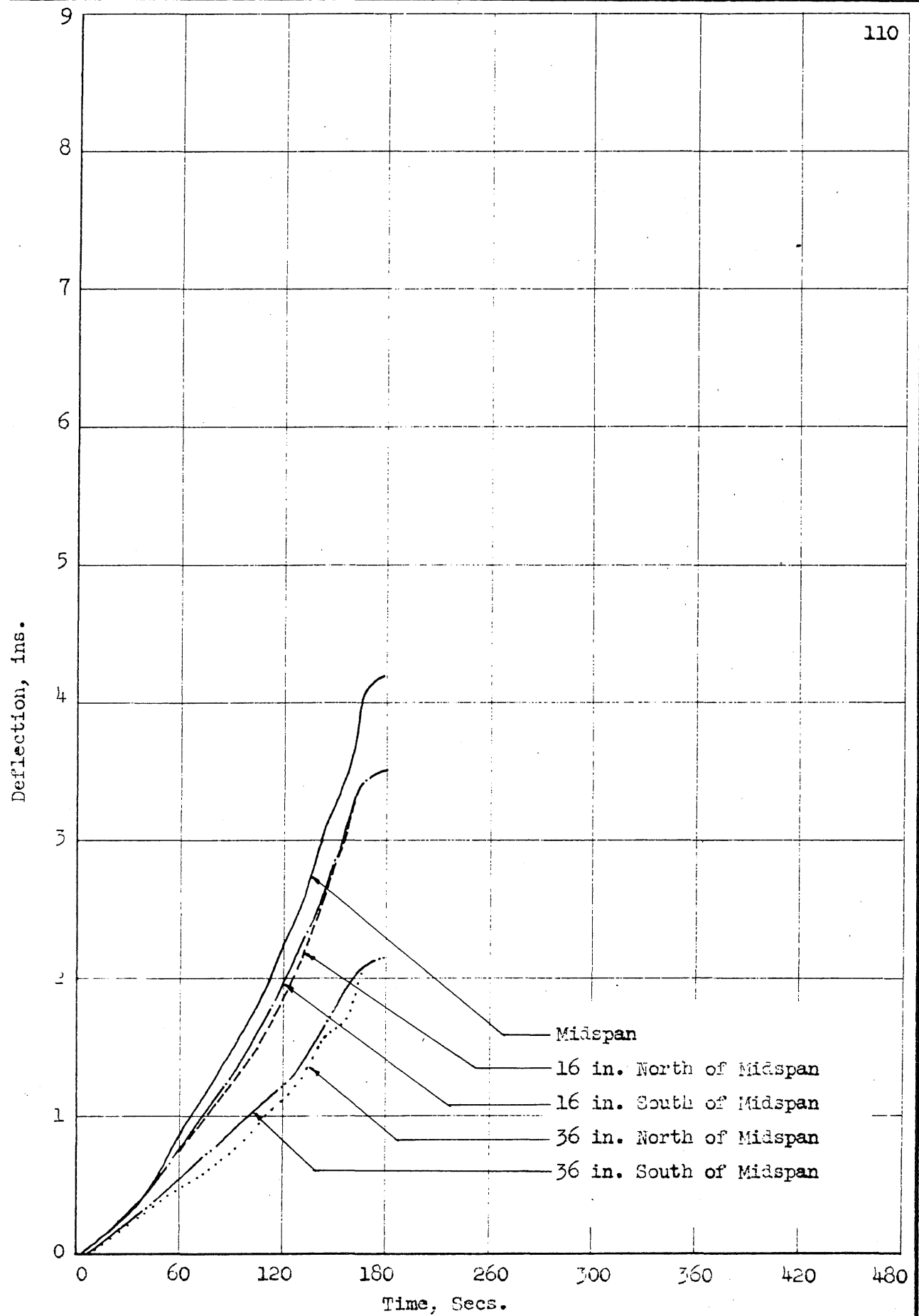


FIG. AL2b: RECORDED DATA FROM TEST CFRS

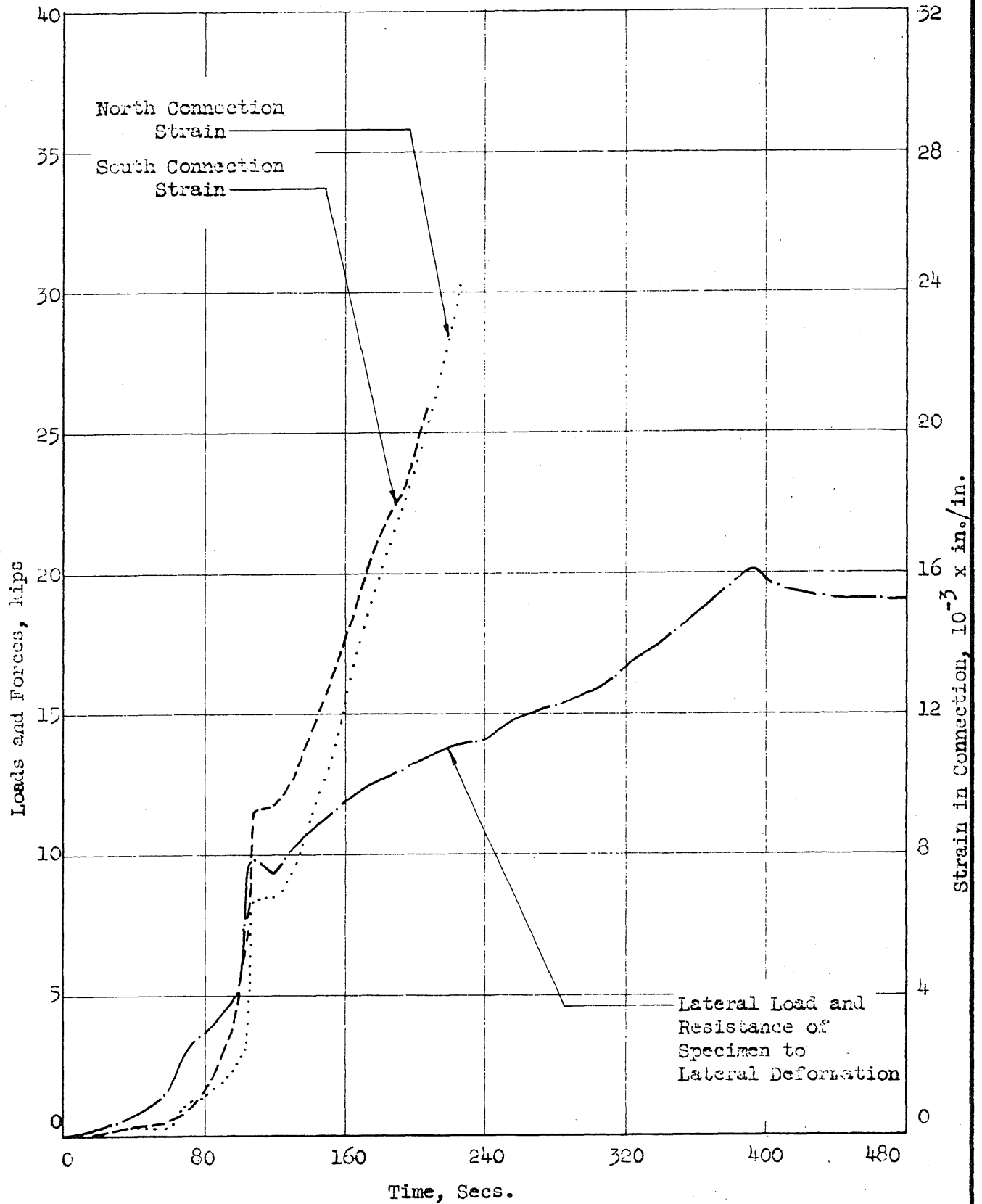


FIG. A13a: RECORDED DATA FROM TEST CWBS

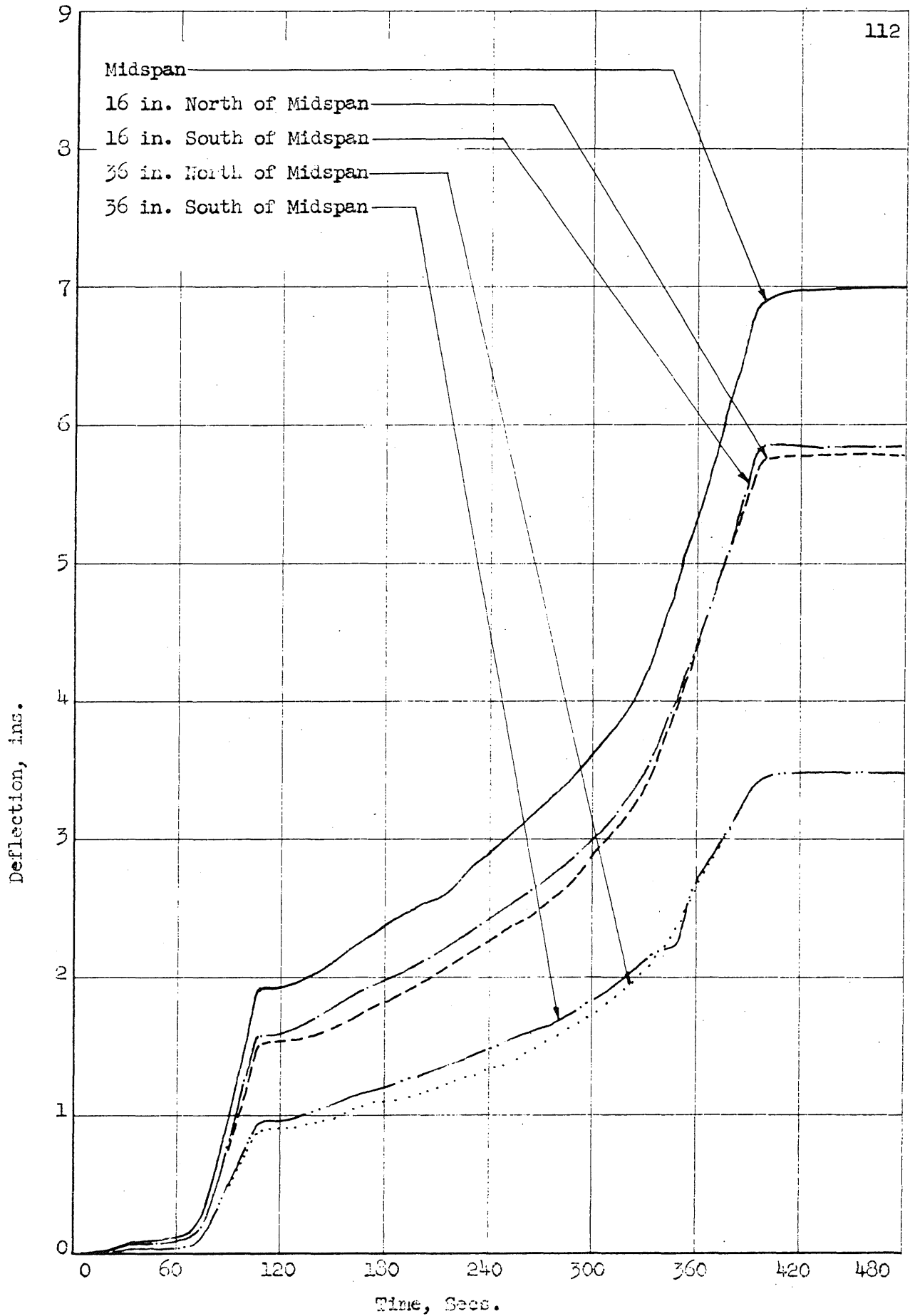


FIG. A131: RECORDED DATA FROM TEST CWBS

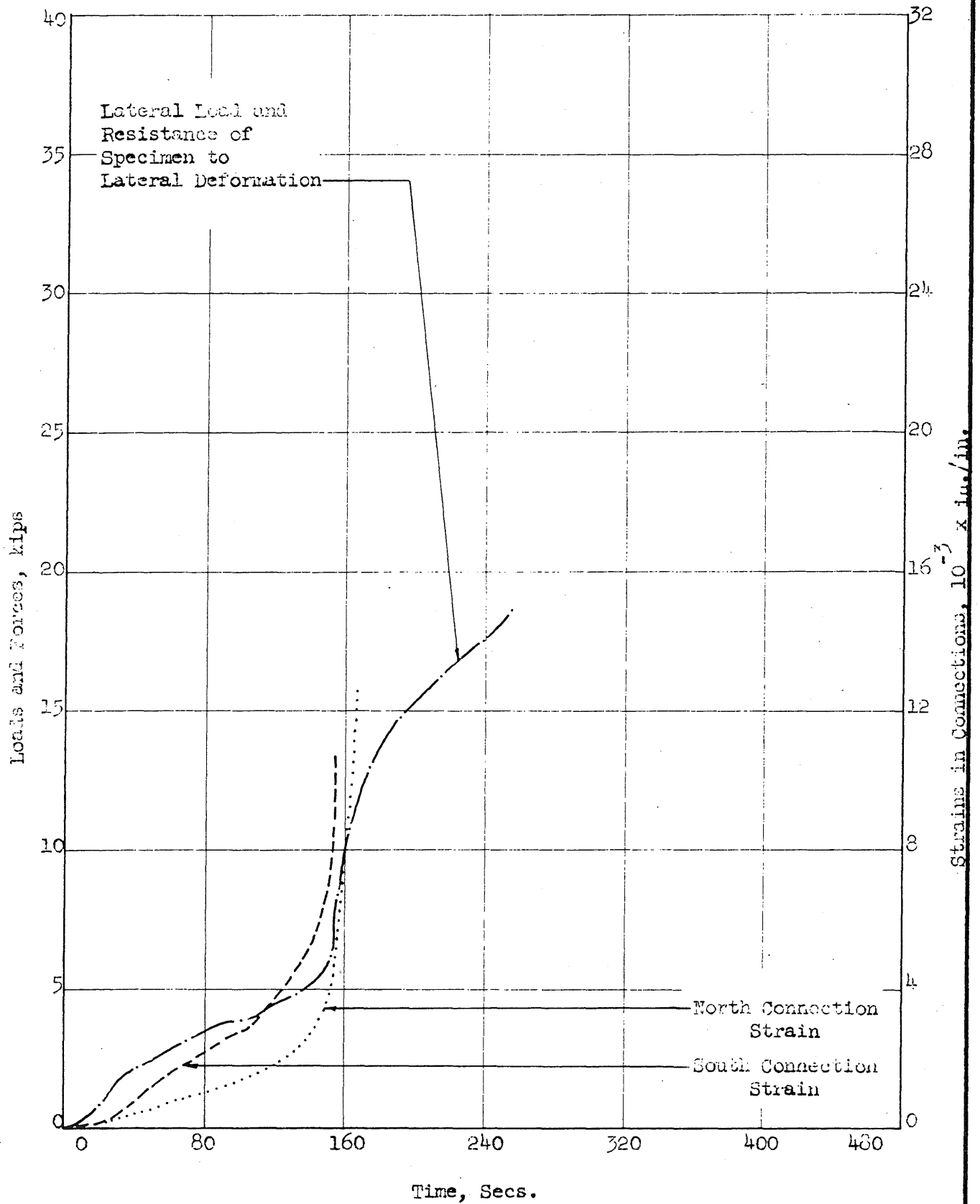


FIG. A14a: RECORDED DATA FROM TEST CMRS

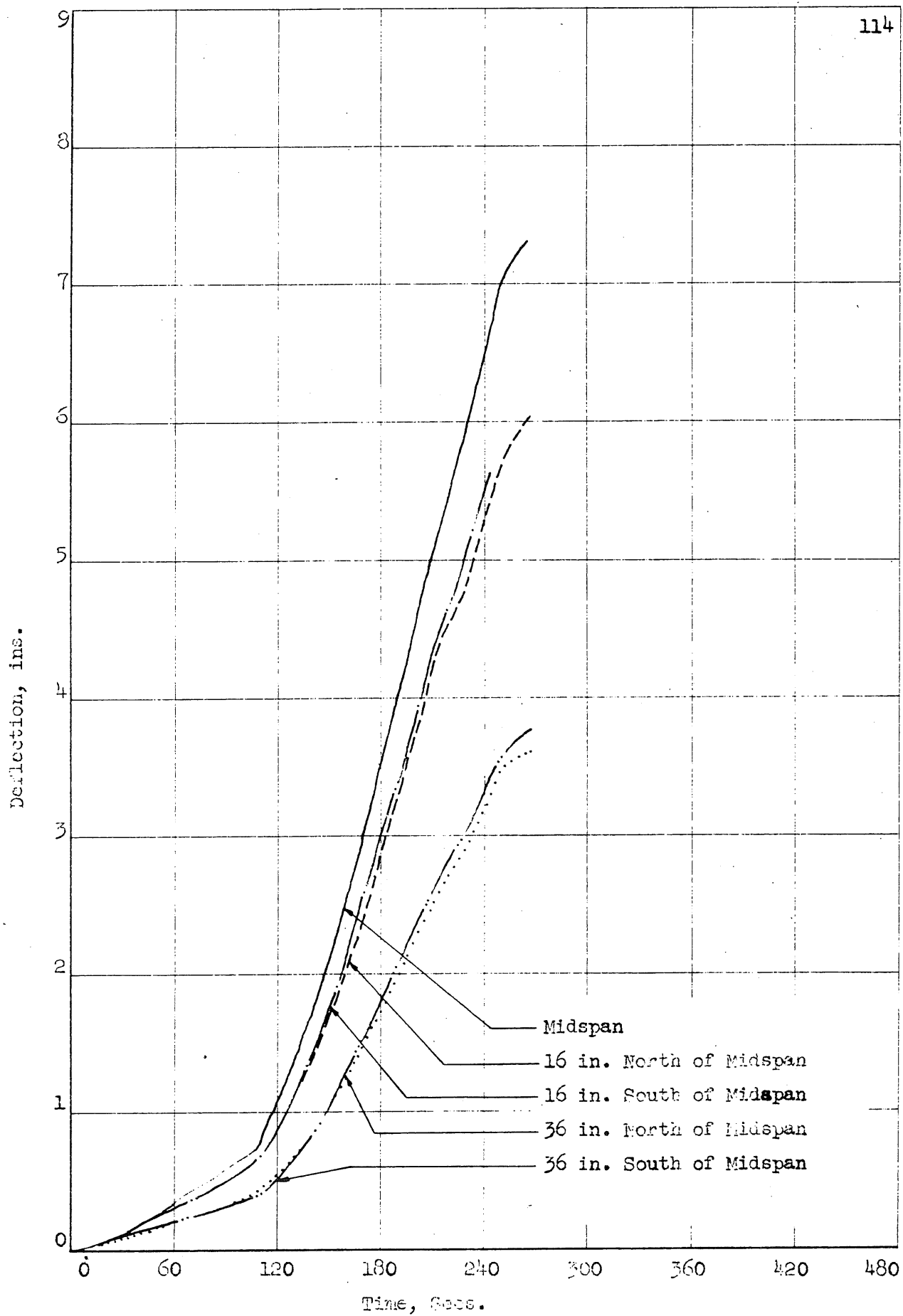


FIG. A14b: RECORDED DATA FROM TEST CURVES

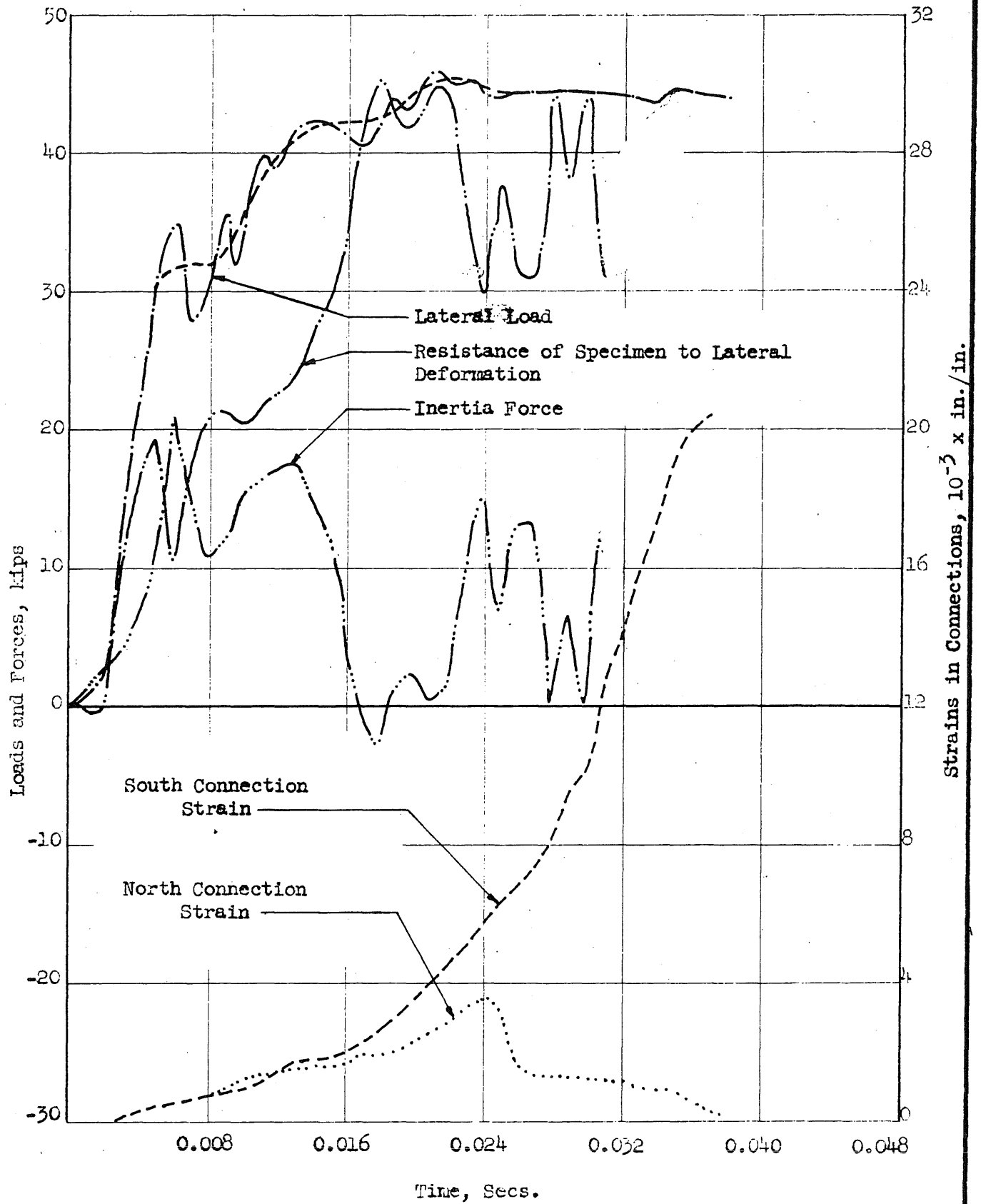


FIG. A15a: RECORDED DATA FROM TEST CTBR

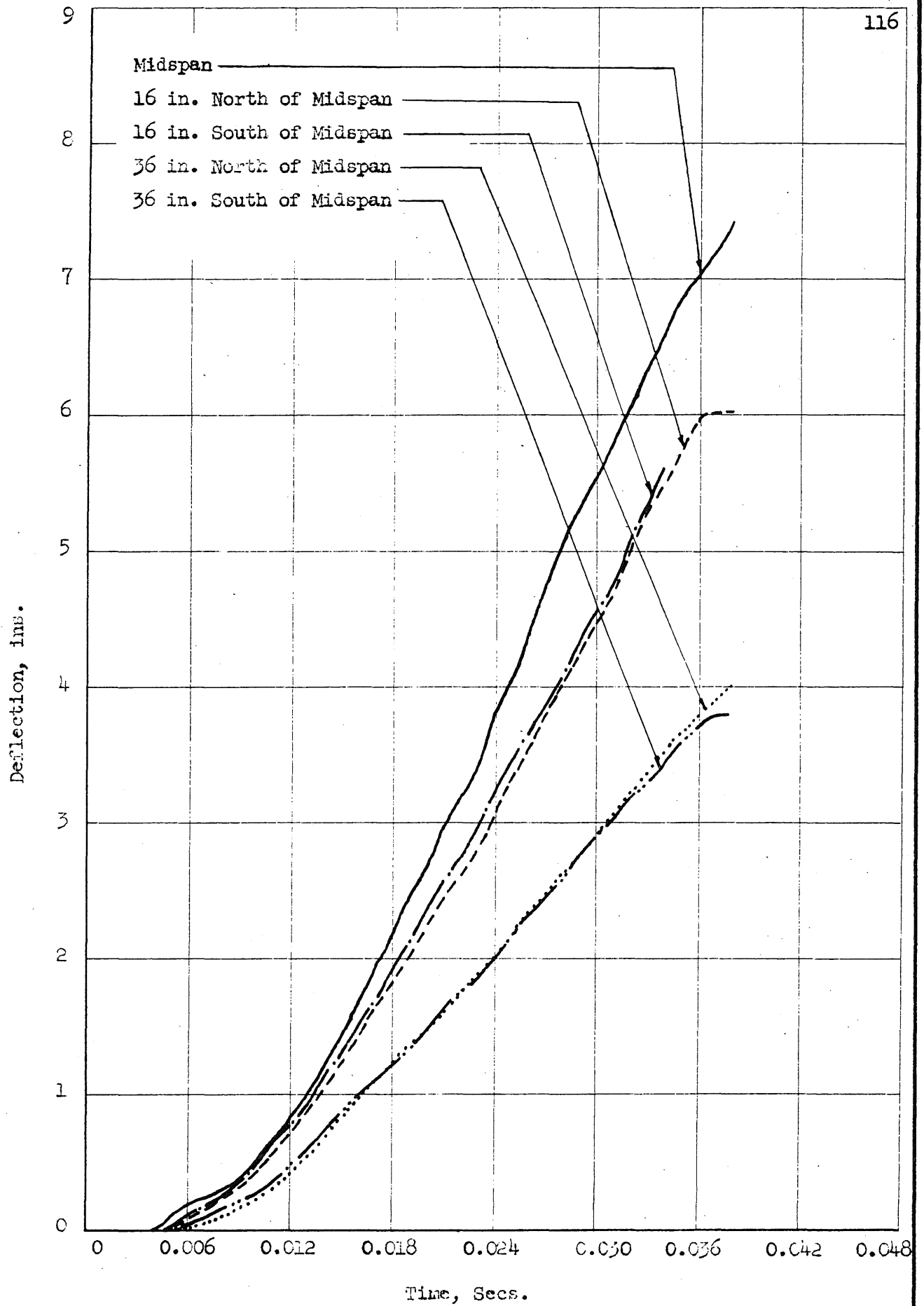


FIG. A15b: RECORDED DATA FROM TEST CTBR

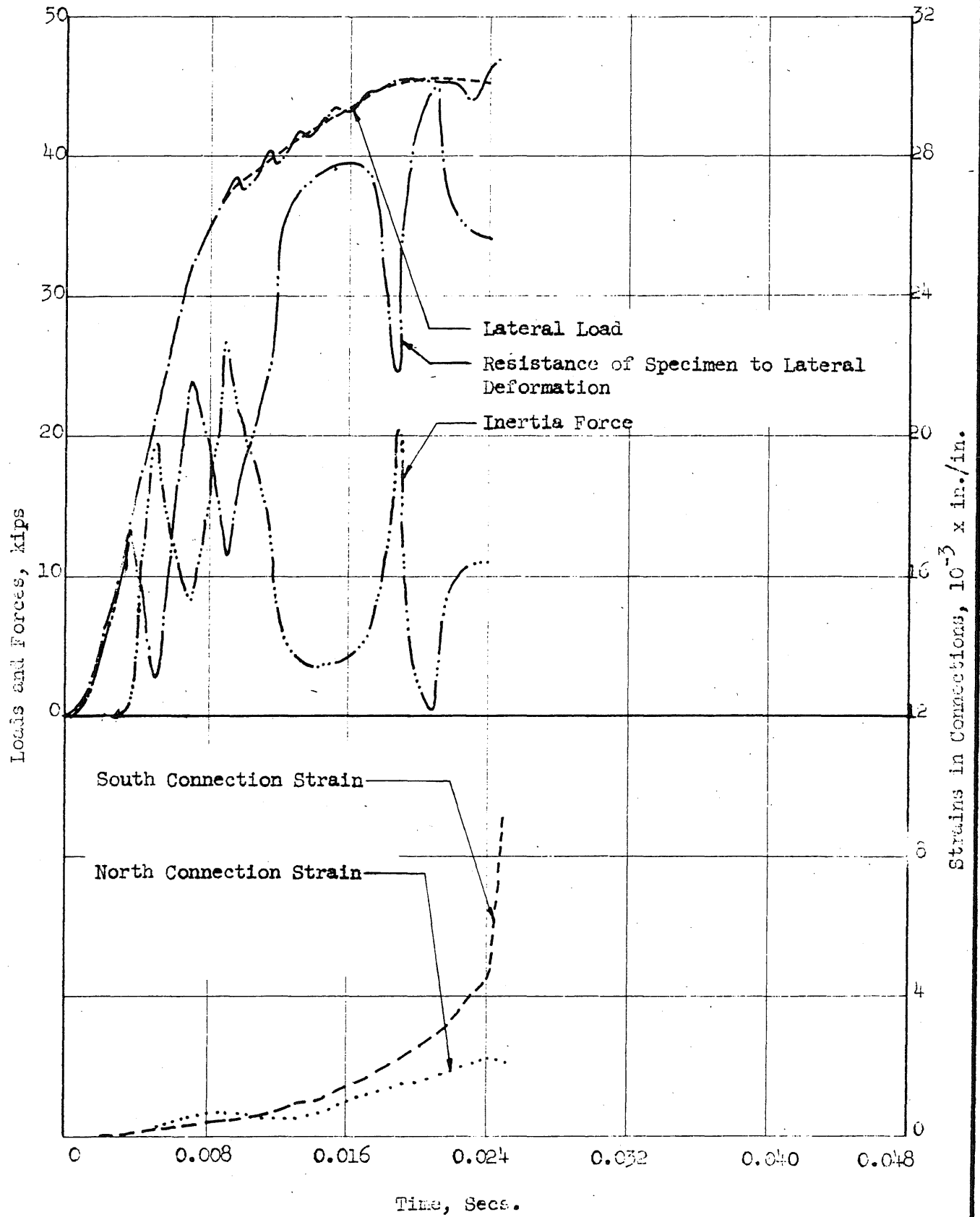


FIG. A16a: RECORDED DATA FROM TEST CTRR

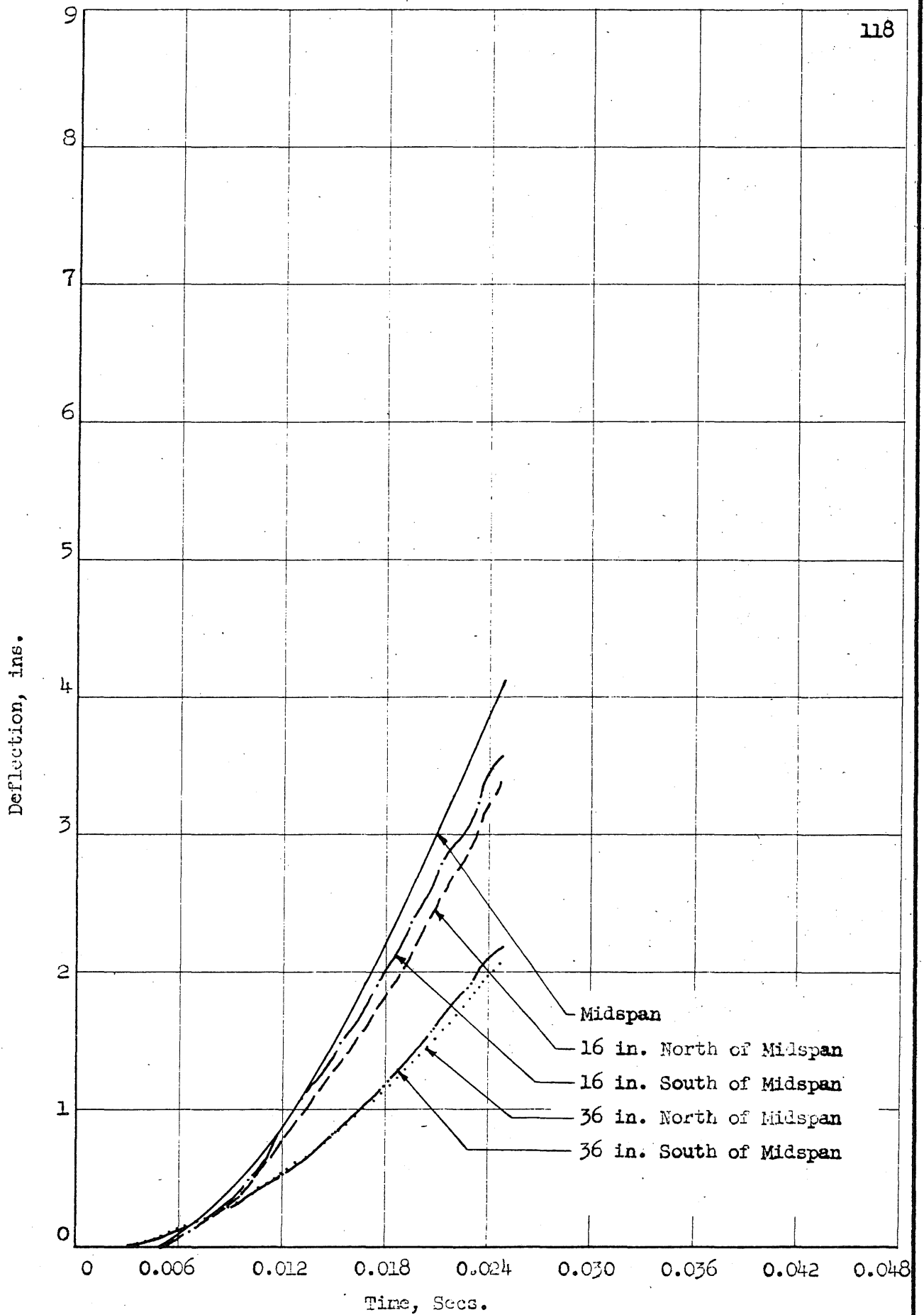


FIG. A16b: RECORDED DATA FROM TEST CTRR

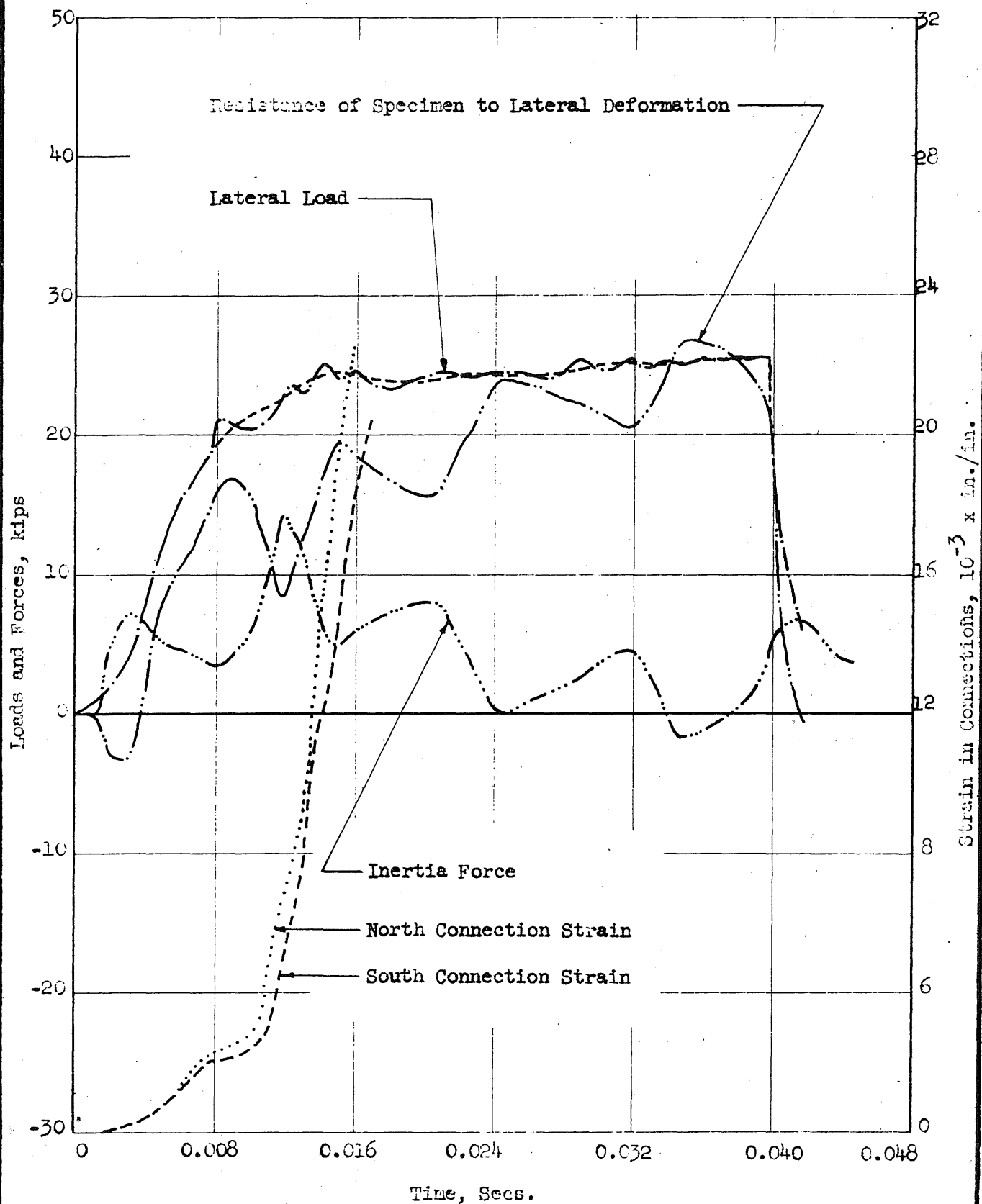


FIG. A17a: RECORDED DATA FROM TEST CFBR

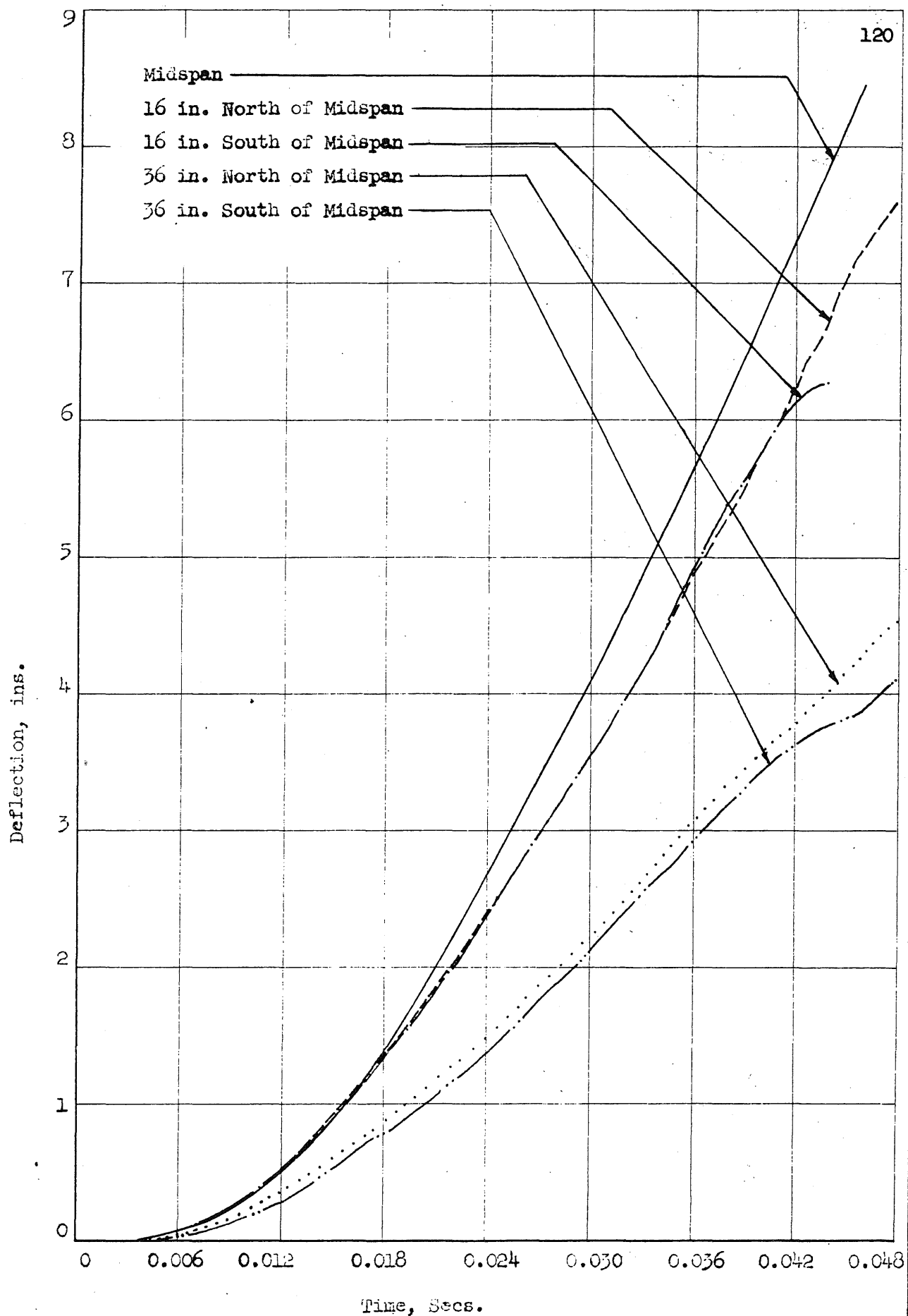


FIG. A17b: RECORDED DATA FROM TEST CTBR

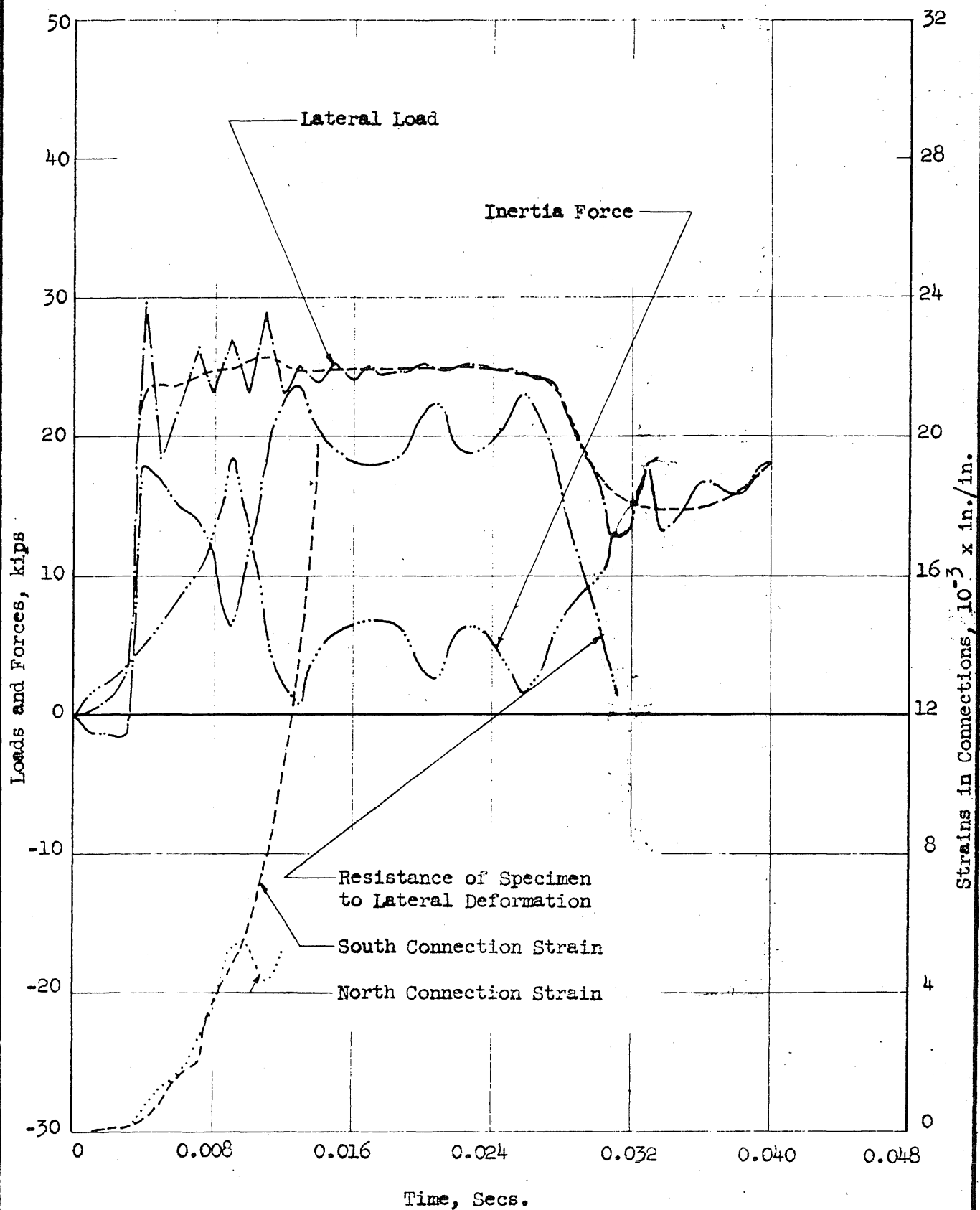


FIG. A18a: RECORDED DATA FROM TEST CFRR

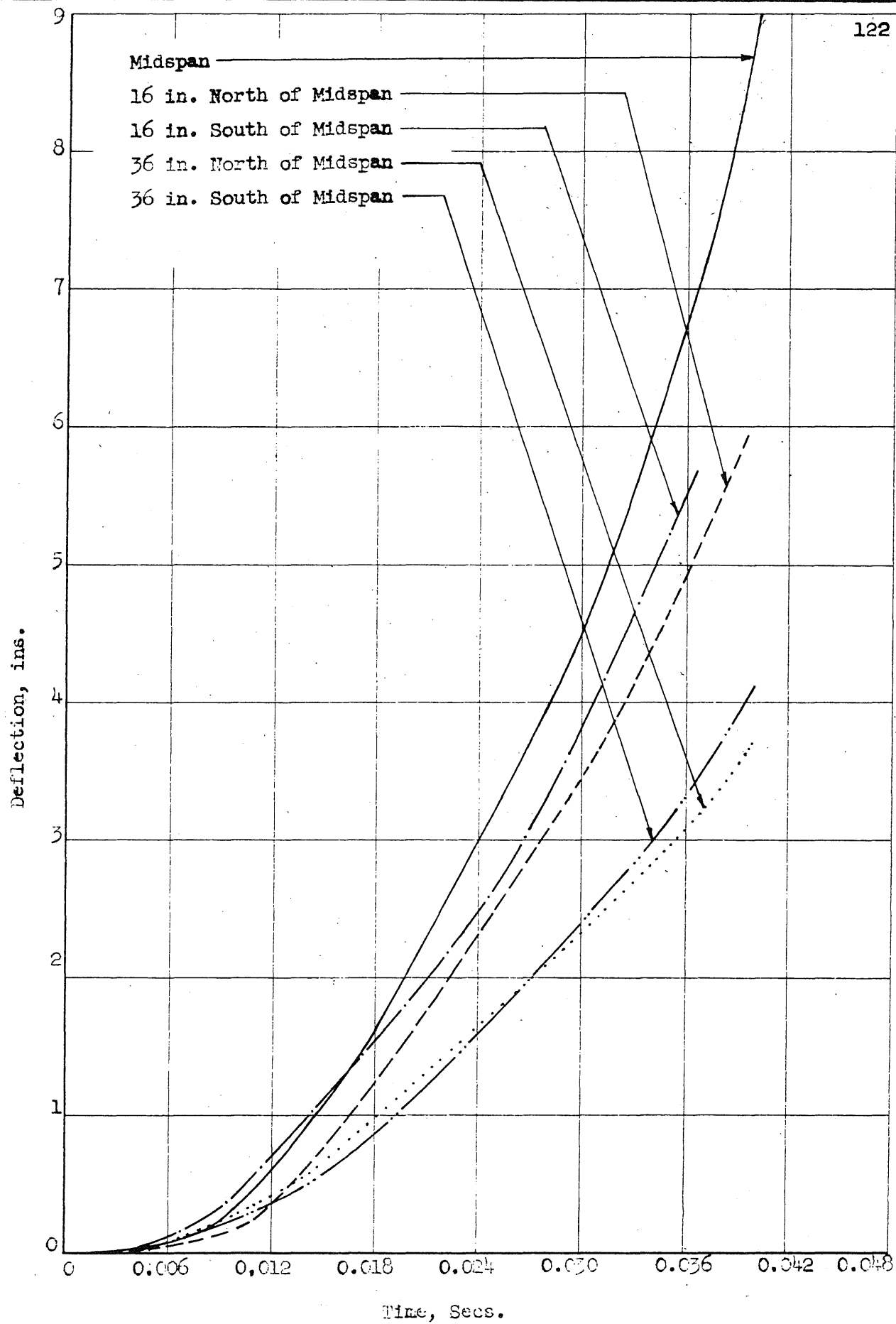


FIG. A18b: RECORDED DATA FROM TEST CFRR

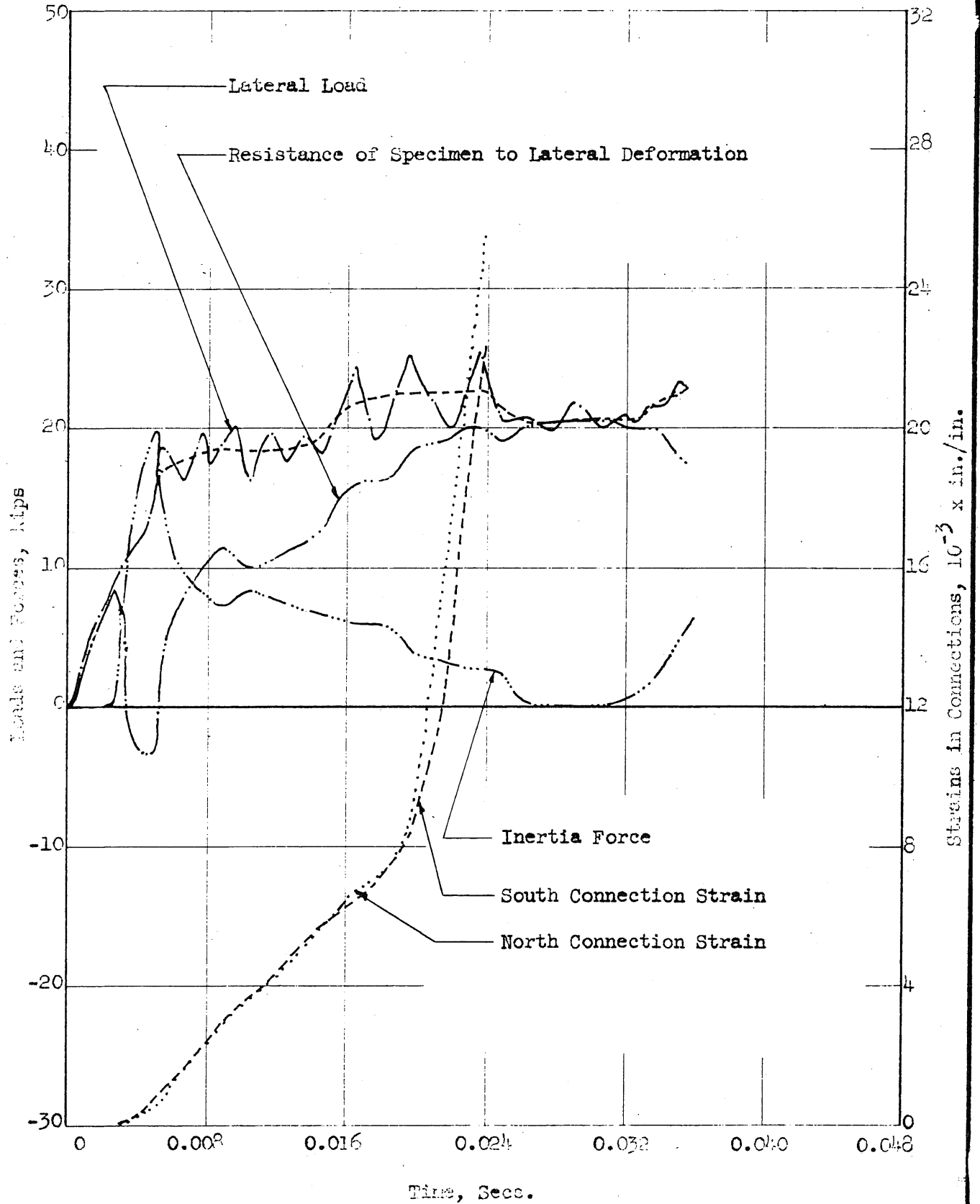


FIG. A19a: RECORDED DATA FROM TEST CWBR

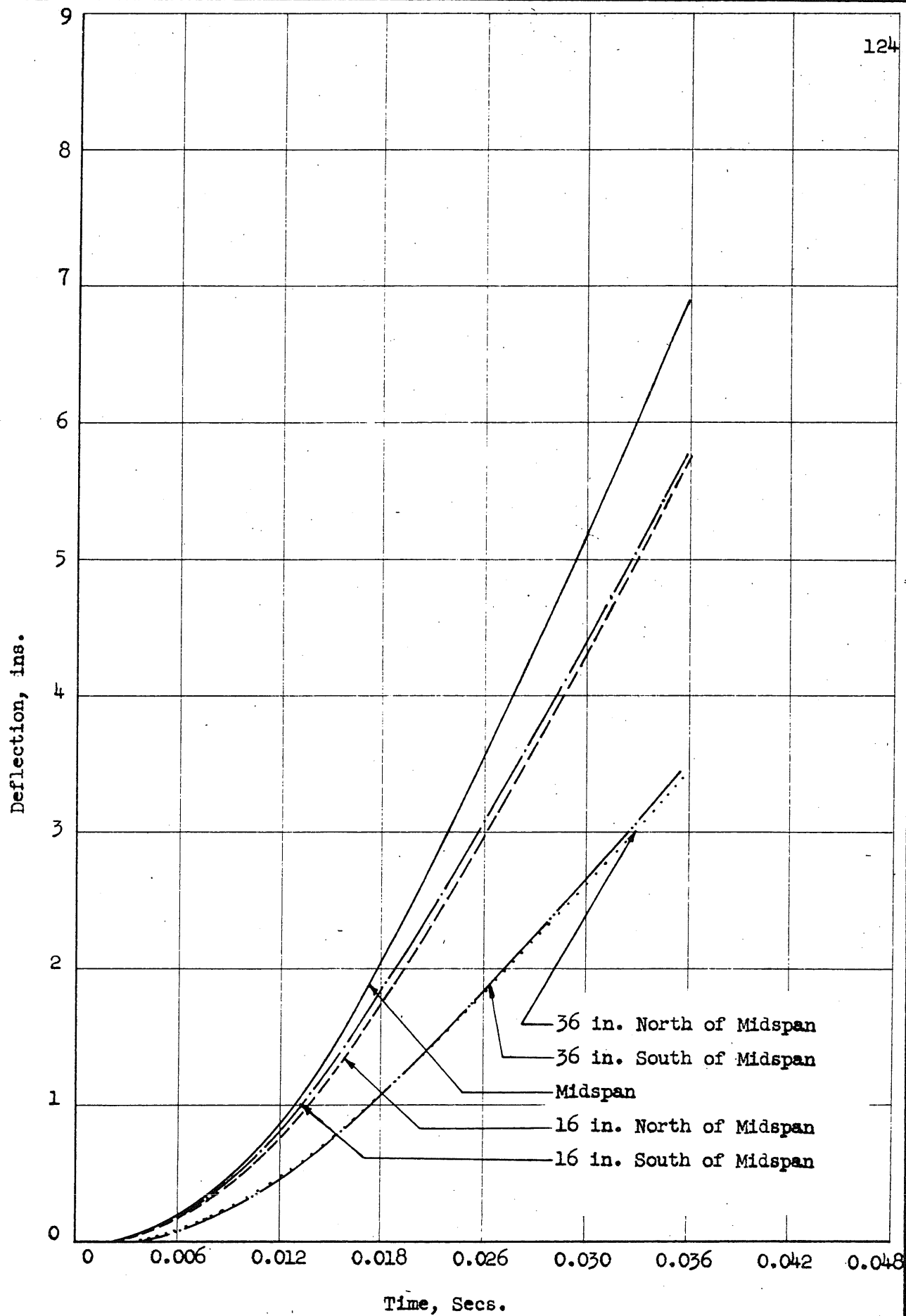


FIG. A19b: RECORDED DATA FROM TEST CWBR

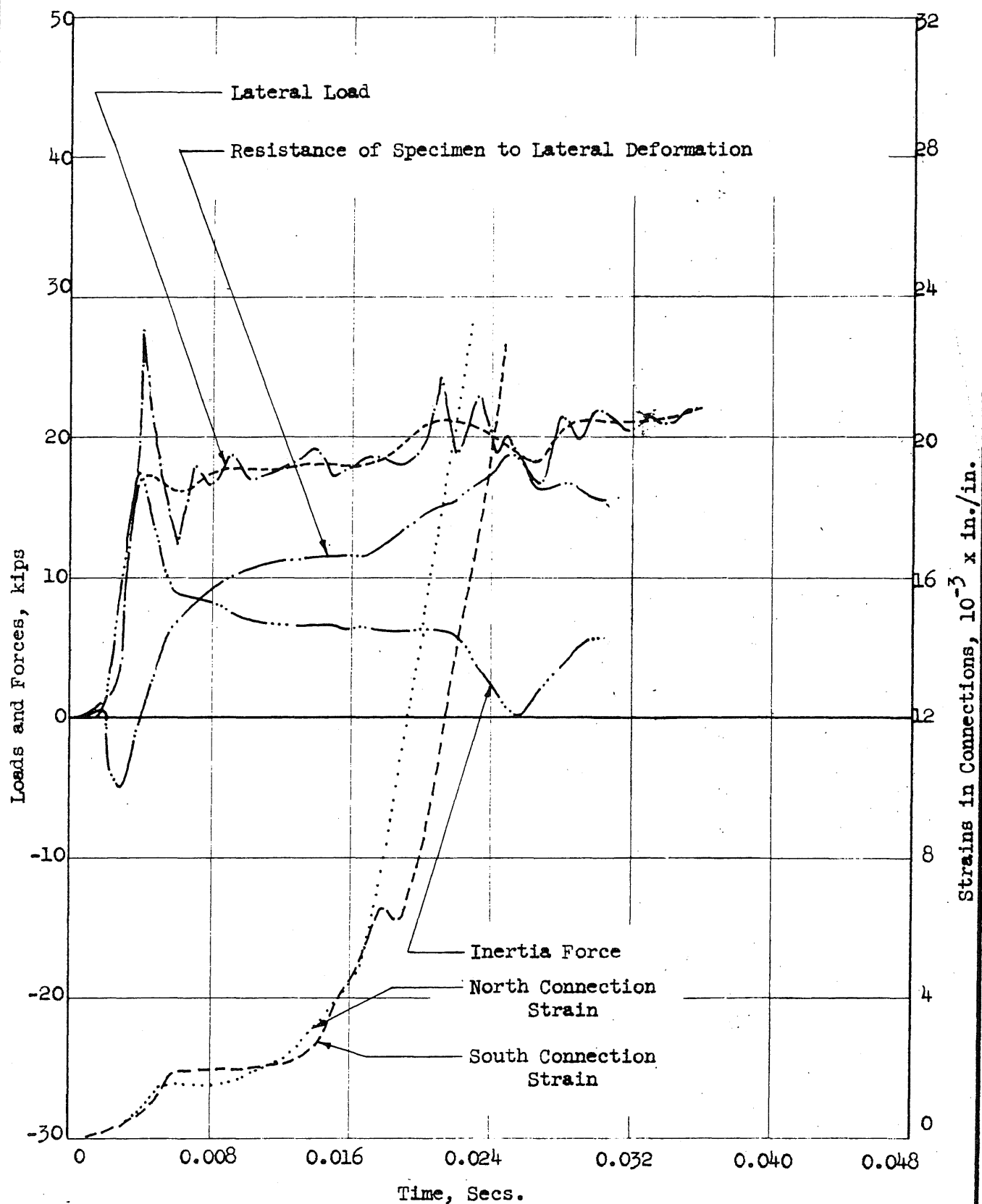


FIG. A20a: RECORDED DATA FROM TEST CWRR

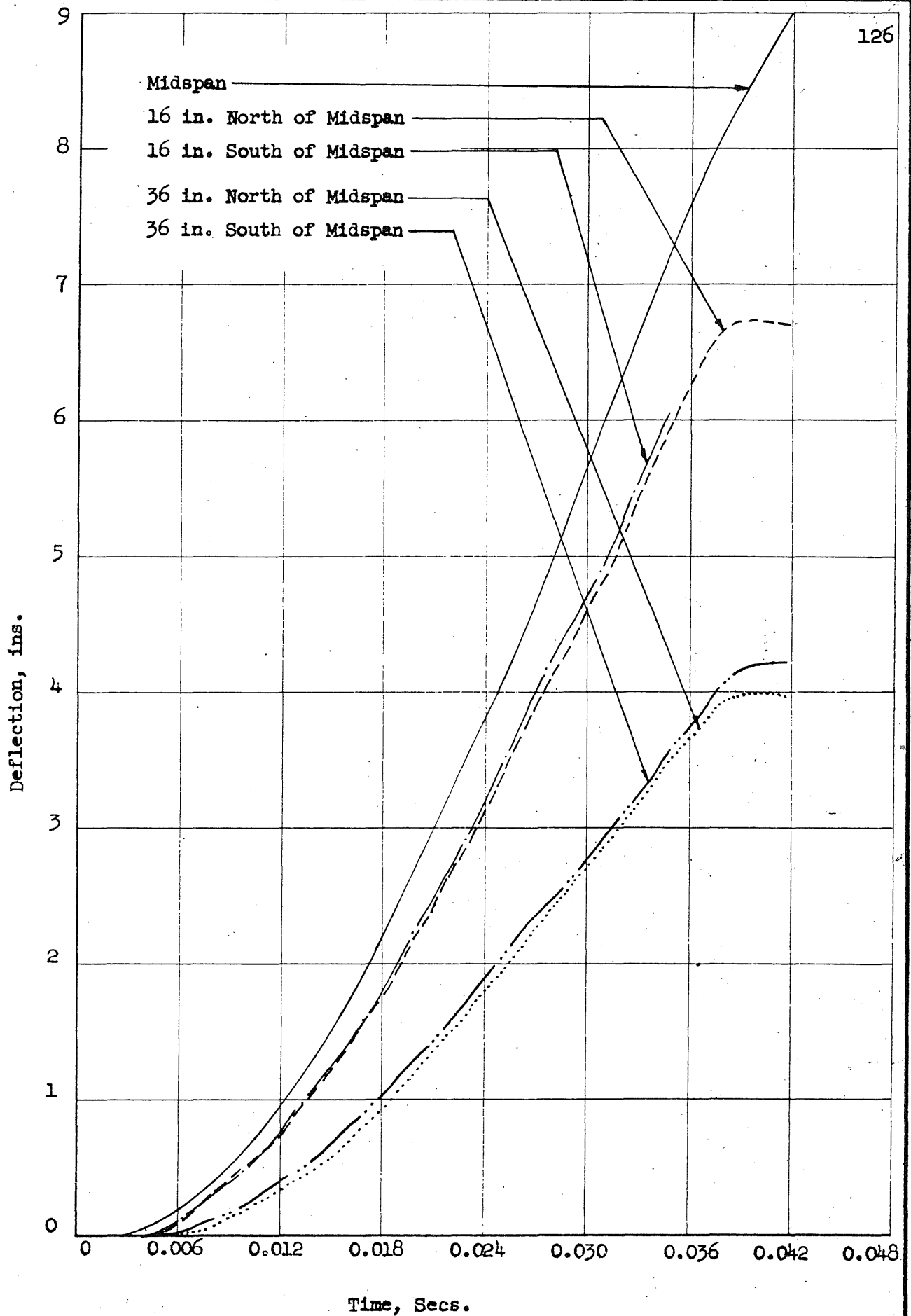
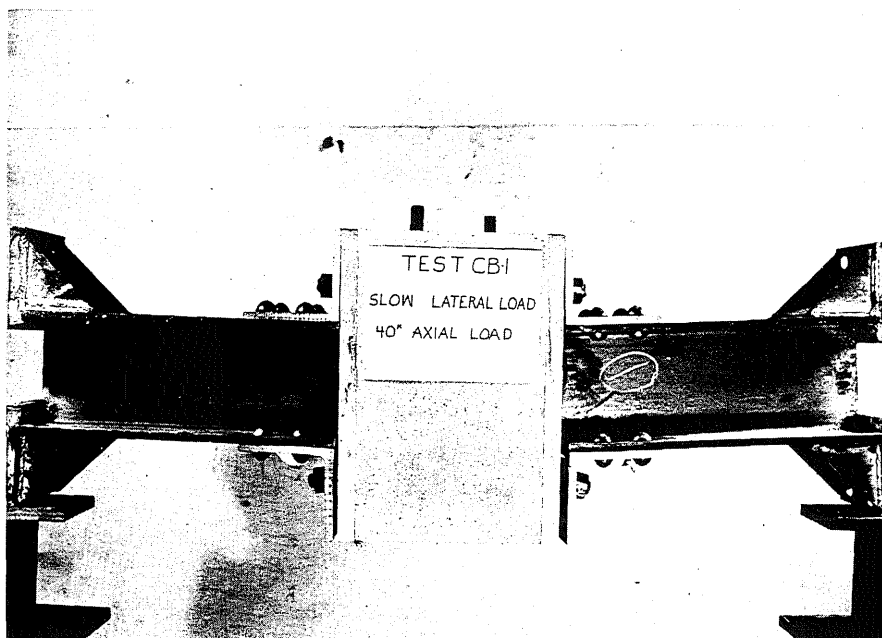


FIG. A206: RECORDED DATA FROM TEST CWRR

APPENDIX B
PHOTOGRAPHS OF SPECIMENS AFTER TESTING

<u>Figure</u>		<u>Page</u>
B1	Specimen CB1 After Testing	128
B2	Specimen CB2 After Testing	128
B3	Specimen CB3 After Testing	129
B4	Specimen CB4 After Testing	129
B5	Specimen CB5 After Testing	130
B6	Specimen CB6 After Testing	130
B7	Specimen CB7 After Testing	131
B8	Specimen CB8 After Testing	131
B9	Specimen CTBS After Testing.	132
B10	Specimen CTRS After Testing.	132
B11	Specimen CFBS After Testing.	133
B12	Specimen CFRS After Testing.	133
B13	Specimen CWBS After Testing.	134
B14	Specimen CWRS After Testing.	134
B15	Specimen CTBR After Testing.	135
B16	Specimen CTRR After Testing.	135
B17	Specimen CFBR After Testing.	136
B18	Specimen CFRR After Testing.	136
B19	Specimen CWBR After Testing.	137
B20	Specimen CWRR After Testing.	137
B21	Close-up of Brittle Fracture, Specimen CFBR.	138



(Specimen Straightened Somewhat During
Removal from Testing Frame)
Note: Brittle Fracture, Lower Right Angle

FIG. B1 SPECIMEN CB1 AFTER TESTING

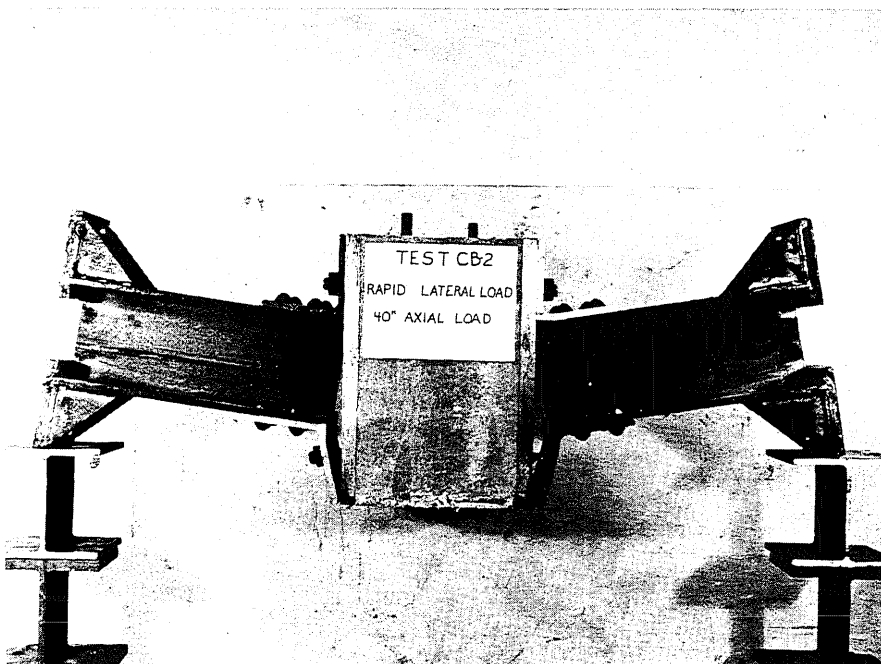


FIG. B2 SPECIMEN CB2 AFTER TESTING

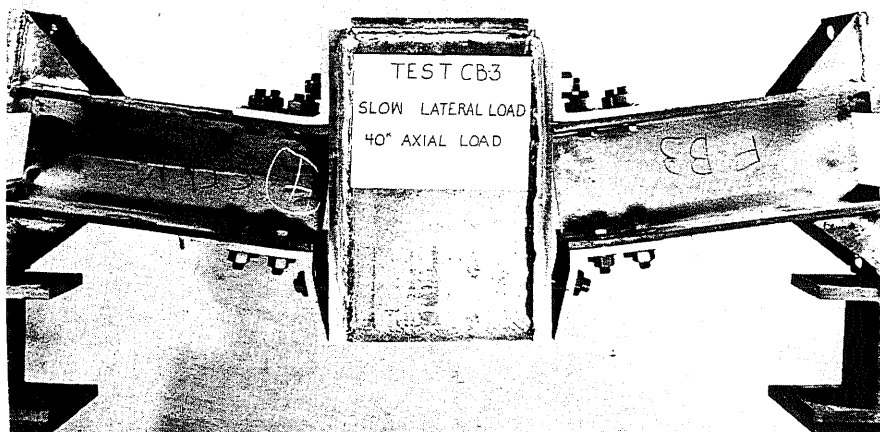


FIG. B3 SPECIMEN CB3 AFTER TESTING

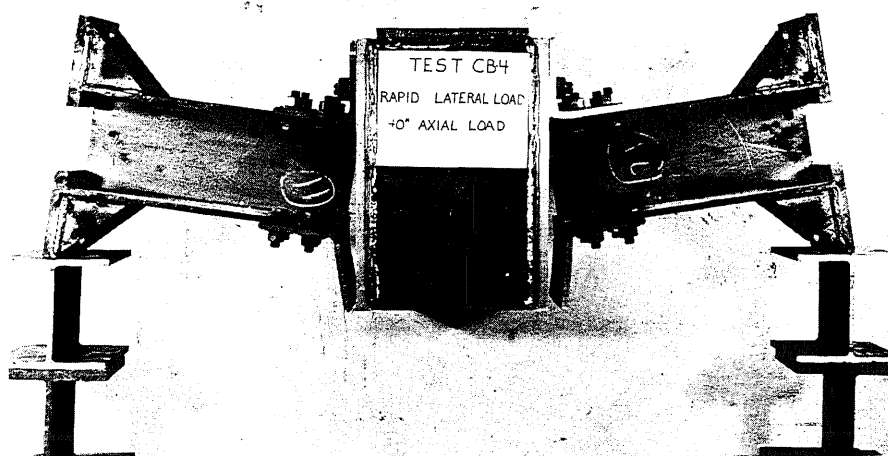


FIG. B4 SPECIMEN CB4 AFTER TESTING

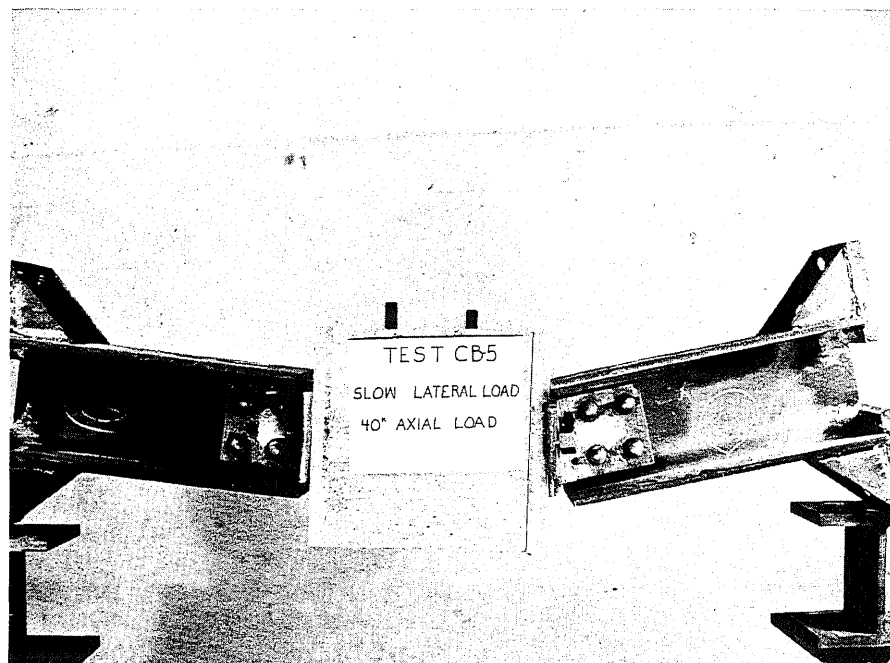


FIG. B5 SPECIMEN CB5 AFTER TESTING

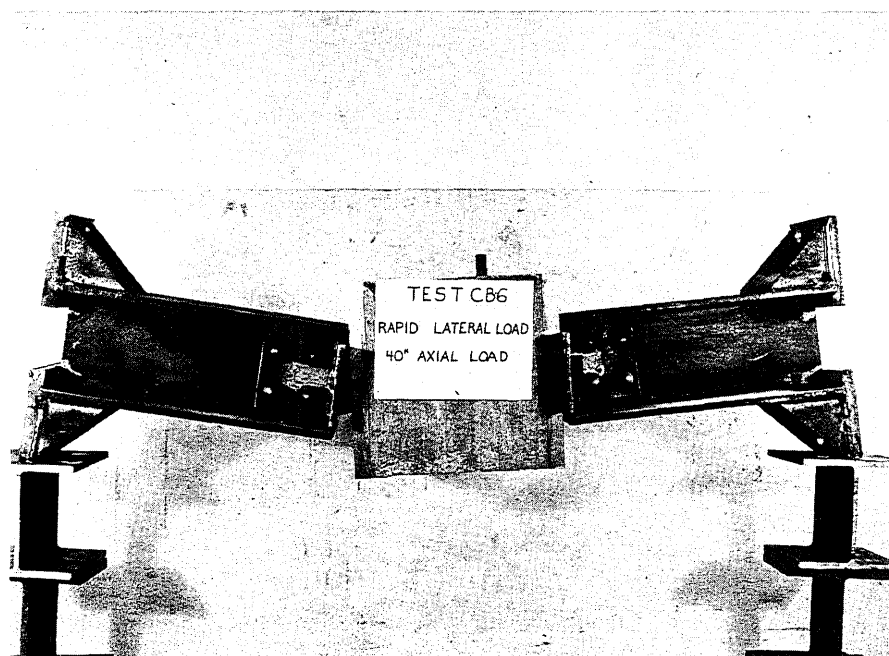


FIG. B6 SPECIMEN CB6 AFTER TESTING

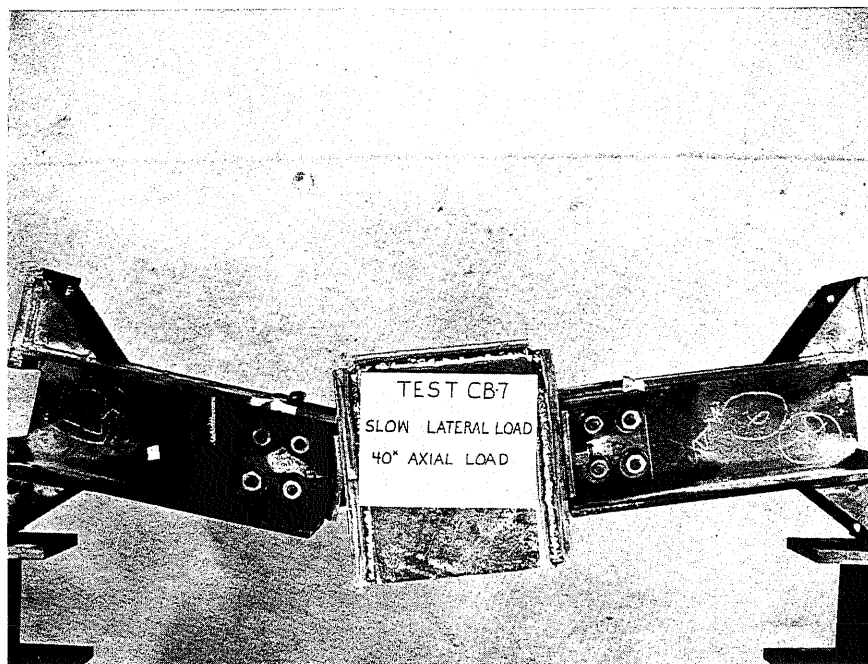


FIG. B7 SPECIMEN CB7 AFTER TESTING

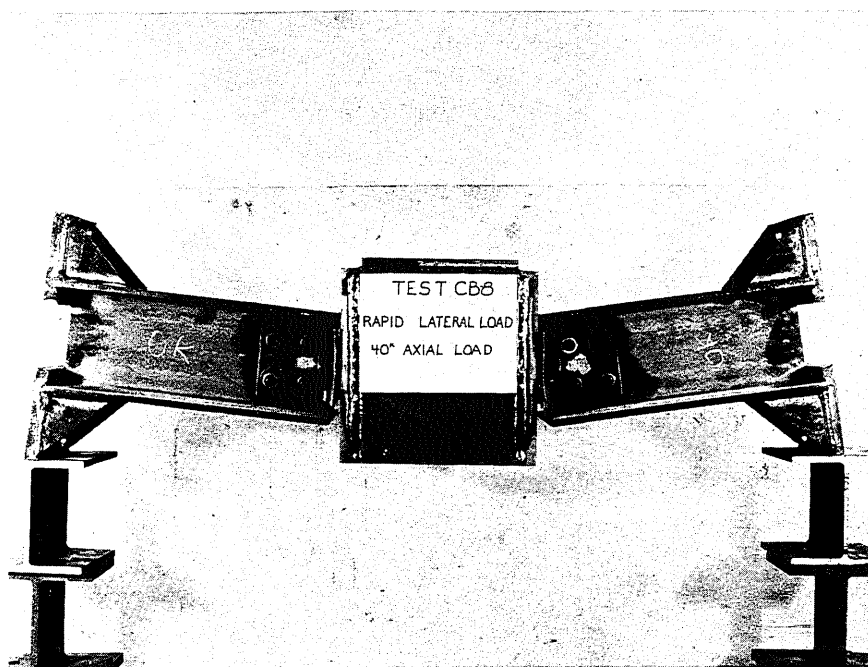


FIG. B8 SPECIMEN CB8 AFTER TESTING

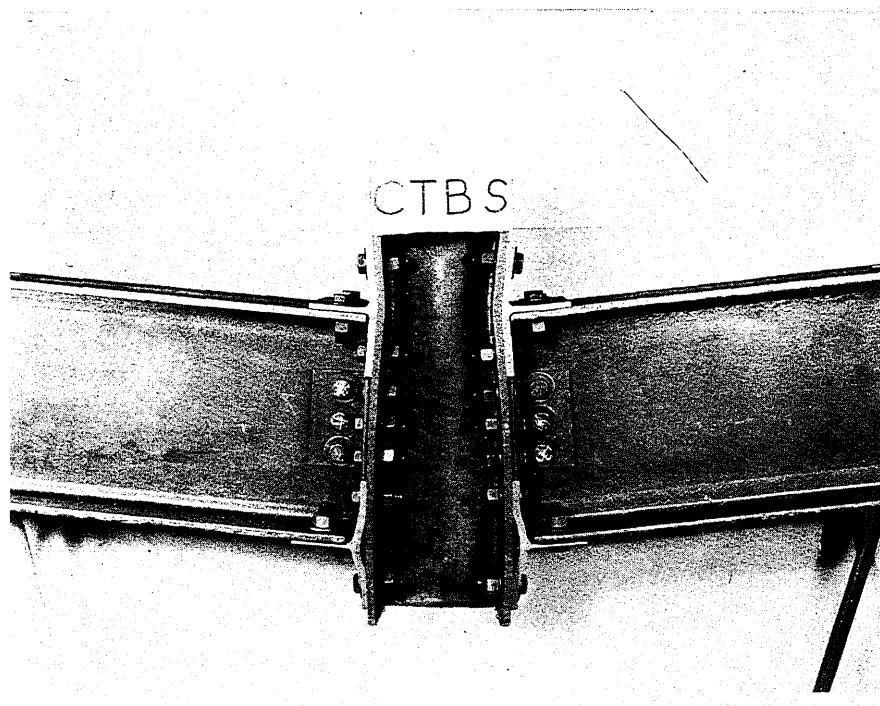


FIG. B9 SPECIMEN CTBS AFTER TESTING

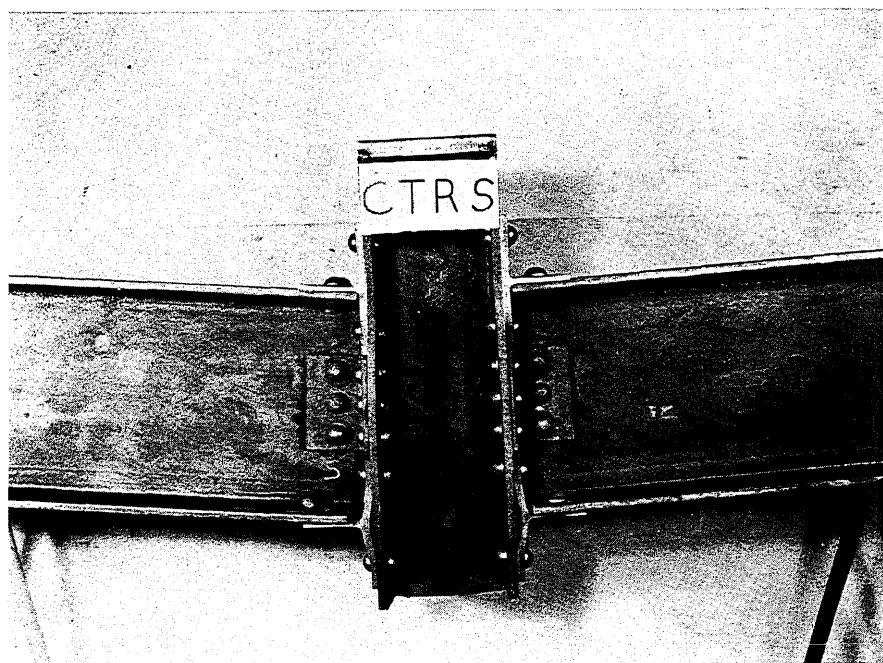
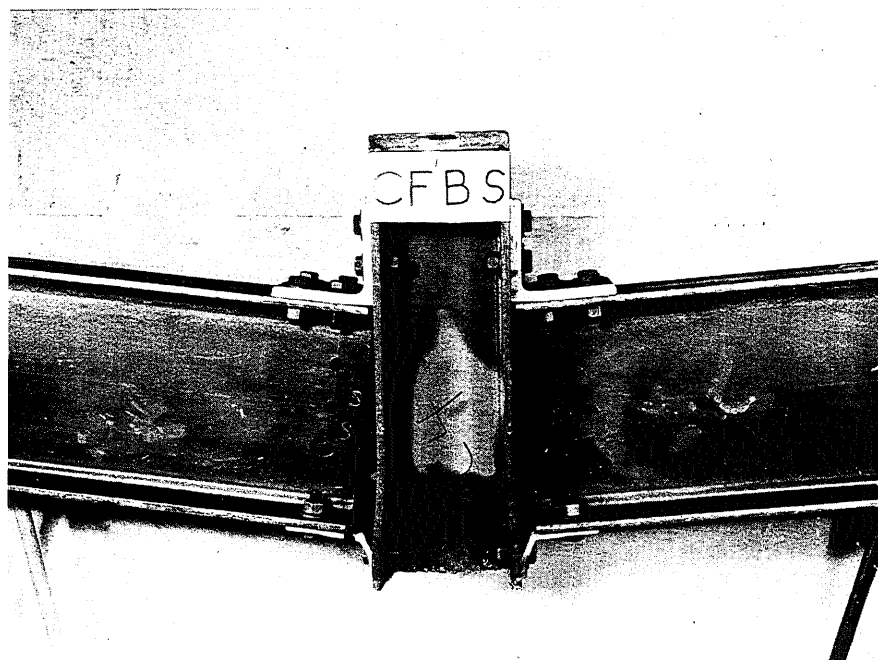
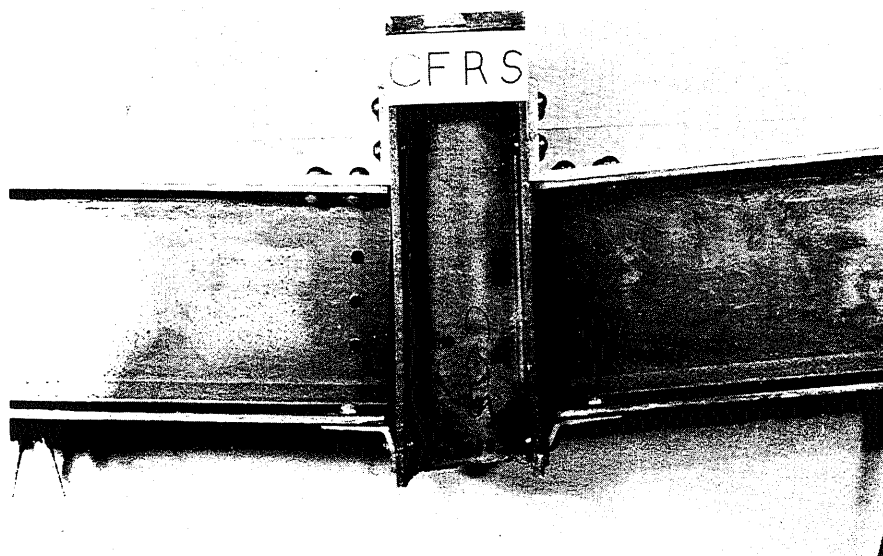


FIG. B10 SPECIMEN CTRS AFTER TESTING



Note: Web Holes Unused

FIG. B11 SPECIMEN CFBS AFTER TESTING



Note: Web Holes Unused

FIG. B12 SPECIMEN CFRS AFTER TESTING

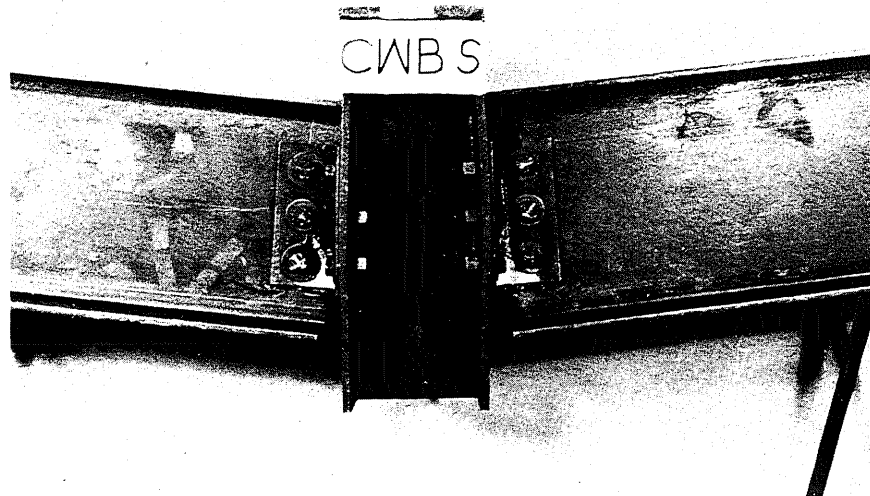


FIG. B13 SPECIMEN CWBS AFTER TESTING



FIG. B14 SPECIMEN CWR S AFTER TESTING

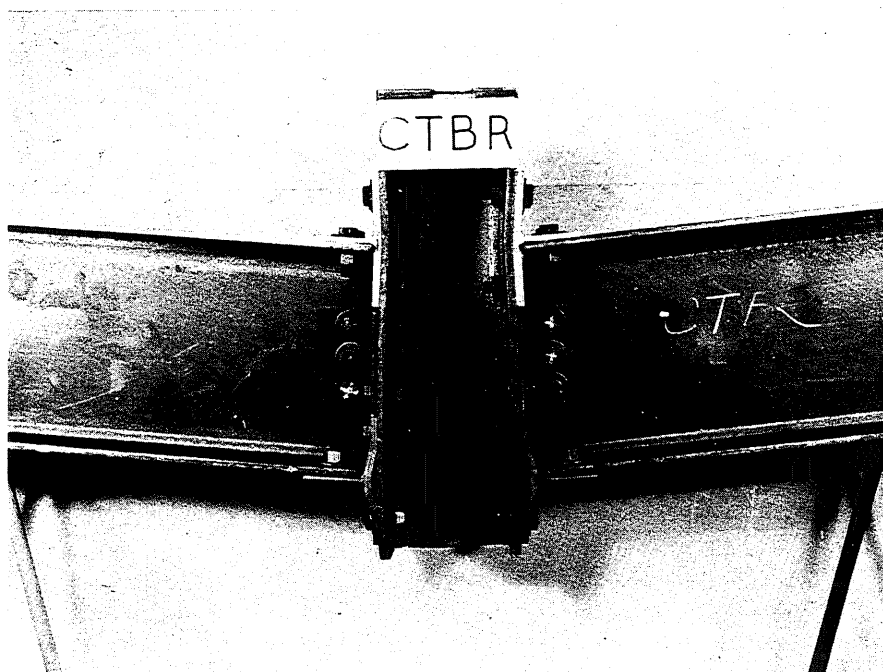


FIG. B15 SPECIMEN CTBR AFTER TESTING

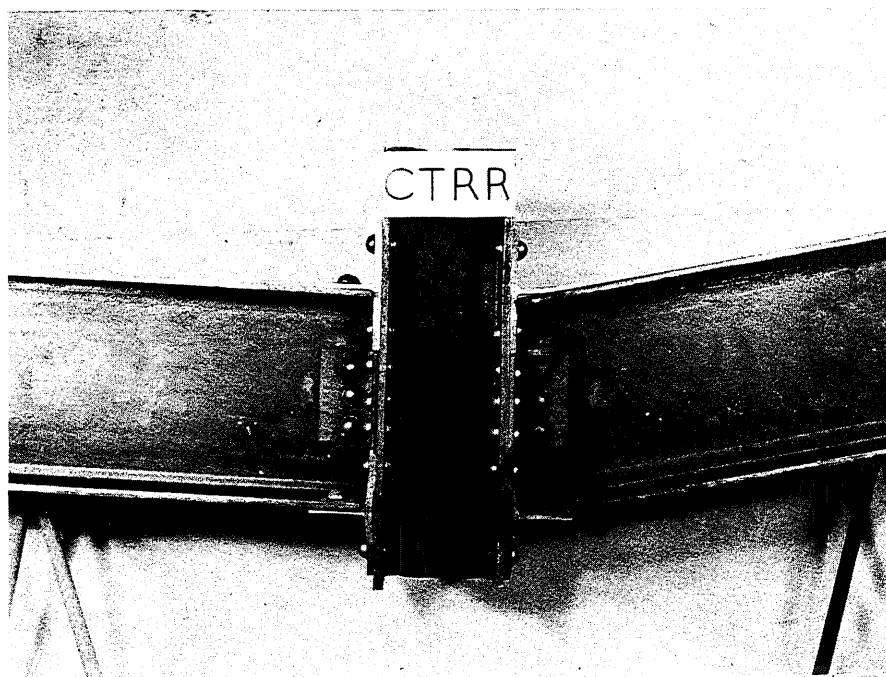


FIG. B16 SPECIMEN CTRR AFTER TESTING



Note: See Fig. B21 for Detail of Brittle Fracture in Lower Left Angle

FIG. B17 SPECIMEN CFBR AFTER TESTING



FIG. B18 SPECIMEN CFRR AFTER TESTING

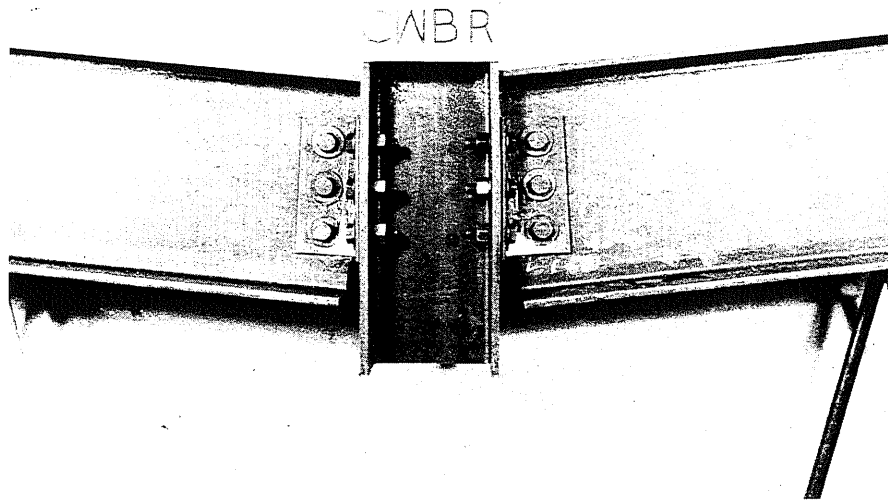


FIG. B19 SPECIMEN CWBR AFTER TESTING

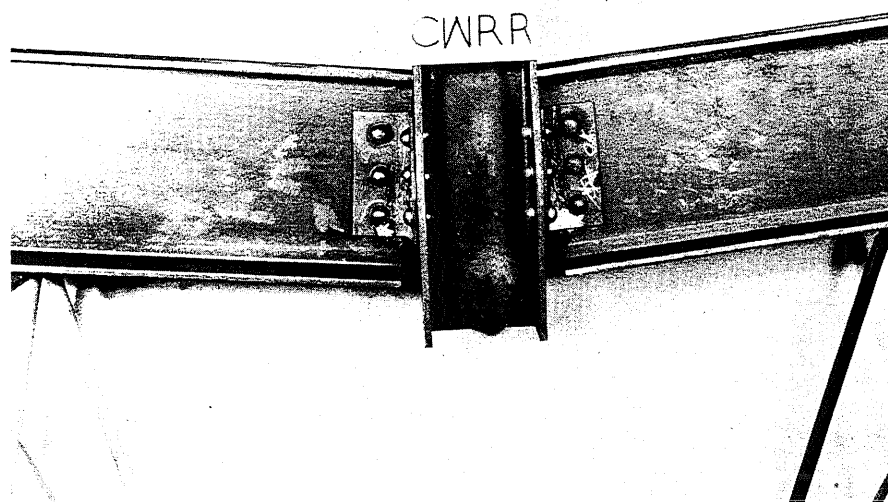


FIG. B20 SPECIMEN CWRR AFTER TESTING



FIG. B21 CLOSE-UP OF BRITTLE FRACTURE, SPECIMEN CFBR